Fall 1979

A PHYSIOCHEMICAL AND SPECTRAL CHARACTERIZATION OF THE EXTRAPALLIAL FLUID OF MYTILUS EDULIS

MILTON JOHN MISOGIANES
University of New Hampshire, Durham

MISOGIANES, MILTON JOHN

A PHYSIOCHEMICAL AND SPECTRAL CHARACTERIZATION OF THE EXTRAPALLIAL FLUID OF MYTILUS EDULIS

University of New Hampshire PH.D. 1979

A PHYSIOCHEMICAL AND SPECTRAL CHARACTERIZATION OF THE EXTRAPALLIAL FLUID OF *MYTILUS EDULIS*

BY

MILTON J. MISOGIANES
B.A., University of Vermont, 1974

A DISSERTATION

Submitted to the University of New Hampshire
in Partial Fulfillment of
the Requirements for the Degree of

Doctor of Philosophy
in
Chemistry

September, 1979

This thesis has been examined and approved.

N. Dennis Chasteen

Thesis director, N. Dennis Chasteen
Professor of Chemistry

Alexander R. Amell

Alexander R. Amell, Professor of Chemistry

Kenneth K. Andersen

Kenneth K. Andersen, Professor of Chemistry

Gerald L. Klippenstein

Gerald L. Klippenstein, Professor of Biochemistry

James H. Weber

James H. Weber, Professor of Chemistry

June 29, 1979

Date

This thesis is dedicated to my parents.

Acknowledgements

The author wishes to express his sincerest appreciation for the help and encouragement extended by his research director, Dr. N. Dennis Chasteen, who has been a counselor and always will be a friend. He would also like to thank the faculty of the Department of Chemistry. Gratitude is expressed to Dr. G. Klippenstein, Dr. J. Stuart, Marianne Borowski, and E. Robin Plummer of the Biochemistry Department for helpful discussions.

Sincerest appreciation is expressed to Suzanne Dimmit, Sue Mead, Dan Templeton, and Bob Saar for their assistance in the preparation of this manuscript. The author would like to thank the University of New Hampshire for financial assistance in the form of teaching and research assistantships.

Finally, the author would like to thank his favorite person in the world, Louie, for his friendship.

TABLE OF CONTENTS

LIST OF TABLES

LIST OF FIGURES

ABSTRACT

A PHYSIOCHEMICAL AND SPECTRAL CHARACTERIZATION
OF THE EXTRAPALLIAL FLUID OF
MYTILUS EDULIS

by

MILTON JOHN MISOGIANES

University of New Hampshire, August, 1979

This study was undertaken to investigate the calcification process in molluscs by characterizing the medium from which shell components are formed. The medium, termed the extrapallial fluid, was analyzed for inorganic and organic constituents. Disc gel electrophoresis revealed the presence of at least five protein components. The insoluble fraction was sulfated carbohydrate material while the ultrafiltratable portion contained free amino acids. Fifteen trace metals were present in the fluid. Sodium, calcium, magnesium, iron and copper remained after centrifugation and dialysis.

Atomic absorption spectroscopy along with ion specific electrode experiments showed that the concentration of calcium in the fluid was 9.8 ± 0.4 mM, 85% of which was complexed. 74.3% of the calcium in the fluid was bound to small molecules, 9.2% was associated with insoluble carbohydrate, 15.3% was free, and 0.88% was associated with soluble macromolecular

components. The calcium bound by these soluble macromolecular components was tenaciously bound.

EPR measurements indicated that the majority of manganese present in the native fluid was also bound to small molecules. Titrations of the native fluid with Mn^{2+} and H^{+} established that the chelating capacity of the fluid was nominally 10^{-4}M. Mn^{2+} formed 1:1 complexes in the fluid having an average pK' value of 5.2. Iron and copper EPR signals observed indicated that these metals were associated with the soluble macromolecular components of the fluid.

The protein components in the fluid were separated into two distinct fractions (1 and 2) by gel filtration chromatography. The apparent molecular weights of 1 and 2 were 80,000 and 30,000 daltons respectively. When each fraction was subjected to anion exchange chromatography, nine protein components were present. Two primary components, a glycoprotein (1A) and an enzyme (1B) were studied in detail.

The glycoprotein (1A) was demonstrated to be homogeneous with respect to charged isomers by disc gel electrophoresis at three different gel concentrations. Amino acid analyses indicated that glutamic and aspartic acid residues accounted for one third of the total amino acids in the protein. The carbohydrate content was 30%. Optical emission spectroscopy showed the presence of sodium, magnesium, and calcium. Atomic absorption spectroscopy on several samples determined the molar ratio of calcium to 1A as 3.1 ± 0.3 and magnesium to be 1.8 ± 0.2.

Metal binding studies with Mn^{2+}, Mg^{2+}, and Ca^{2+} were performed using EPR, ultrafiltration and flow dialysis techniques. The glycoprotein contained five divalent cation bindings sites: two high affinity Mg^{2+} binding sites that also bound Mn^{2+} and Ca^{2+} and three high affinity Ca^{2+} binding sites that bound Ca^{2+} but not Mg^{2+} or Mn^{2+}. The glycoprotein might serve as an initiator of calcification.

A phenoloxidase (1B) detected in the fluid was found to catalyze the dehydrogenation of catechols to form quinones. These quinones are responsible for crosslinking presclerotin protein subunits of periostraca. The electrophoretic properties, activity, pH optimum, amino acid content and metal association of the enzyme were reported.

Chapter 1

Introduction

The deposition of calcium salts in skeletal structures is a widespread physiological activity in the animal kingdom. Common examples of calcified tissue include bones of mammals, egg shells of birds, and exoskeletons of molluscs.[1] All skeletal materials consist of two components: an organic phase and an inorganic phase.[2] In vertebrates, the organic and inorganic phases are the fibrous protein collagen and apatite ($Ca_3P_2O_8$), respectively. The organic phase of invertebrates varies widely while the inorganic phase is calcium carbonate ($CaCO_3$) in the form of calcite, aragonite, or vaterite.

All skeletal materials are products of extracellular biological processes and are characterized by a high degree of organization of the mineral and organic phases. The process of calcification is complex, involving genetic material, enzymes, structural proteins, and carbohydrates as well as small organic molecules and inorganic ions. The interplay of these materials appears to dictate a highly ordered event.

The identification of mineral and organic species in extracellular environments where calcification occurs is important to understanding the mechanism of nucleation and

crystal growth. In vertebrates, skeletal material is usually deposited from the extracellular fluid[3] (Figure 1.1). The fluid is quite diffuse, therefore, direct analysis is difficult. In contrast, some molluscs contain microenvironments termed the extrapallial fluid. Localized in this fluid are species important in calcification. Because extrapallial fluid is readily accessible for direct analysis, it could serve as a useful model for biomineralization processes in higher animals where such analyses are difficult to perform.

This work reports the partial characterization of the extrapallial fluid of Mytilus edulis, with the goal of establishing the mechanism of shell deposition.

General Description of the Shell Forming System of Molluscs

In describing the general process of mineral deposition, it is useful to consider separately the four components of the biomineralization system, namely the external medium, mantle, extrapallial fluid, and shell (Figure 1.2). All are interconnected, permitting ions to pass from one compartment to another.

The External Medium

This compartment is either seawater or fresh water. A portion of the carbonate, calcium, and other inorganic species utilized in crystal formation originates here.

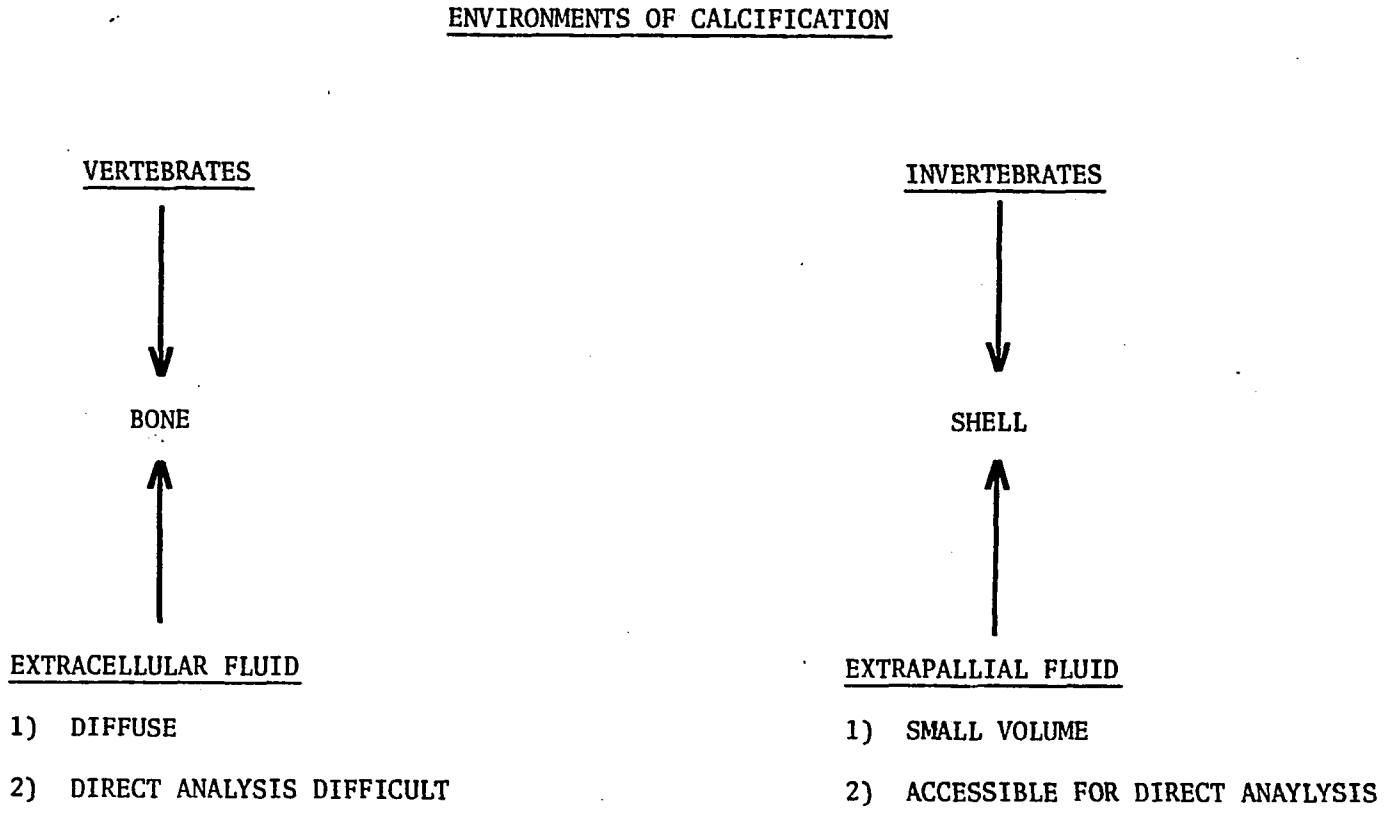

Figure 1.1. Comparison of environments of calcification for vertebrates and invertebrates.

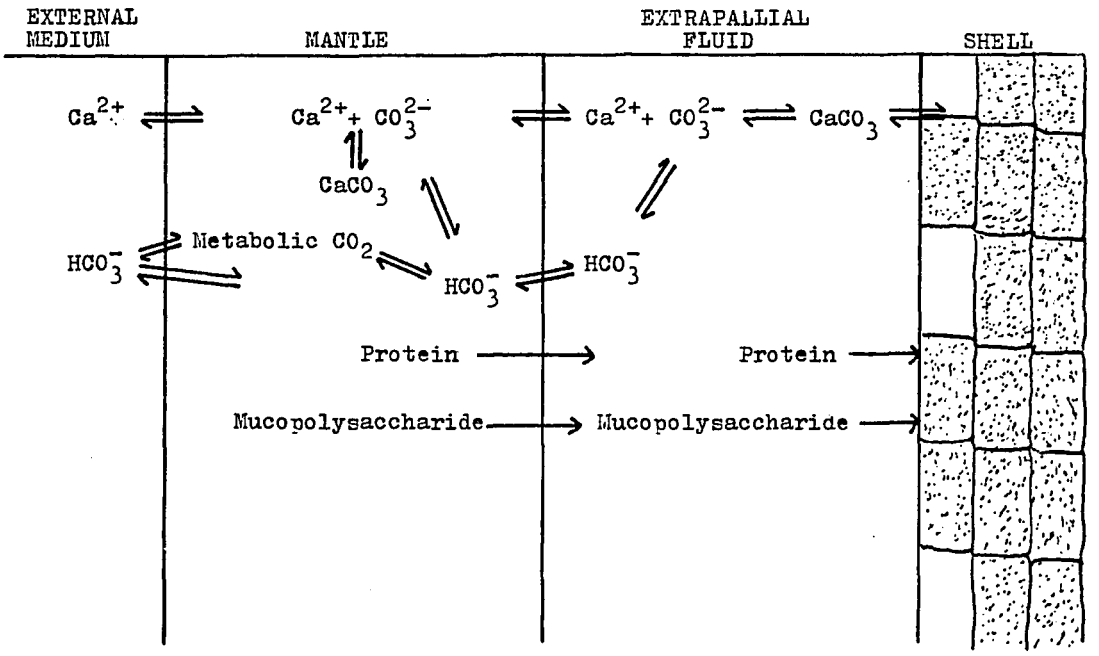

Figure 1.2. Diagram of compartments in molluscs showing ions and organic compounds involved in shell formation. (Adapted from Ref. 38.)

The Mantle

The mantle is a tissue separating the viscera and external medium from the extrapallial fluid. This tissue is responsible for synthesizing the organic components of the shell. The mantle secretes components such as proteins, polysaccharides, amino acids, organic acids, simple sugars, and peptides. Present here also are solubilized calcium and metabolic carbon dioxide, providing another source for skeletal material.

The Extrapallial Fluid

The extrapallial fluid is the medium from which the inorganic and organic phases of the shell are formed. The fluid transports mantle products to the growing shell. The composition of the fluid determines the skeletal organic components, rate, and type of mineral formation.[4]

The Shell

The shell is primarily composed of $CaCO_3$ with smaller amounts of $MgCO_3$, $CaSO_4$, SiO_2, $Ca_3(PO_4)_2$, protein and mucopolysaccharides.[5-7] Trace quantities of many other elements have also been found.[8-9] The shell consists of two or more layers. The inner layer is mostly $CaCO_3$ which is found in one or more of three crystalline forms--calcite, aragonite, or vaterite. The crystals are separated by an organic matrix made of protein--mucopolysaccharide material which serves as a cement. Covering this layer in many species is the periostracum, an acid resistant, quinone-tanned

protein.[10] Tanning occurs by enzyme catalyzed oxidations of phenolic compounds.[11]

During calcification of a multiple layered shell, the following events take place within the four compartments:

1. The mantle secretes the periostracum which becomes a substratum upon which outer crystalline shell layer is deposited

2. Calcium ions and carbonate in the form of bicarbonate and metabolic carbon dioxide pass through the mantle to the extrapallial fluid where crystals of $CaCO_3$ are formed

3. Concurrently, the mantle synthesizes and then deposits the organic matrix into the fluid onto the inner shell surface

4. Crystal nucleation then occurs on the matrix on the surface of deposited crystals. Oriented crystal growth then proceeds in a precise fashion

Theories of Calcification in Molluscs

The preceding discussion represents only a general chemical description of extracellular calcification in molluscs. The overall process is complicated and hence, several theories have been postulated.

Calcium and Bicarbonate Pumps

Based upon the supposition that calcium and carbonate ions are pumped from within mantle cells into the extrapallial fluid, one theory proposes that the fluid becomes supersaturated with $CaCO_3$, and deposition occurs. Circumstantial

evidence supports this scheme. Experiments using the muscles of molluscs have shown that intracellular Ca^{2+} is quite low (10^{-6}M) and is maintained in that state by outwardly directed pumps.[12] Power for these pumps is supplied by CaATPase[13] or by energy obtained from Na^+ pumps.[14] Current thought suggests that all cells possess Ca^{2+} pumps, and it is conceivable that they could concentrate calcium at extracellular sites. Bicarbonate pumps, consisting of Na^+/H^+ and Cl^-/HCO_3^- exchange systems[15] have been detected in various invertebrates.

To support this theory, analysis of the extrapallial fluid of some molluscs has been performed.[16] Interpretation of the results was difficult because data on calcium binding to organic species was not available. Moreover, there was difficulty in estimating carbonate ion (CO_3^{2-}) concentrations.

Proton Removal

The proton removal theory is premised on the notion that calcification is merely pH controlled. The scheme posited is shown below:

1. $CO_2 + OH^- \rightleftharpoons HCO_3^-$

2. $Ca^{2+} + HCO_3^- \rightleftharpoons CaCO_3 + H^+$

3. $H^+ + OH^- \rightleftharpoons H_2O$

where the energy for the reactions comes from removal of protons. Reaction 1 may be catalyzed by the enzyme carbonic anhydrase,[17] which is found in many molluscan tissues.[18-19] Reaction 2 depicts the formation of mineralized $CaCO_3$ and the release of protons while reaction 3 represents the removal of protons by hydroxyl ion. Consequently, a slight drop in pH at sites of calcification should be observed. This is in accord with data shown in Table 1.1, where the extrapallial fluid of molluscs is more acidic than the blood.[20] A major drawback to this proposed scheme concerns the origin of hydroxyl ions necessary for proton removal. The hydroxyl ion concentration at these pH's is only 10^{-6} - 10^{-7}M and thus is insufficient to adequately neutralize the protons produced.

Campbell and Speeg[21] observed high concentrations of ammonia at sites of shell formation in molluscs. The possible effect of NH_3 in the deposition of $CaCO_3$ is shown by equation 4:

$$4.\quad NH_3 + HCO_3^- + Ca^{2+} \rightleftharpoons CaCO_3 + NH_4^+$$

where the proton from bicarbonate is removed by NH_3. Their hypothesis is reasonable in view of the fact that neutralization of protons by NH_3 occurs commonly in biological systems. For example, protons are neutralized by NH_3 in kidneys during acidosis[22] and this reaction serves to regulate the acidity of perspiration.[23] Simkiss[24] has pointed out a

Table 1.1

Comparisons of Extrapallial Fluid and Blood pH Values[16,19,20]

Species	Extrapallial Fluid	Blood
Crassostrea virginica	7.41	7.43
Aequipecten irradians	7.43	7.53
Mytilus edulis	7.39	7.50
Mercenaria mercenaria	7.35	7.52
Chlamys nipponensis	~ 7.2	~ 7.5
Modiolus demissus	7.39	7.34

major problem associated with the proposal of Campbell and Speeg. Because NH_3 is neutral and mobile, the molecule can cross cell membranes. The charged NH_4^+ ion, however, cannot penetrate cell membranes easily, and would tend to accumulate in the extrapallial fluid. If ammonia does play a part in calcification, how is the NH_4^+ ion removed?

Counterion Movement

This proposal is based on the suggestion that calcium moves through an electrochemical gradient established by the movement of some other ion.[24] In molluscs, the shell side of the mantle is thought to be positively charged relative to the blood; a potential of this kind would tend to move calcium away from the extrapallial fluid. Such a potential could be produced by the movement of an anion such as chloride into the animal.

The Semiconductor Theory

This hypothesis, proposed by Digby,[25] suggests that ions are continually diffusing out of the animal across the mantle, extrapallial fluid, and shell. Various ions diffuse at different rates, resulting in a potential gradient where the outer surface is relatively positive. The shell behaves as a semiconductor by creating a flow of electrons from the inner surface rich in hydroxyl ions towards the outer surface abundant in protons. The semiconductor properties of the exoskeletons are due mainly to the periostraca of the animals. Using Mytilus edulis as an example, Digby has

proposed that the periostracum is polarized, being acidic outside and alkaline inside. Formation of carbonate ions would be favored in the inner surface, facilitating deposition of $CaCO_3$ crystals as is suggested by a pH of 9.4 in the extrapallial fluid near the shell edge of M. edulis.[20] In addition, model experiments in which seawater was forced through the periostracum produced the potential gradient and pH changes as predicted by the hypothesis.

In order to resolve the question of the mechanism of mineral deposition, a complete characterization of the extrapallial fluid in molluscs is essential. While the importance of the extrapallial fluid has been emphasized by many,[2-7] most investigations of biomineralization processes in molluscs have concentrated on the mantle and shell, omitting consideration of this fluid. The next section presents a description of the fluid known before this work began.

Description and Composition of the Extrapallial Fluid of Molluscs

The organic and inorganic constituents of skeletal material precipitate and polymerize from the extrapallial fluid. The fluid composition determines the chemical nature and microscopic pattern of the organic matrix and periostracum, the rate and character of crystal growth, and the polymorphic type of $CaCO_3$ crystals.[20]

In some molluscs such as Chlamys nipponensis, the fluid is directly exposed to the external medium, whereas in other species such as Mytilus edulis, it is not. Regardless, the

fluid differs in composition from the external medium.[16,26]

Knowledge of the composition of the fluid is limited due to various difficulties in sampling. The volume obtainable from a specimen may vary from microliter amounts (Crassostrea virginica) to several milliliters (Anodonta lavta, Modiolus demissus). All analyses of the fluid are confronted with the problem of changing composition due to (1) varying rates of secretion by the mantle and (2) decreasing amounts of constituents during the biomineralization process.[20] The fluid is a complex mixture of proteins, mucopolysaccharides, glycoproteins, amino acids, peptides, organic acids and inorganic ions. Figure 1.3 presents a general outline of the known make-up prior to this dissertation.

In 1930,[27] deWaele provided the first analysis on the fluid. In his study the following ions were found to be present: sodium, potassium, calcium, magnesium, manganese, chloride, sulfate, and phosphate. The molluscan fluid was thought to be equivalent to the blood of the animal, with similar proportions of constituents present. However, later studies indicated that the two fluids were distinct.[16,28]

The presence of mucopolysaccharides in the fluid has been shown directly for several species by electrophoresis[29] and indirectly by histochemical tests in the organic matrix of the shell.[30,31] Proteins of various species have also been examined qualitatively by electrophoretic techniques.[29,32] Of several species examined, those with strictly a calcitic shell had a single fraction, while species with an aragonitic

COMPOSITION OF EXTRAPALLIAL FLUID

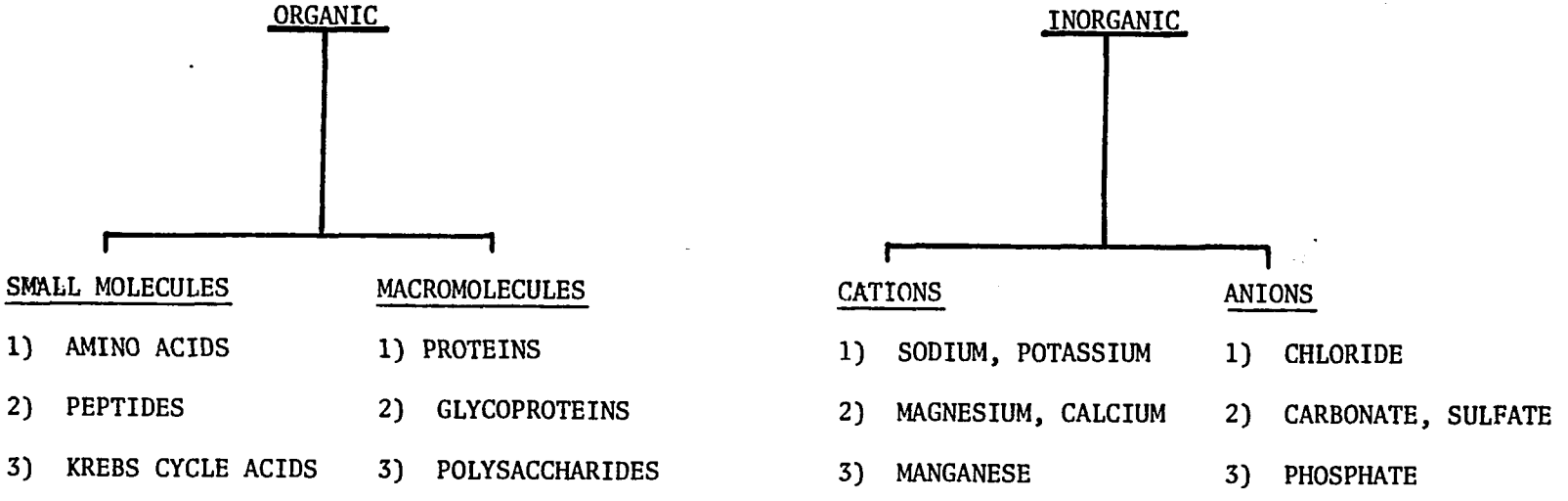

Figure 1.3. Outline of the known make-up of the extrapallial fluid of various molluscs before this study was undertaken.

shell or a shell of both aragonite and calcite has three or more protein components. The number of protein fractions also corresponded to that in the blood of the animals. This difference in number of proteins in calcitic and aragonitic species implicated a relationship between protein and crystal form.

In addition to polymeric organic constituents, Crenshaw[33] has detected succinic and lactic acid in the fluid of the mollusc, Mercenaria mercenaria. Results of this study indicated that these acids, produced by metabolism of the animal, may be instrumental in the regulation of skeletal material formation. A proposed reaction scheme is shown in Figure 1.4.

In another finding, Crenshaw[16] found differences between the fluid and external medium in that all major cations and total carbon dioxide were higher in the extrapallial fluid. The concentrations of the principal cations and some anions in the fluid and seawater are given in Table 1.2. The Donnan ratios of the cations between extrapallial fluid and environmental water were similar within a species and fell between 1.03 and 1.05 except for ionic calcium, which was 1.15. The bound calcium appeared to occur as a calcium-protein complex in both the extrapallial fluid and shell of the animals.[16,34]

The extrapallial fluid and organic matrix of the shell are both derived from the mantle and are in intimate contact with each other.[20] However, their amino acid composition is

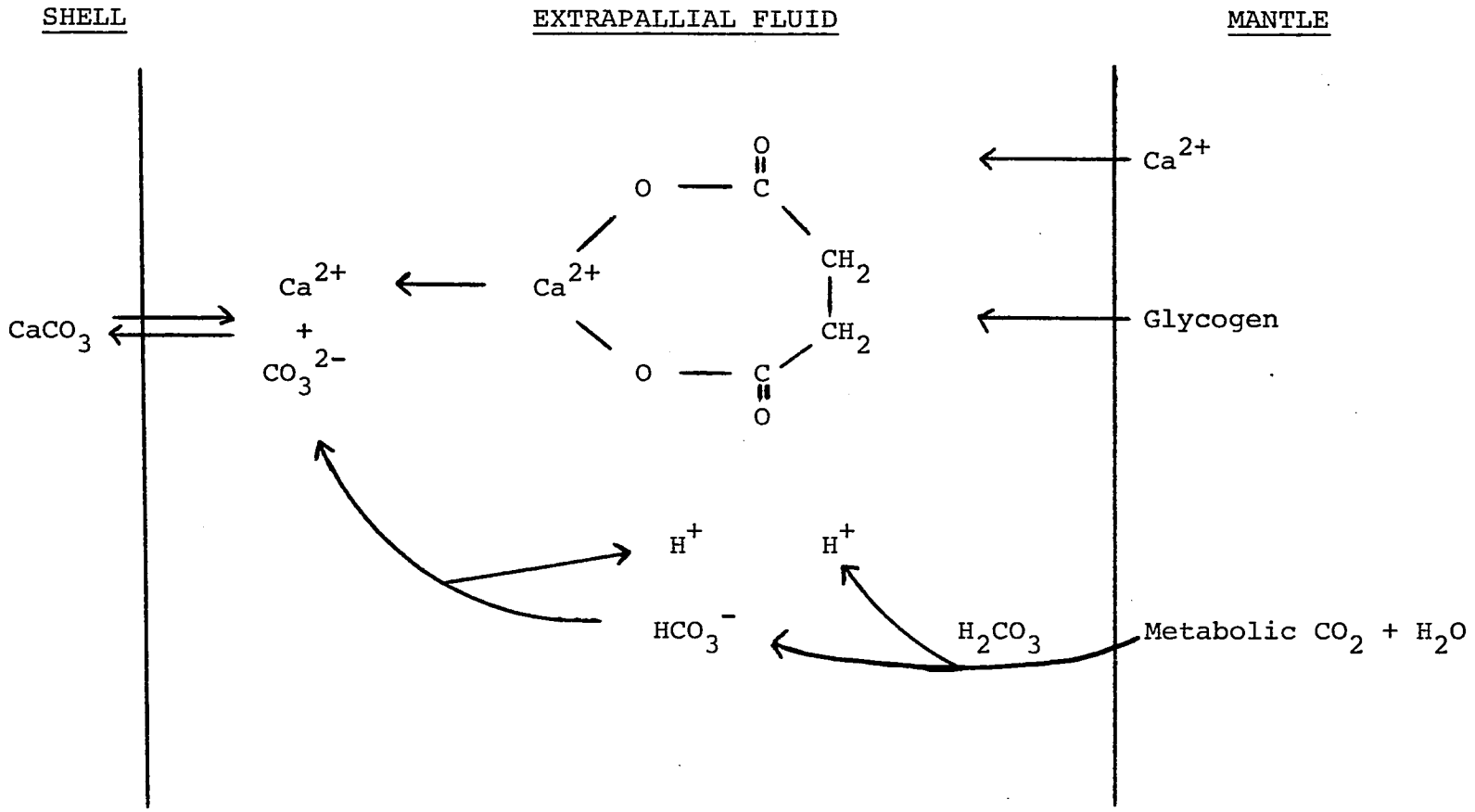

Figure 1.4. Proposed involvement of succinic acid in the calcification process.
(Adapted from Reference 33)

Table 1.2

Inorganic Composition of Extrapallial Fluids[1]

(Adapted from Ref. 19)

	Na (mN)	K (mN)	Ca (mN)	Mg (mN)	Cl (mN)	SO_4 (mN)	CO_2 (mM)
Mercenaria mercenaria	444±9	9.6±0.8	23.6±2.0	120±10	472±8	46.1±5.1	5.2±1.9
Crassostrea virginica	441±9	9.4±0.5	21.5±1.7	114±6	480±9	48.3±2.3	5.0±0.8
Mytilus edulis	442±10	9.5±0.5	21.3±1.2	116±6	477±8	47.3±2.3	4.2±0.5
Seawater	427±9	9.0±0.1	18.5±0.4	106±5	496±6	51.1±2.6	2.5±0.1

[1]Numbers exhibit means and standard deviations. mN = millinormal; mM = millimolar.

different, as shown in analyses of several species of molluscs.[35-37] This implies that the mechanism by which protein material is deposited on the inner shell surface is a selective process.

The extrapallial fluid is a mixed solution of electrolytes and contains proteins and mucopolysaccharides. In such a solution, the interaction between calcium ions with proteins, mucopolysaccharides, and small molecules (metabolic and amino acids) appears instrumental in controlling $CaCO_3$ deposition. Since the chemical composition of organic species has not been determined, it is my belief that characterizing the organic fluid components completely would provide new insights into the process.

Chapter 2

Overview of Investigations

Molluscan biomineralization is primarily the deposition of structural $CaCO_3$, which is intimately related to metabolism of the animals. Theories for calcification in molluscs were reviewed in Chapter 1. A reexamination of molluscan extrapallial fluid with biophysical techniques can contribute significantly towards the development of a comprehensive theory of calcification.

It is appropriate to pose questions that would be answered by such a study.

1. What relationships exist between the composition of the fluid and shell structure?

2. How is calcium distributed in the fluid?

3. What controls the mechanism of $CaCO_3$ calcification?

4. Does the calcification mechanism have a role in incorporating other metals into the shell?

5. What is the relative importance of organic components in this process?

Studies were directed in four basic areas, each of which are developed as separate chapters in this dissertation. The final chapter provides a base for future investigations.

A Chemical and Spectral Characterization of the Extrapallial Fluid of M. edulis

Studies were done with Mytilus edulis, the edible blue mussel, since it is commonly found along the New Hampshire coast and is readily accessible. The structure (Figure 2.1) of the shell has been studied in detail.[39,40] It is composed of three layers. The outer layer (periostracum) has been recently examined.[41] The blue crystalline layer just beneath the periostracum is the prismatic region and contains anvil-like prisms of calcite. The inner layer (nacre) consists of aragonite crystals packed in horizontal rows. Individual crystals in the latter two layers are surrounded by the organic matrix. An important part of the study focused on the relationship of the fluid to the composition and structure of the shell.

A survey of the organic constituents by electrophoretic and colorimetric techniques show the organic portion of the fluid to consist of several proteins, polysaccharides, and amino acids. Optical emission spectroscopy reveals the presence of many metals, of which some, including calcium, are selectively associated with macromolecular components of the fluid.

The distribution of calcium in the fluid is determined using ion specific electrodes, atomic absorption spectroscopy and dialysis procedures. The dependence of calcium binding on the conformation of protein constituents is demonstrated by employing ion specific electrodes.

Electron paramagnetic resonance (EPR) studies indicate

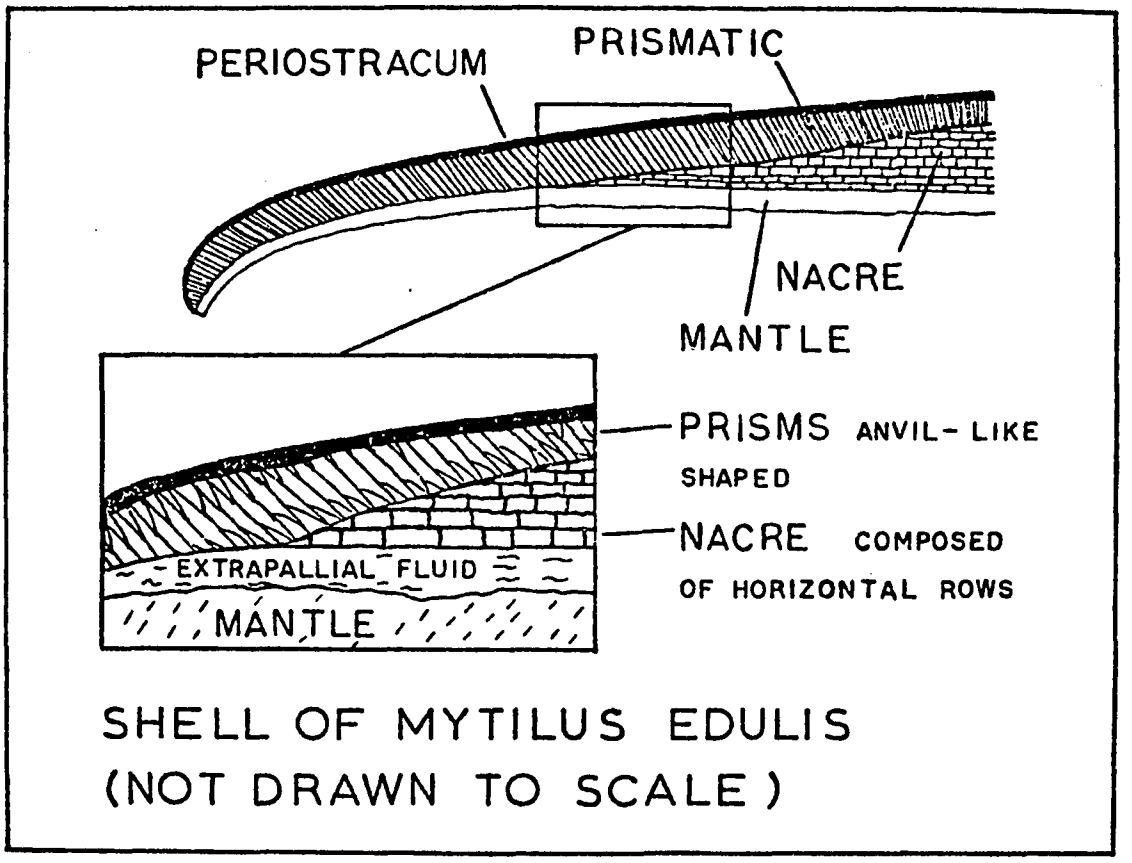

Figure 2.1. Sketch of the shell structure, extrapallial fluid, and mantle for Mytilus edulis.

the various oxidation states and chemical environments of trace paramagnetic transition metal ions. EPR studies utilizing divalent manganese establish the chelating capacity and apparent pK's of the chelating ligands. The detailed results of these studies are presented in Chapter 3.

Separation of Protein Components of the Fluid

Preliminary experiments with disc gel electrophoresis revealed the presence of several protein constituents in the fluid. Further separation would permit the determination by other techniques of structure, identity, and finally function of particular proteins.

Column chromatography has proved to be invaluable in the separation and purification of complex biological mixtures. Literally thousands of articles have been published which describe the use of column chromatography in the separation of proteins. When working with complex mixtures, e.g., physiological fluids, substances cannot be fractionated in a single operation, and often several steps are needed to isolate particular species.

The separation scheme shown in Figure 2.2 is applicable to our mixture. Centrifugation and dialysis techniques are performed on the native fluid to reduce the amounts of material to quantities more suitable for chromatography, and to also remove gross contaminants. Gel filtration chromatography, which separates molecules on the basis of size, allows estimation of molecular weight and reduces the number

SCHEMATIC REPRESENTATION OF MAIN OBJECTIVES

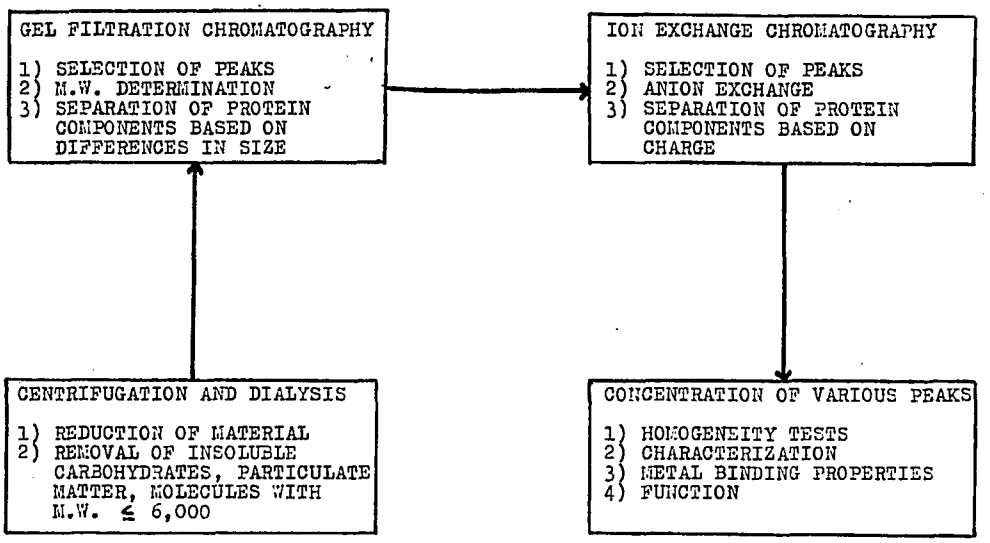

Figure 2.2. Schematic representation for the separation of fluid proteins.

of components to be subsequently separated by ion exchange chromatography.

The fractions were concentrated by ultrafiltration. Various fractions were then tested for homogeneity, structurally characterized and evaluated with respect to functionality in later studies.

The protein components in the fluid were separated into two distinct fractions by gel filtration chromatography. The apparent molecular weights of each fraction were then estimated.

By anion exchange chromatography, several proteins were found in the fluid. Two primary components, a glycoprotein (1A) and an enzyme (1B) were studied in some detail. The results of the chromatographic separation of protein components are presented in Chapter 4.

Partial Characterization, Metal Binding Properties and Proposed Function of a Glycoprotein (1A)

Proteins are thought to play an important part in molluscan calcification processes. Initiation of crystal formation, calcium transport and storage, and regulation have all been mentioned as possible roles. Nearly all previous studies have concentrated on the isolation of proteins in the shell. Crenshaw[42] isolated a glycoprotein from Mercenaria mercenaria that specifically binds calcium by ester sulfate groups. Krampitz et al.[43] also isolated a calcium binding protein from the shell protein of the snail Nassa reticulata. This protein has a high content of aspartic and glutamic acid

residues and is believed to play a role in initiating mineralization. The molecular weight and amino acid composition of Krampitz's protein differs from the protein described by Crenshaw.[43]

Weiner and Hood[44] have studied a variety of shell proteins and found a significant portion of them to be composed of aspartic acid (15-45 mole percent) using mild hydrolysis techniques, which cleave proteins on both sides of this residue. Significant quantities of glycine and serine are released. These results indicate protein chain sequences to be of the type $(Asp\text{-}Y)_n$, in which Asp is aspartic acid and Y is predominantly serine or glycine. Weiner and Hood hypothesized that the negative charge on carboxyl groups of aspartic acid could bind calcium and, in effect, serve as a template for $CaCO_3$ formation and growth.

Although proteins in the fluid have been detected,[16, 29,32] experimenters have not attempted to isolate, characterize, and relate them to molluscan calcification. Peak 1A, identified as a glycoprotein, was isolated through methods described in Chapter 4. The protein is demonstrated to be homogeneous with respect to charged isomers by disc gel electrophoresis at three different gel concentrations. Subsequent studies[45] show that the specie contains two identical subunits and is acidic ($pI < 5.0$). The amino acid analysis and carbohydrate content are determined. Optical emission spectroscopy shows the presence of calcium, sodium, and magnesium bound to this fraction. The stoichiometry of

calcium and magnesium are determined by atomic absorption spectroscopy. Metal binding studies with Mn^{2+}, Ca^{2+}, and Mg^{2+} are performed using a variety of techniques (EPR, Ultrafiltration, Flow Dialysis). A function for this glycoprotein is proposed on the basis of these measurements. Results of the experiments are detailed in Chapter 5.

Detection, Partial Characterization, and Preliminary Examination of Phenoloxidase (1B)

Two enzymes are almost invariably associated with calcification of molluscs. The first is carbonic anhydrase, which catalyzes the hydration of carbon dioxide and is known to exist in "high activity" and "low activity" forms.[46] Secondly, there are general phosphatases which also exist in various isoenzyme forms.[47] The suggested function of this enzyme has varied from synthesizing matrix material[48,49] to removing crystal poisons.[50]

In addition, phenoloxidases appear to be associated with the calcification process. This enzyme catalyzes the dehydrogenation of catecholic compounds to form quinones, which crosslink proteins in an undetermined manner. Presumably, the enzyme aids in the formation of periostraca which is composed of quinone-tanned protein.

The periostracum might be the most important part of molluscan exoskeletons. Since this layer is formed before all other portions of the exoskeleton, it must polymerize rapidly to resist solubilization.[51] The reactivity of quinones as crosslinking agents is considered fundamental to the

inertness and durability of this layer.

The enzyme has recently been extracted from the mantle and periostracum of the mollusc, Modiolus demissus.[51] In Chapter 6, the isolation and detection of a phenoloxidase from the extrapallial fluid of Mytilus is discussed. The electrophoretic properties, specific activity, amino acid content, and metal association are reported.

Future Studies

This chapter will present suggestions for future work in this area. In outline form, several biomineralization studies are given below:

Current and Future Studies

I. Protein Components
   - A. Isolation and characterization
   - B. Enzymatic activity
   - C. Metal binding studies - Lanthanide probes
   - D. Function

II. Carbohydrate Components
   - A. Structure and function

III. Dialyzable Material
   - A. Presence of peptides, sugars, organic acids
   - B. Inorganic composition
   - C. Metal binding studies - Chelating capacity

Each of the general headings could be developed as separate projects. A description of specific experiments will be given in Chapter 7.

Chapter 3

A Spectral and Chemical Characterization of the Fluid

As part of the overall scheme in studying the calcification process, the work in this chapter represents an examination into the macro-properties of the fluid. In this chapter, the chemical and spectral characteristics of the fluid are reported.

Experimental Procedures

Sampling. The extrapallial fluid used in this work was obtained from samples of Mytilus edulis periodically from June, 1975 to October, 1978. All animals were collected at low tide near Seabrook, New Hampshire. After opening the valves with a scalpel, a syringe was inserted between the mantle and nacre of each animal, being careful that the tip of the needle was in contact with the inner surface of the shell. The fluid was then withdrawn by gentle suction, yielding approximately 300 µl of fluid per animal. The pH of the pooled fluid was taken immediately and normally ranged from 7.2 to 7.4, in agreement with values reported previously.[16] The fluid was stored in a polypropylene container at 4°C with several drops of toluene added to prevent bacterial growth. Fluid samples were normally used within two weeks.

Isolation and characterization of insoluble and

and soluble fractions. The extrapallial fluid was centrifuged for 30 minutes at 8,000 x g to remove various particulate matter. A portion of the supernatant was passed through an Amicon ultrafiltration apparatus fitted with PM-10 (MW cutoff 10,000) membrane under nitrogen pressure. The ultrafiltrate was analyzed for amino acid content. The remainder of the supernatant was dialyzed against a 300-fold volume excess of 50 mM Tris-HCl buffer at pH 7.5 for 48 hours at room temperature, using Spectrapor membrane tubing (MW cutoff 6,000 - 8,000). The precipitate which had formed during the dialysis was then centrifuged at 10,000 x g for 30 minutes and labeled the insoluble fraction. The resultant supernatant was labeled the centrifuged-dialyzed fluid.

Carbohydrate, elemental and amino acid analyses. The carbohydrate content of the native fluid, insoluble fraction, and the centrifuged-dialyzed fluid was determined using the anthrone reaction.[52] The method was calibrated using standard glucose samples. Spectral measurements were carried out with a Bausch and Lomb Spectronic 710 spectrophotometer using 5 cm quartz cells and a wavelength of 620 nm. The carbon, hydrogen, and nitrogen analyses were performed on an F and M Model 185 CHN analyzer. Samples for the amino acid analyses were hydrolyzed with constant boiling 6M HCl under reduced pressure in sealed tubes at 105° for 24 hours. The amino acid contents of the hydrolysates were determined on a Beckman 120C analyzer by the method of Guire et al.[53]

Electrophoresis. The disc gel electrophoretic system, described by Hedrick and Smith,[54] employing a Tris-HCl buffering system, was utilized to estimate the distribution pattern and number of protein bands of native fluid, centrifuged-dialyzed fluid and ultrafiltrate. Electrophoresis proceded toward the positive electrode with Bromphenol blue as the leading tracker. Gels were stained with 0.5% Napthol blue to visualize protein components. Gel concentrations were 7%, sample sizes were normally 150 µg, and the pH was 9.5. A Beckman Acta CIII double beam spectrophotometer with gel scanner adapter was used to scan the Napthol blue stained gels at 600 nm.

Metal analyses. EPR spectra of VO^{2+}, Mn^{2+}, Fe^{3+}, and Cu^{2+} were measured on a Varian E-4 spectrometer operating at X-band frequency (9.2 GHz), and 100 KHz magnetic field modulation. A Varian Techtron Model AA-3 spectrometer modified with AA-5 electronics was used for atomic absorption analyses of calcium. The wavelength and slit width employed was 422.67 nm (100 µ). A Type AB-51 burner was used with an air-acetylene flame. All samples except the centrifuged-dialyzed fluid were diluted 100-fold in 1.2N HCl and made 1.25% in lanthanum to suppress matrix effects prior to analysis. Standards were prepared similarly. A Baird Associates Eagle Mount grating spectrograph was used for optical emission work. To remove organic matter, all samples were ashed prior to analysis in a graphite electrode crater at 550°C.

Calcium electrode. Calcium measurements were made on various fluids during the calcium titrations with an Orion model 710 recording electrometer fitted with an Orion model 92-20 calcium ion electrode and a Corning saturated calomel reference electrode. Solutions were made to 0.1M KCl for the titrations of the centrifuged-dialyzed fluid with urea. The supporting electrolyte for the standards used for all other Ca^{2+} ion determinations by selective electrode was .05M NaCl, .001M KCl, and .005M $MgCl_2$. Samples were adjusted to the appropriate pH with .01M HCl or NaOH. The calcium electrode was standardized just prior to and immediately after each titration and sample measurement.

Materials. Stock solutions of vanadyl sulfate $VOSO_4 \cdot 5H_2O$ (Fischer Scientific) 2×10^{-2}M, were standardized spectrophotometrically using $\varepsilon = 18.0$ $cm^{-1}M^{-1}$ at 750 nm.[55] Thiourea, glucose and anthrone were purchased from Sigma Chemical Company and used without further purification. All other chemicals were the best commercially available.

Results

Characterization of components--native fluid profile. The profile of protein components in dialyzed extrapallial fluid was estimated using polyacrylamide disc gel electrophoresis. The results are shown in Figure 3.1. At least five protein components are present in the dialyzed fluid. The amino acid compositions of the native fluid, periostracum, and total shell matrix, less periostracum are listed in Table 3.1. A 1 mg sample of lyophilized dialyzed fluid was

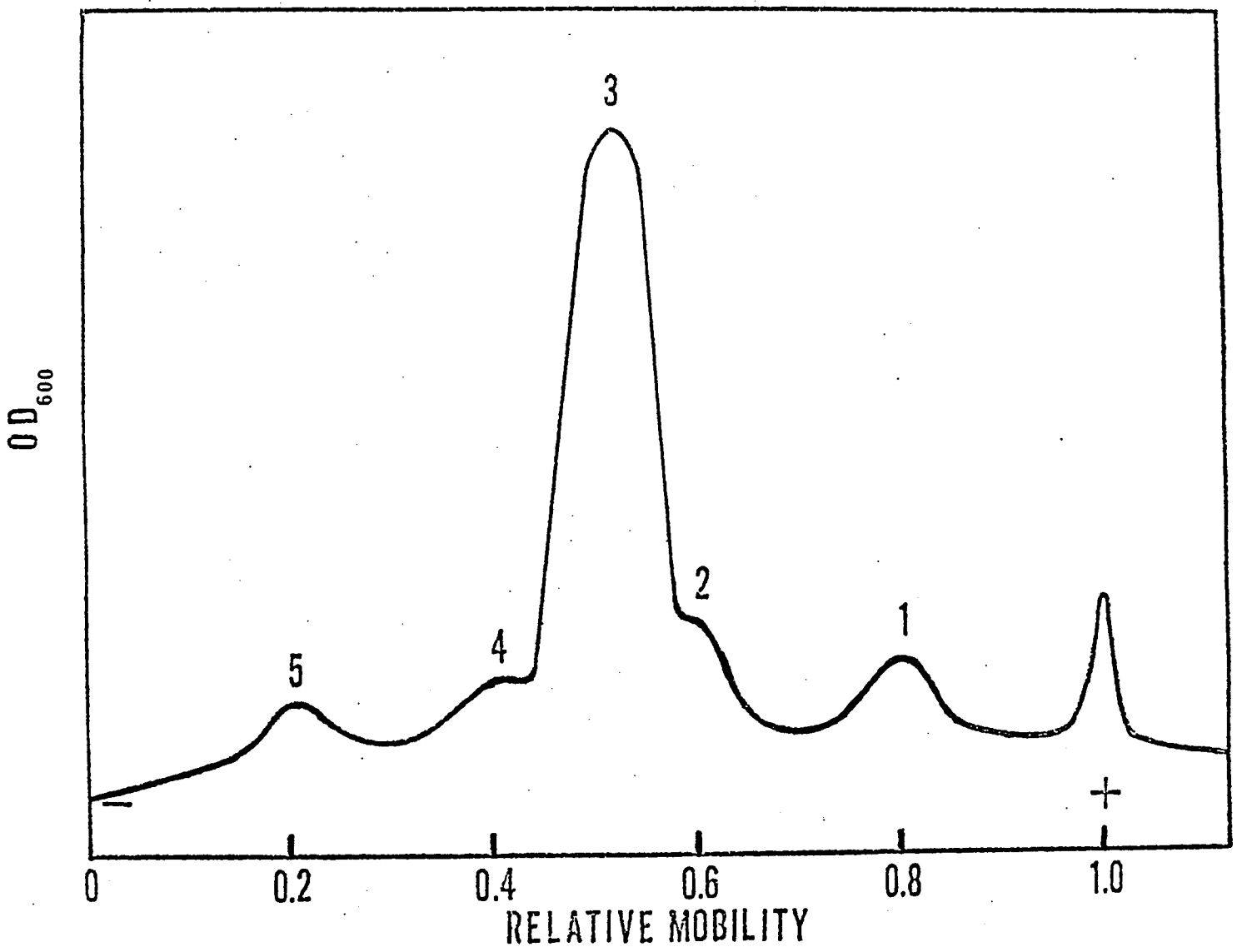

Figure 3.1. Profile of protein components in the fluid by disc gel electrophoresis.

Table 3.1

Amino Acid Analysis of Native Extrapallial Fluid, Centrifuged-Dialyzed Fluid, Ultrafiltrate, Periostracum, and Decalcified Shell Matrix, Less Periostracum of *M. edulis*

(Amino Acid Residues per 1000 total)*

	Native fluid	Centrifuged-dialyzed fluid	Ultrafiltrate	Periostracum†	Shell matrix†† less perio.
Lysine	42	53	42	15	19
Histidine	8	10	7	12	5
Arginine	26	30	16	46	25
Aspartic acid	72	127	17	52	118
Serine	64	101	11	15	98
Threonine	41	62	9	19	17
Glutamic acid	91	123	31	60	41
Proline	5	9	---	24	15
Glycine	316	104	592	510	291
Alanine	121	72	178	38	216

Table 3.1 - Continued

	Native fluid	Centrifuged-dialyzed fluid	Ultrafiltrate	Periostracum[†]	Shell matrix less perio.[††]
Cystine	2	5	---	43	11
Valine	48	74	15	16	29
Methionine	12	18	3	27	6
Isoleucine	44	67	5	2	18
Leucine	51	66	39	3	48
Tyrosine	27	33	14	97	20
Phenylalanine	30	46	21	21	17

[*]To convert from Residues total to molar concentration, use the equation:

Residue/1000 x $[\text{Amino acid}]_{total}$ = [Amino acid], where

$[\text{Amino acid}]_{total}$(Ultrafiltrate) = 9.02×10^{-5}M

$[\text{Amino acid}]_{total}$(Centrifuged-dialyzed) = 11.0×10^{-5}M

$[\text{Amino acid}]_{total}$(Native fluid) = 20.1×10^{-5}M

[†]Reference 56

[††]Reference 57

found to be 40% carbohydrate by weight expressed as hexose by the anthrone reaction.

Ultrafiltrate. The amino acid analysis is presented in Table 3.1. Ensuing qualitative tests to detect the presence of small protein or peptide moieties which could pass through the PM-10 ultrafiltration membrane were negative. No bands could be observed with disc gel electrophoresis experiments. Moreover, attempts to precipitate out protein species with trichloroacetic acid were unsuccessful, and the characteristic purple color normally observed for proteins or peptides, was not produced by the biuret reaction.[58] These results suggest that a significant fraction of the amino acids in the ultrafiltrate exist in their free form.

Centrifuged-dialyzed fluid. Disc gel electrophoresis of the centrifuged-dialyzed fluid exhibited identical gels to that of the dialyzed fluid. The carbohydrate content was found to be 15% by weight. The amino acid analysis is presented in Table 3.1.

Insoluble fraction. A 1 mg sample of the insoluble fraction was determined by the anthrone reaction to be 95% carbohydrate. The elemental analysis C-29.30%, H-4.01%, N-6.26% is likewise consistent with carbohydrate material. These compare favorably with values reported for sulfated glucosamine polymers, common in various invertebrates:[59] C-30%, H-3.9% and N-6.0%. The presence of sulfate was confirmed by the appearance of a $BaSO_4$ precipitate when $BaCl_2$ was added to a hot solution of the fraction that had been

digested in 6N HNO_3. No further work was done on this fraction.

Metal content and association. Qualitative optical emission spectroscopy of the native fluid evaporate indicates the presence of large amounts of Na, Mg, Ca, and K and trace quantities of Cu, Fe, Mn, Al, Cr, Pb, Ti, Ag, Sn, Sr, and Ba. The centrifuged-dialyzed fluid evaporate shows the presence of significant amounts of Na, Mg, Ca, Fe, and Cu, which must be associated with the macromolecular components of the fluid. The results are summarized in Figure 3.2.

Atomic absorption spectroscopy was used to determine the distribution of calcium in the fluid. The value of 9.8 ± 0.4mM for the native fluid based on five different samples is in good agreement with the results previously reported.[16,20] Dialysis reduces the calcium value to 0.90 ± 0.04 mM, indicating that approximately 90% of the calcium in extrapallial fluid is not strongly associated with macromolecular components. Centrifugation of the dialyzed fluid further reduces the calcium level to 0.087 ± 0.004mM based on 10 samples. This result demonstrates that approximately 10% of the calcium in the native fluid is strongly associated with the precipitating carbohydrate component. Less than 1% of the calcium originally present in the native fluid remains associated with the soluble macromolecular components after centrifugation and dialysis. This calcium is termed tightly bound. Figure 3.3 outlines the relative distribution

METALS DETECTED IN EXTRAPALLIAL FLUID OF M. EDULIS - OPTICAL EMISSION SPECTROSCOPY

NATIVE FLUID

I A	II A	III A	TRANSITION METALS	IV A
Na	Mg	Al	Ti	Sn
K	Ca		Cr	Pb
	Sr		Mn	
	Ba		Fe	
			Cu	
			Ag	

CENTRIFUGED-DIALYZED FLUID

I A	II A	TRANSITION METALS
Na	Mg	Fe
	Ca	Cu

Figure 3.2. Summary of metals detected in the fluid with optical emission spectroscopy.

DISTRIBUTION OF CALCIUM IN EXTRAPALLIAL FLUID OF M. EDULIS

ATOMIC ABSORPTION SPECTROSCOPY

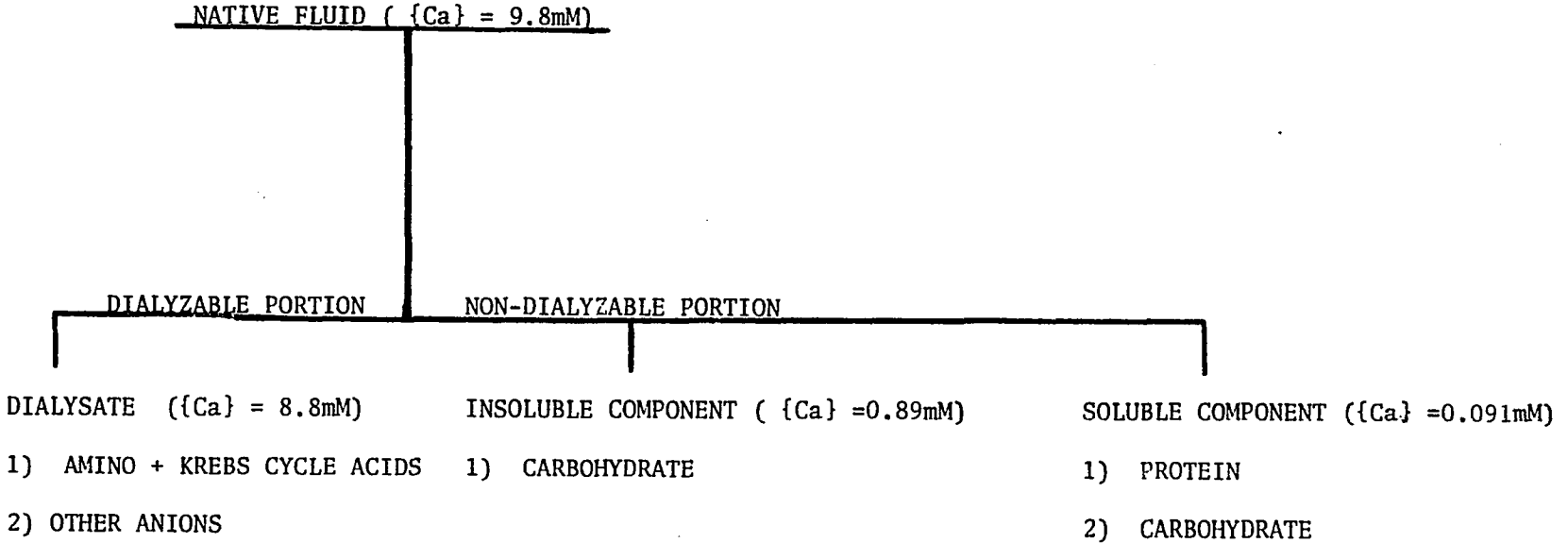

Figure 3.3. Relative distribution of calcium in the fluid.

of the metal in the fluid. Subsequent calcium ion electrode measurements on samples, diluted 10-fold with distilled-deionized water, of the native fluid, ultrafiltrate and sea water indicate that only 15% of the calcium exists in an unbound ionic form in the extrapallial fluid, while 92% of the calcium in diluted sea water is ionized (Figure 3.4). This demonstrates that the majority of calcium in the fluid is complexed to small chelates. Table 3.2 summarizes the distributions of calcium in the extrapallial fluid expressed as percentages.

EPR spectroscopy-trace metal speciation and binding of manganese by native fluid. Figure 3.5A shows the room-temperature solution EPR spectrum of the native fluid at pH 7.4. The 6-line first-derivative spectrum is characteristic of free Mn^{2+}, I = 5/2. In most instances only unchelated Mn^{2+} ions are observable in room-temperature solutions by EPR.[60] When 25 µl of 12N HCl is added to 500 µl of native fluid there is a reduction in pH to 1.2 and concomitant large increase in the $Mn(H_2O)_6^{2+}$ EPR signal intensity, indicating that much of the Mn^{2+} present in the fluid is complexed in some fashion. By comparison of the acidified fluid with that obtained from $MnCl_2$ solutions of known concentration, we estimate the total Mn^{2+} concentration in the fluid to be 9×10^{-6}M. Details of this type of analysis have been given elsewhere.[61]

Addition of 1 µl of 2×10^{-2}M $VOSO_4$ to a 500 µl sample of the native fluid results in a two-fold increase in the

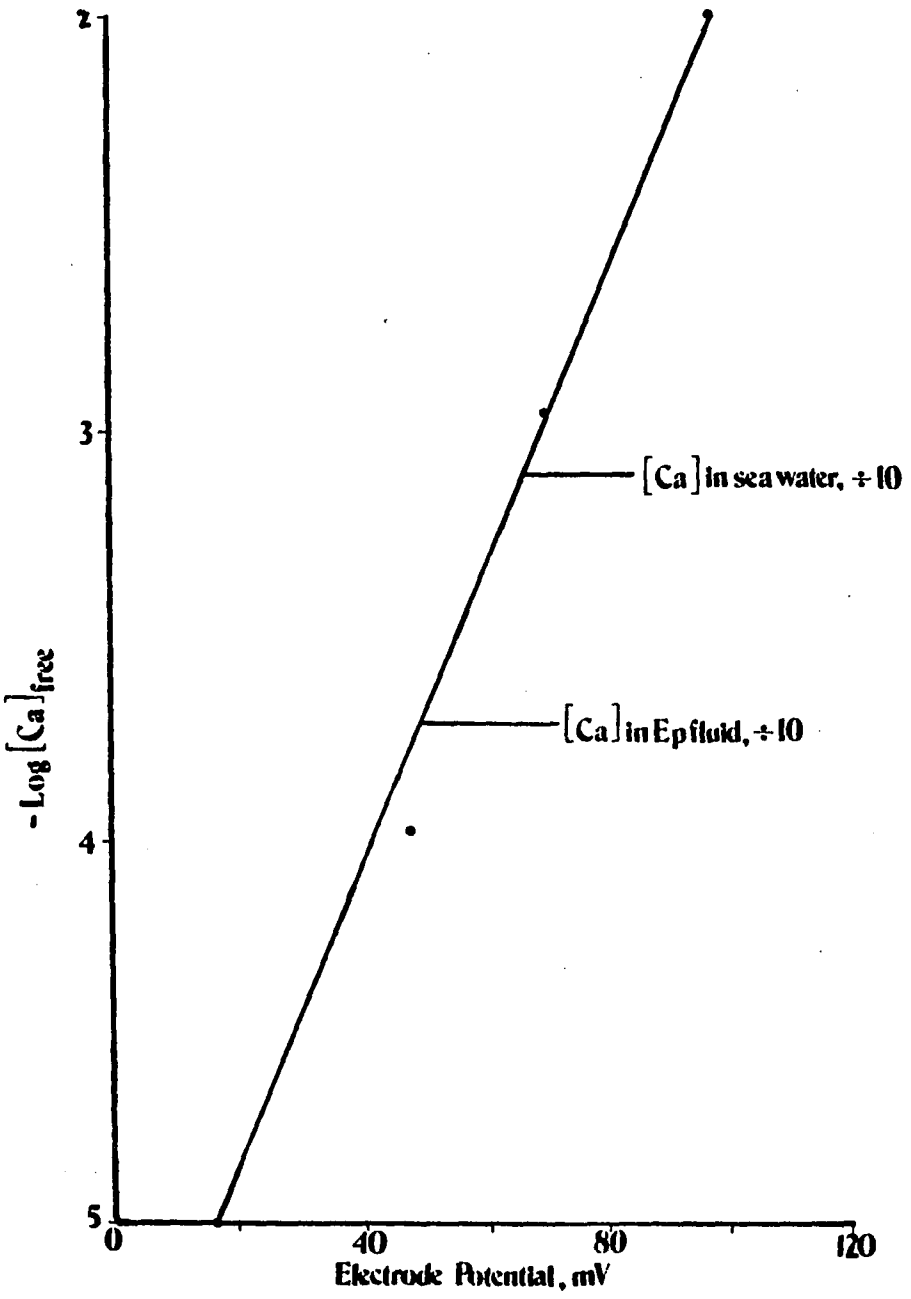

Figure 3.4. Determination of $[Ca^{2+}]_{free}$ in environmental water and fluid with calcium ion specific electrode.

Table 3.2

Calcium in Extrapallial Fluid of *M. edulis*

Calcium species	% Total
Free	15.3 ± 0.5
Bound to small chelates	74.3 ± 0.8
Bound to insoluble carbohydrate	9.2 ± 0.6
Bound to soluble macromolecular components	0.88 ± .04

Figure 3.5. (A) Room temperature X-band EPR spectrum of the native fluid, pH 7.4. (B) 500 µl of the native fluid with 1 µl of 2 x 10^{-2}M $VOSO_4$ added, pH 6.9.

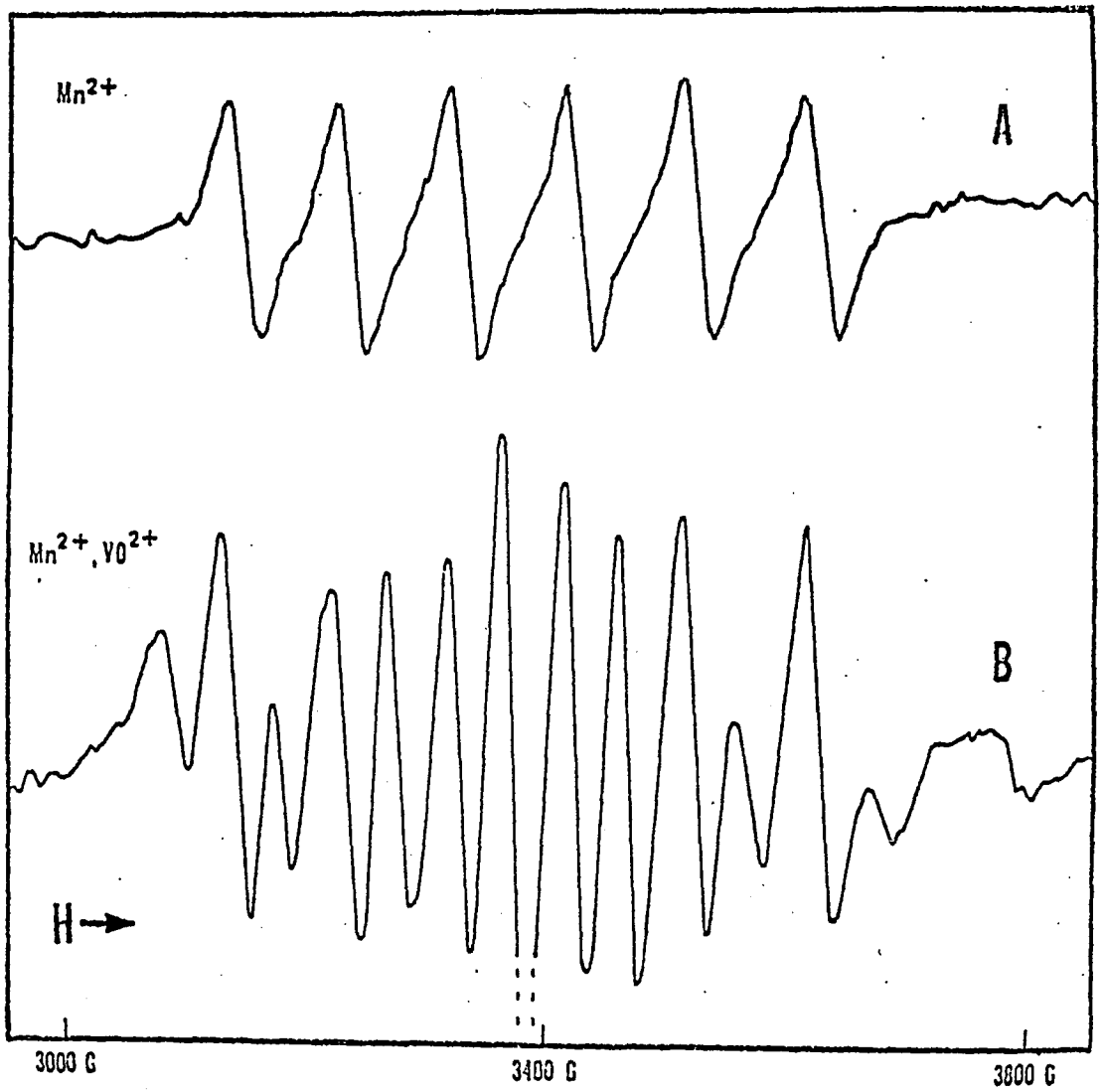
Mn^{2+}
A
Mn^{2+}, VO^{2+}
B
H→
3000 G
3400 G
3800 G

$Mn(H_2O)_6^{2+}$ signal intensity. (A small reduction in pH from 7.3 to 6.9 is observed but is not sufficient to account for the increase.) Eight additional lines appear in the EPR spectrum (Figure 3.5B) because of the presence of complexed VO^{2+} ion, I = 7/2. It is apparent that the VO^{2+} ion competes with the Mn^{2+} ion for some of the binding sites. The resulting isotropic VO^{2+} spectrum is typical of a VO^{2+} - small chelate specie.[62] Uncomplexed VO^{2+} exists as an EPR silent hydroxide species at pH 7.0.[63]

In order to further examine the manganese binding capabilities of the native fluid, a titration was performed. 1.0 ml of native extrapallial fluid was placed in an acid washed test tube. The pH = 7.4 was recorded, and the concentration of free manganese ion was measured by the intensity of its electron spin resonance spectrum compared to that of a series of solutions of known concentration. A predetermined amount of stock $MnCl_2$ dissolved in distilled-deionized water (2×10^{-3}M, pH = 5) was delivered to the fluid by microliter syringe such that the resultant concentrations covered the range of (1.4 to 11.9) $\times 10^{-5}$Mn total. After each successive addition, the pH was taken and the EPR spectrum of free manganese was monitored. In Figure 3.6, a plot of EPR signal height divided by the instrument gain vs. concentration of Mn^{2+} (original plus added) shows a break at 8×10^{-5}M, thus establishing the chelating capacity of the native fluid for Mn^{2+} as nominally 10^{-4}M.

The intensity of the solution spectrum of Mn^{2+} in

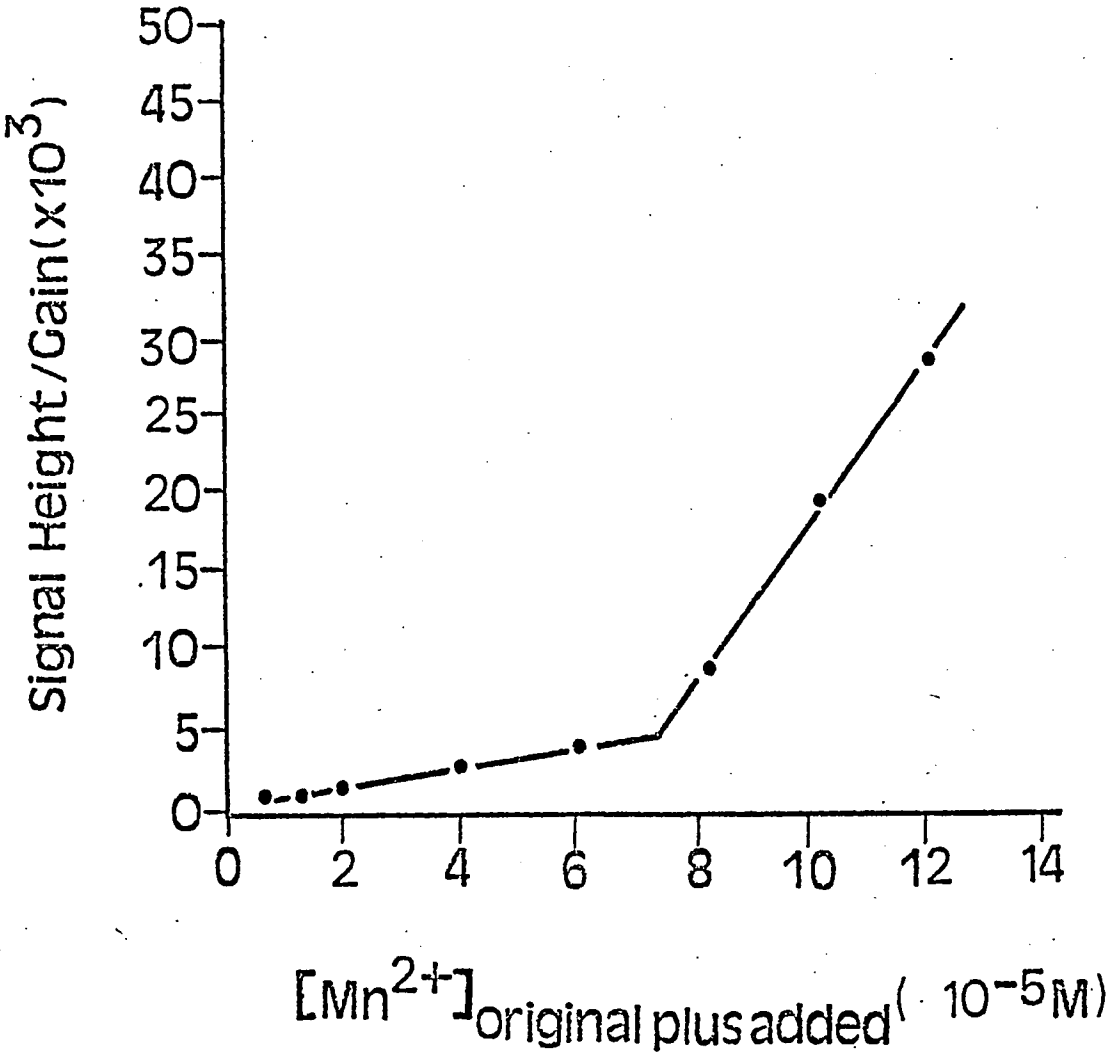

Figure 3.6. Plot of Mn^{2+} EPR signal height divided by the instrument gain vs. concentration of Mn^{2+} added.

the native fluid increases markedly as the pH is reduced by the addition of 12N HCl. The displacement of Mn^{2+} from its ligands by acid was monitored from pH 7.25 to 2.4. Approximately 10^{-4} equivalents of H^+ per liter were needed to obtain maximum signal intensity, in accord with a chelation capacity of $\sim 10^{-4}$M (Figure 3.7). This result indicates that only one functional group is ionized per Mn^{2+} ion found, i.e., a 1:1 complex is formed. The data were plotted in the form of a Henderson-Hasselbalch equation,

$$pH = pK_a' + \frac{1}{n} \log \frac{(base)}{(acid)} = pK_a' + \frac{1}{n} \log \frac{h_{max}-h}{h}$$

where h is the peak-to-peak height of the $Mn(H_2O)_6^{2+}$ EPR signal at a particular pH and h_{max} is the maximum signal height obtained in a completely acidified solution, pH = 2.4. n is the number of functional groups ionized per ligand bound to the metal. A linear regression yields n = 0.82 and pK' = 5.2 with a correlation coefficient of 0.96 (Figure 3.8).

A plot similar to that described by Scatchard et al.[64] was used to verify the chelation capacity and the stability constant, K, for the metal-ligand association. Bound Mn^{2+} for the plot was determined by the relationship $[Mn^{2+}]_{bound} = [Mn^{2+}]_{added} - [Mn^{2+}]_{free}$, where $[Mn^{2+}]_{free}$ is measured directly from the EPR intensity. If there is one class of sites then the data should obey the equation:

$$\frac{[Mn^{2+}]_{bound}}{[Mn^{2+}]_{free}} = -K\,[Mn^{2+}]_{bound} + n[L]_{total}$$

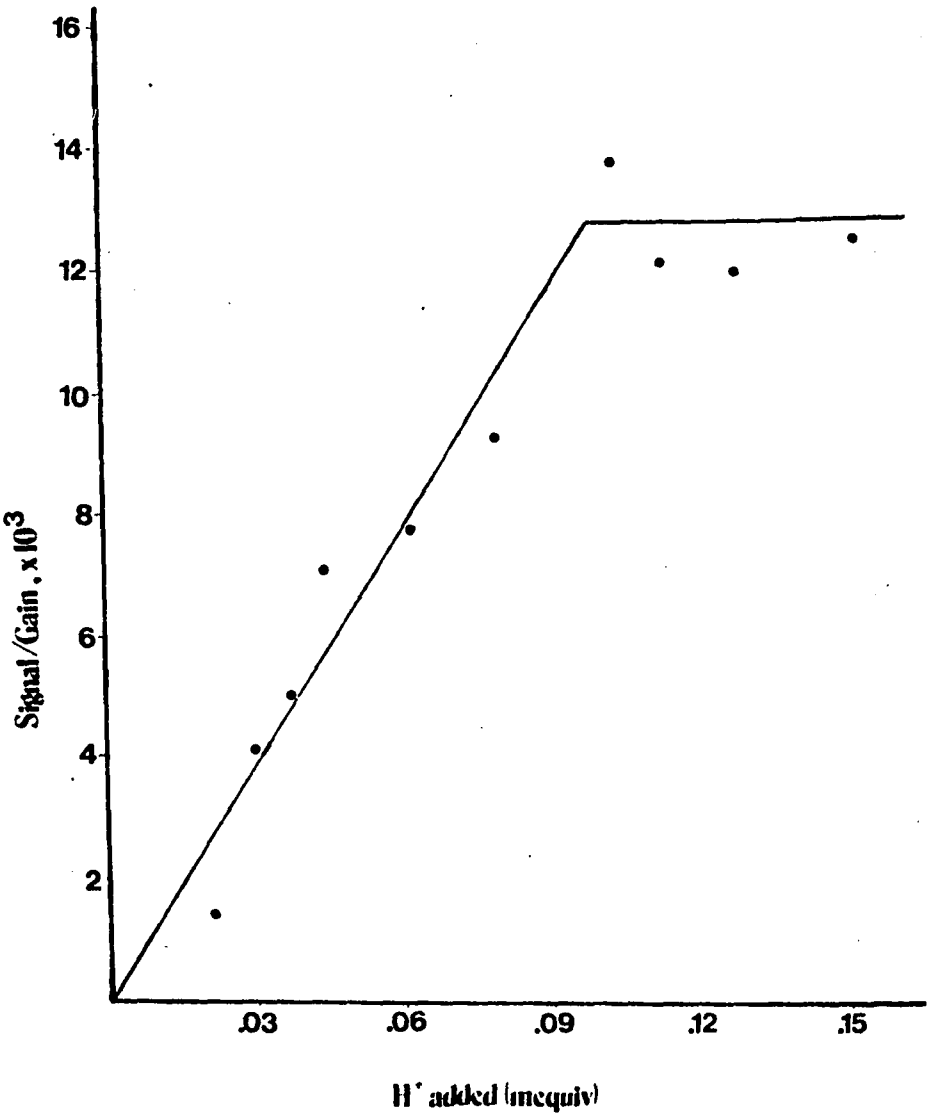

Figure 3.7. Plot of Mn^{2+} EPR signal intensity versus H^{+} added.

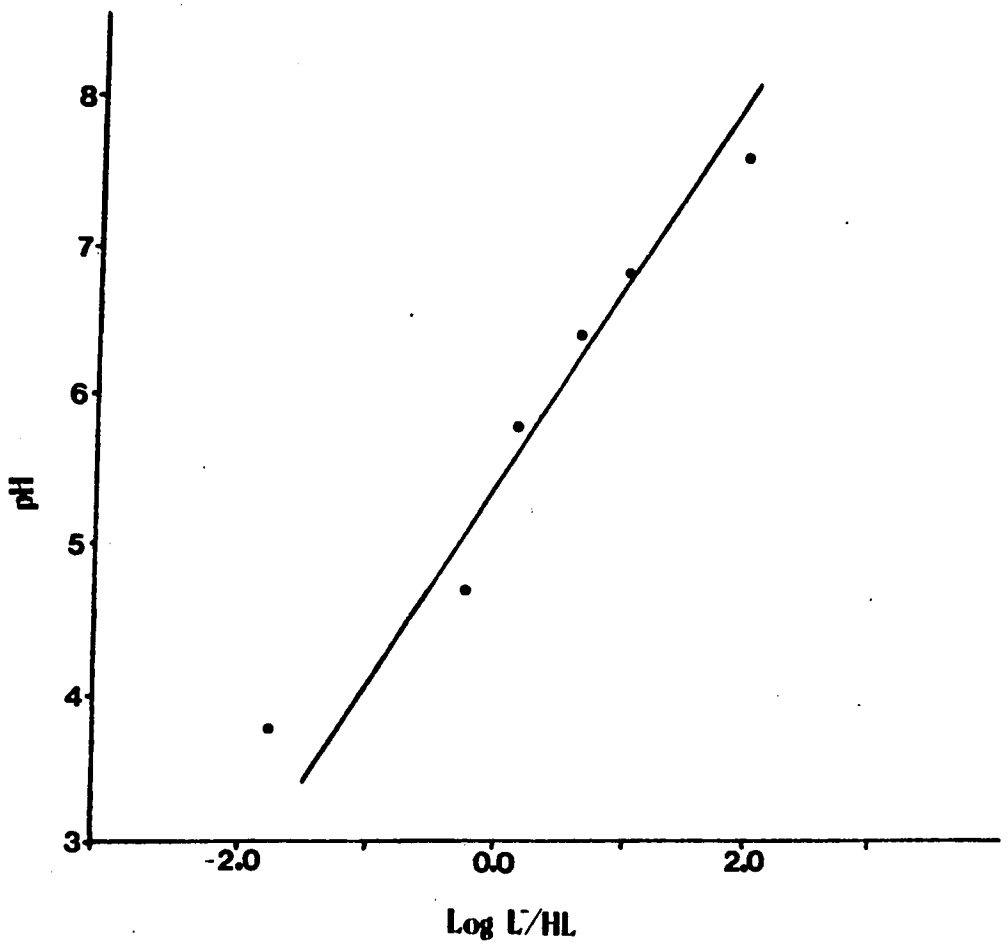

Figure 3.8. Plot of data obtained in Figure 3.7 in the form of a Henderson-Hasselbalch equation.

where n is the ligand to metal ratio in the complex and $[L]_{total}$ is the total concentration of ligand. In this case n = 1 (vide supra) and $[L]_{total}$ is therefore the chelation capacity. The data are plotted in Figure 3.9 from which we obtain $[L]_{total} = 9.0 \times 10^{-5}M$ and $K = 1.7 \times 10^{5}M^{-1}$.

Figure 3.10 shows the 77°K spectra of lyophilized native fluid and lyophilized centrifuged-dialyzed fluid. The native fluid exhibits a weak Fe resonance at g = 4.3 and a Mn^{2+} spectrum at g = 2.0 (Figure 3.10A). Centrifugation and dialysis of the fluid followed by lyophilization produces the spectrum obtained in Figure 3.10B. The strong resonance near g = 4.3 and the associated line at g = 9.5 are characteristic of high spin Fe^{3+} complexed in a low symmetry environment. These signals are frequently observed with non-heme iron proteins.[65] Note the absence of Mn signals in Figure 3.10B after dialysis indicating that the metal is associated with small chelates and/or weakly bound to macromolecules. The appearance of a signal in Figure 3.10B near the g = 2.2 region and the associated hyperfine splitting to slightly lower field show the presence of Cu^{2+}. The room-temperature solution spectrum is anisotropic, indicative of a copper-macromolecule complex.[66] The relatively sharp line at g = 2.0 suggests that possibly a radical species is present. This resonance may be related to those observed in the nacre and periostracum of the shell.[40]

Calcium binding by the centrifuted-dialyzed fluid. The influence of the protein denaturing agent urea on the

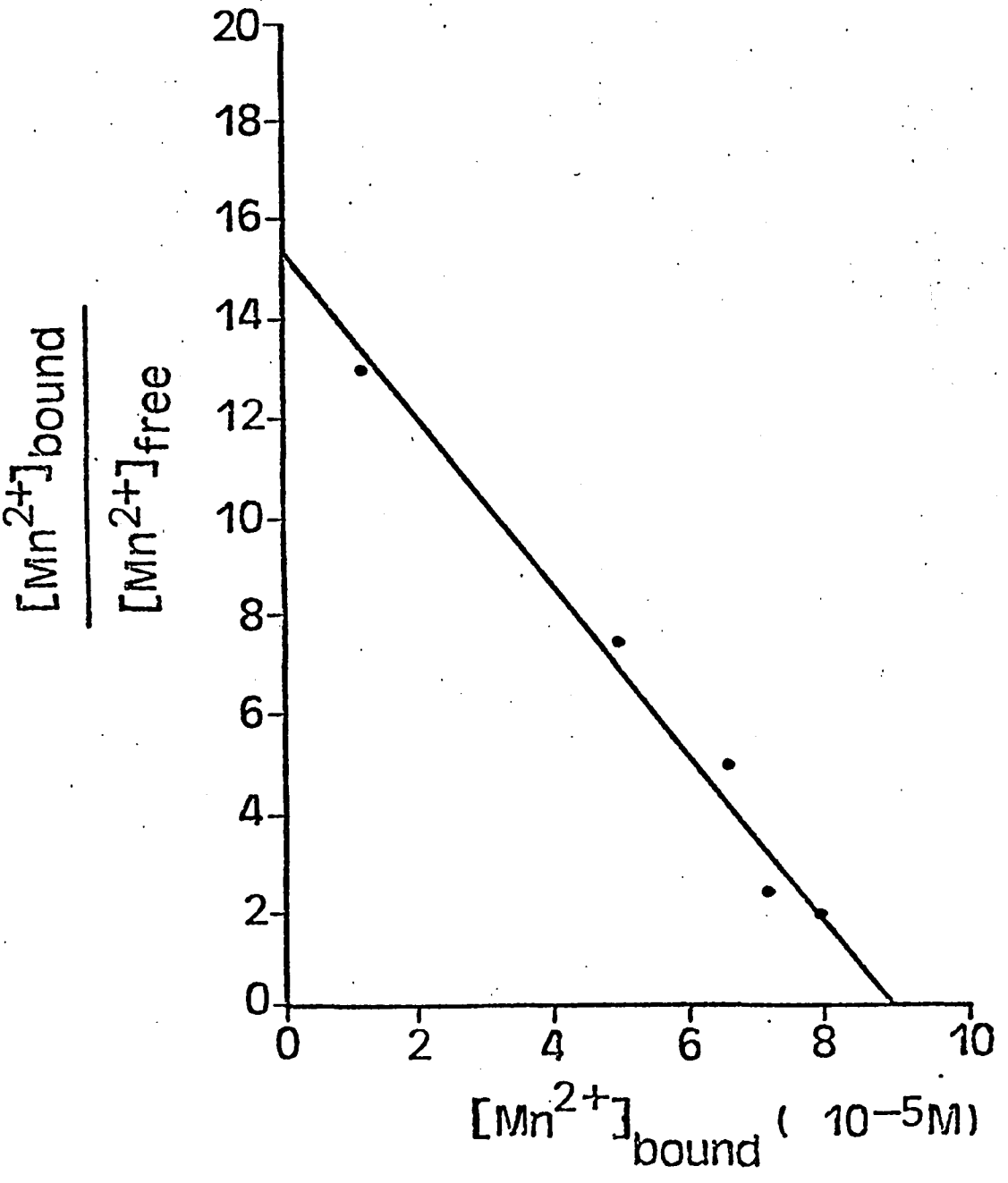

Figure 3.9. Scatchard plot of the titration of the fluid with Mn^{2+}.

Figure 3.10. (A) 77°K X-band EPR spectrum of lyophilized native fluid. (B) 77°K X-band EPR spectrum of lyophilized centrifuged-dialyzed fluid.

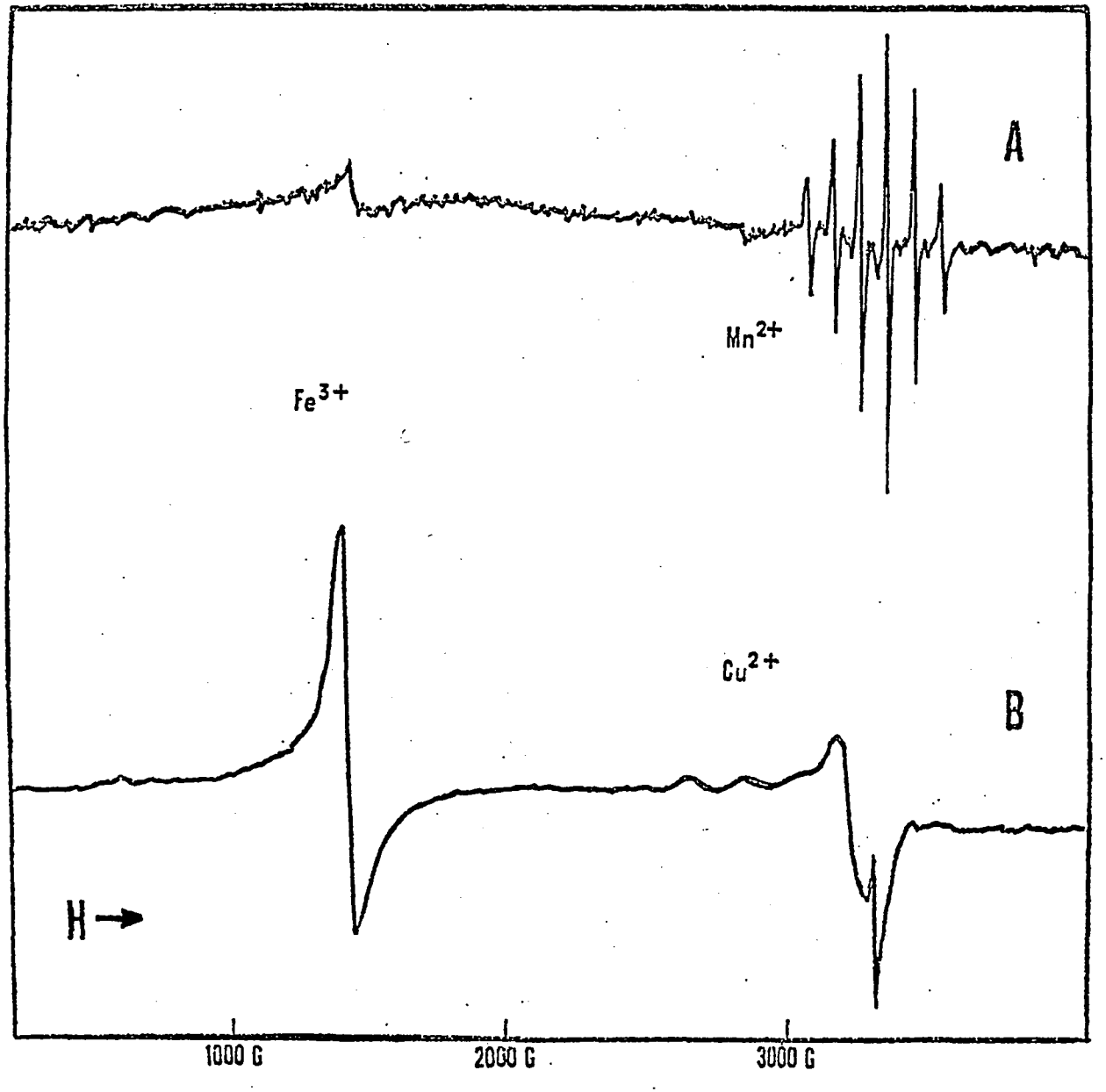
A
Mn^{2+}
Fe^{3+}
Cu^{2+}
B
H
1000 G
2000 G
3000 G

calcium binding of the centrifuged-dialyzed fluid was determined by titration. The centrifuged-dialyzed fluid was titrated with freshly prepared 10M urea while the ionic calcium was monitored with a calcium electrode. The results, adjusted for dilution effects, are shown in Figure 3.11, where $[Ca^{2+}]_{free}$ divided by $[Ca^{2+}]_{total}$ versus urea concentration is plotted. At 2M urea concentration, the amount of calcium released corresponds to 90% of the tightly bound calcium (0.087 mM) of the centrifuged-dialyzed fluid. These results demonstrate that the complexation of the tightly bound calcium is dependent on the conformation of the protein or possibly other macromolecular components of the fluid.

Dialysis of the centrifuged-dialyzed fluid against a 300-fold volume excess of 0.1M sodium ethylenediaminetetraacetate (EDTA), pH 7.2 for 48 hours results in no appreciable loss of the tightly bound calcium. Moreover, only 10% of the tightly bound calcium is released, as monitored by a calcium ion electrode, when the pH of the fluid is reduced to 4.1. However, when both 0.1M EDTA and a reduction in pH to 4.6 are employed, 90% of the calcium is removed by dialysis.

The calcium binding in the centrifuged-dialyzed fluid is reversible. A sample was dialyzed against 300-fold excess 0.1M EDTA, pH 4.6 to remove 90% of the tightly bound calcium. After the EDTA was removed by dialysis against 4mM sodium citrate, pH 4.2, the sample was further dialyzed against 0.5M $CaCl_2$ in 4mM sodium citrate at pH 4.5 for 48 hours. The pH of the dialysate was then slowly brought

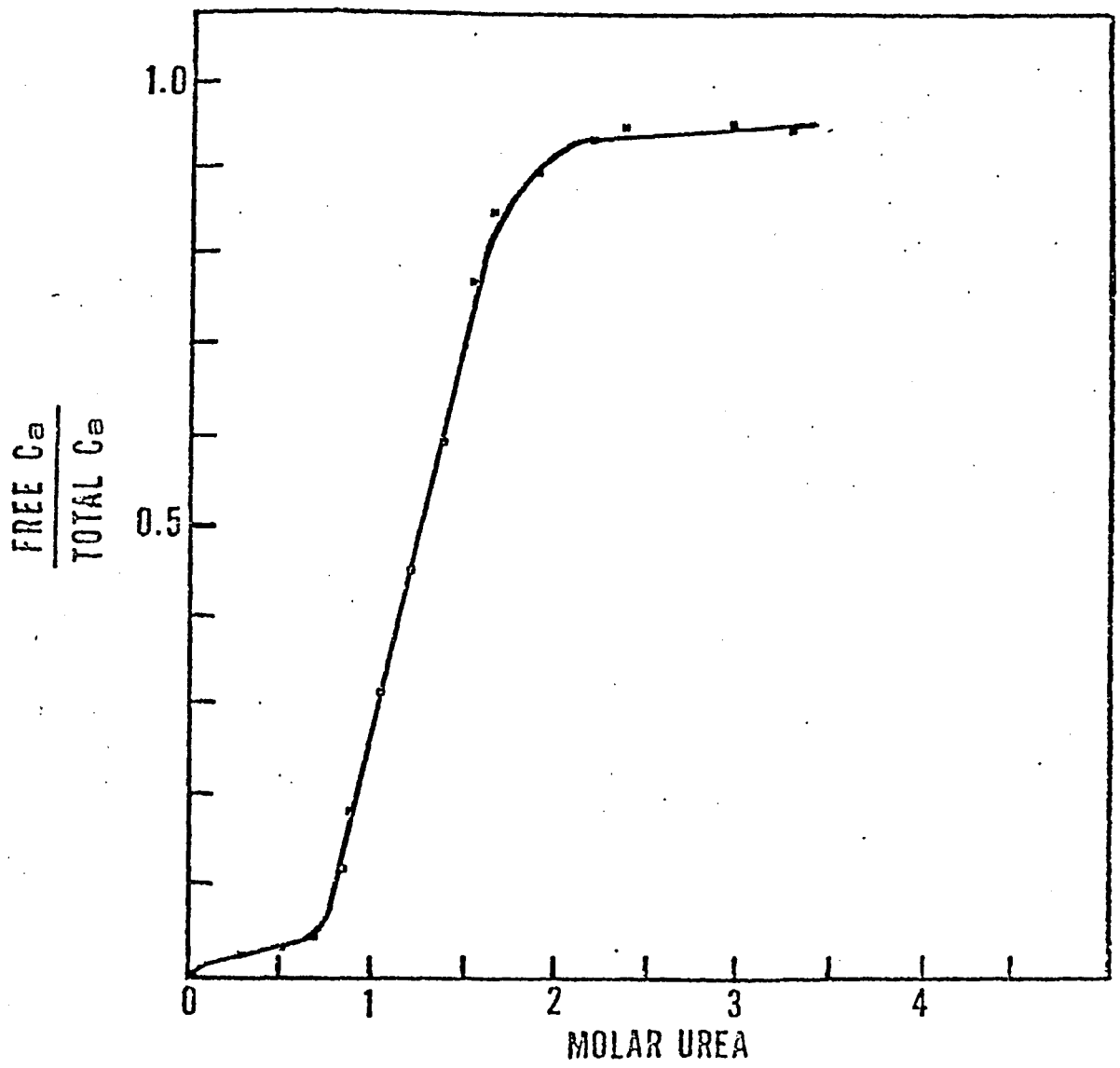

Figure 3.11. Plot of free [Ca^{2+}] divided by total [Ca^{2+}] vs. urea concentration.

up to pH 7.0 with 0.1M NaOH and the sample was dialyzed for an additional 24 hours. The sample was then divided into two fractions; one of which was dialyzed against 50 mM Tris buffer, pH 7.1, while the other against 0.1M EDTA, pH 7.1. The concentration of calcium (0.16 mM) by atomic absorption spectroscopy in the fraction dialyzed against Tris buffer was nearly twice the 0.086 mM of the other sample (which was the same as the original tightly bound Ca^{2+}). These results show that at pH 7.1 EDTA removes the introduced calcium which is not tightly bound. Moreover, some of the introduced calcium binds weakly to the components of the centrifuged-dialyzed fluid and is not easily removed by dialysis against buffer alone.

Discussion

The shell of Mytilus edulis contains two types of calcium carbonate, calcite and aragonite. Disc gel electrophoresis experiments reported here indicate the presence of at least five protein components in dialyzed fluid. This is in accord with work done by others[29,32] who found that three or more proteins were always present in the extrapallial fluid of several molluscs that had both aragonite and calcite components in their shell. These results suggest, but do not demonstrate, that crystal type may be influenced by the protein components of the fluid.

The insoluble fraction of the fluid is carbohydrate material, probably an acid mucopolysaccharide, commonly found in the extrapallial fluid of molluscs. Acid mucopolysaccharides

have been implicated in calcium carbonate formation,[67,68] and they may play a role as ion exchange agents binding metal ions, thereby regulating the deposition of calcium carbonate crystals. This is consistent with our observations that almost 10% of the Ca^{2+} in extrapallial fluid precipitates with the polysaccharide material.

Amino acid analyses of the native extrapallial fluid of M. edulis and its constituents show their composition is different from that of shell protein components. These findings are in accord with studies by others[35-37] in which the amino acid content of the extrapallial fluid and shell components varied greatly.

Results obtained with the ultrafiltrate component suggest that free amino acids are present in the native fluid. These amino acids along with other small organic molecules may function as chelating agents for various metal ions as observed for VO^{2+} added to the fluid. The spectrum of the vanadyl complex has a vanadium nuclear hyperfine splitting of 99G, similar to that of $VO(gly)_2$.[69] This result is consistent with the large amounts of glycine found in the fluid (Table 3.1). Some of the Mn^{2+} is probably complexed with this amino acid as well.

Recently interest has arisen in the possibility of using EPR spectroscopy to obtain information on trace paramagnetic metal ions in calcified tissue.[61,70] Blanchard and Chasteen[40] have investigated the EPR spectrum of different regions of the shell of Mytilus edulis and found iron,

manganese, and radical species in varying amounts. A manganese signal due to substitution of the Mn^{2+} for Ca^{2+} in calcite was observed in the prismatic region. Iron signals similar to those observed in the centrifuged-dialyzed fluid are seen in the periostracum, and radical species noted in both the nacre and periostracum are suggestive of quinone type radicals.

Room-temperature studies with native fluid show the presence of free manganese in solution. The majority of manganese was found to be complexed, and substitution of VO^{2+} into the fluid with a concomitant increase in manganese signal suggests that significant amounts of the manganese exists as a small chelate. The characteristic VO^{2+} small chelate spectrum obtained supports this view. The manganese signal at both room and liquid nitrogen temperatures completely disappears upon dialysis, suggesting the presence of small chelates or weak association with the macromolecular components. Further work involving titrations of the native fluid with Mn^{2+} and H^{+} indicate that the binding capacity of the fluid for manganese is on the order of 10^{-4}M. The observed apparent pK_a' of 5.2 is consistent with carboxylic acid ligation. Recent studies in this laboratory have demonstrated that calcium readily displaces the bound manganese, showing that manganese and calcium also bind to the same ligands in some instances.

Optical emission spectroscopy measurements show that several trace metal ions are present in the native fluid,

some of which may have a physiological role. Some sodium, magnesium, calcium, iron, and copper remain associated with the centrifuged-dialyzed fluid and appear to be tenaciously bound. The observed iron and copper EPR signals may be due to metalloenzymes important in the regulation of calcium carbonate deposition or formation of shell matrix components.

Calcium electrode measurements indicate that over 85% of the calcium in native fluid is bound as compared to sea water, where less than 10% is complexed. By atomic absorption spectroscopy experiments, it was shown that 91% of the metal was also dialyzable and ultrafiltratable. This result along with Ca^{2+} ion electrode measurements indicates that the bulk of the calcium in extrapallial fluid is complexed to small chelates.

The calcium binding properties of the centrifuged-dialyzed fluid appear to be unique in that the metal is bound rather tenaciously. This is not usually observed for typical extracellular calcium binding proteins in the animal kingdom[1] where binding constants are of the order of only $10^3 - 10^4 M^{-1}$.

When the centrifuged-dialyzed fluid is subjected to an excess of calcium, additional calcium becomes associated but is readily removed by dialysis against 0.1M EDTA, pH 7.1. These additional weak binding sites must be quite different in structure from those which bind the tightly associated calcium. The tightly bound calcium sites are probably buried in the interior of the macromolecules and become accessible

to EDTA only through reductions in pH or the addition of urea. The ability of the centrifuged-dialyzed fluid to bind calcium strongly is dependent on the conformation of the protein components and implies that the bound calcium is a polydentate complex. The concomitant loss of binding at pH 4.6 is probably caused by protonation of ligands or unfolding of the protein structure in acid medium. These proteins might provide the correct spatial relationship for strong calcium chelation.

The chelation of calcium may be an important factor in controlling calcification. Calcification occurs from solutions which exceed the solubility product of calcium carbonate. The apparent solubility product of calcium carbonate in a seawater matrix at a specified temperature, pressure and salinity may be expressed as:

$$K'sp = M_{Ca}{}^{2+} \cdot M_{CO_3}{}^{2-} \qquad (1)$$

where $M_{Ca}{}^{2+}$ and $M_{CO_3}{}^{2-}$ are the total concentrations of calcium and carbonate ions in moles/kilogram of seawater. Problems arise in determining solubility products in seawater solutions because the "constant" varies with crystal form, purity, and particle size.[127] In addition, organic matter in extrapallial fluids can affect calcium carbonate solubility in two major ways. The organics may coat solid calcium carbonate, essentially taking the particles out of equilibrium with the solution. Organic matter can also prevent the

nucleation of calcium carbonate crystals from solution. Concepts of solubility products are fundamental however, since they stipulate equilibrium conditions necessary for minerals to exist in solid phases with solutions.

The use of thermodynamic solubility product constants requires the single ion activity coefficients of calcium and carbonate. Because of discrepancies of coefficient values in previous published results,[72,128] it is more convenient to utilize apparent solubility product constants for calculations. At a specified temperature, pressure, and salinity apparent solubility products can be determined without the knowledge of activity coefficients.[73]

The K'sp of calcite in 35% artificial seawater is 4.76×10^{-7} moles^2/Kg^2 at 13°C and one atmosphere pressure.[73] Values for K'sp's of calcite in seawater matrices are directly proportional to salinity.[127] The salinity of the extrapallial fluid is 32%, thus K'sp (adjusted) = 4.3×10^{-7} moles^2/Kg^2.

The ion product ($M_{Ca}2+ \cdot M_{CO_3}2-$) of calcium carbonate in the extrapallial fluid was estimated. $M_{Ca}2+_{total} = 9.5 \times 10^{-3}$ as determined by atomic absorption spectroscopy while $M_{CO_3}2-$ was determined as follows. Total inorganic carbon was measured on a D.O.C. analyzer (Barnstead and Sybron) and found to be 3.6×10^{-3}M. M_{HCO_3-} was assumed to be 3.6×10^{-3}M. The pK_2' of carbonic acid in a seawater matrix at 13°C, 32% salinity and one atmosphere pressure is 9.32.[129] We now calculate $M_{CO_3}2-$ from the Henderson-Hasselbalch equation,

$$pH = pK_2' + \log \frac{M_{CO_3^{2-}}}{M_{HCO_3^-}}$$

By taking the pH of the fluid to be 7.4, we calculate $M_{CO_3^{2-}} = 4.3 \times 10^{-5}$. The ion product using the total calcium concentration would therefore be 4.1×10^{-7} moles^2/Kg^2, a condition of saturation. However in the fluid, the concentration of ionic calcium is 1.45×10^{-3}M, or only 15.3% of the total. This leads to an ion product of 6.2×10^{-8} moles^2/Kg^2, which is below that needed to precipitate the mineral. The fluctuations in the ion products suggest that small chelates could control the deposition of calcium carbonate in the extrapallial fluid.

In addition, the observation that Mn^{2+} substitutes for Ca^{2+} in the calcitic and aragonitic shells of molluscs [40,70,71] and that both metals appear to be associated mostly with small molecules suggests that Mn^{2+} ions might be profitably used to probe calcification processes by EPR spectroscopy. The preliminary experiments reported here for Mn^{2+} as well as the other EPR active metals, Cu^{2+}, Fe^{3+}, and VO^{2+}, indicate that useful information might be obtained from such studies. More detailed investigations along these lines are currently underway in our laboratory.

Chapter 4

Separation of Protein Components in the Fluid

Many biochemical and physical studies have been undertaken to study protein components in molluscan shells. These studies have centered on the products of calcification and conclude little about the processes that occur.[16,19,26] In contrast, I believe an examination of the protein constituents of the extrapallial fluid can aid in understanding details of the calcification process. The first phase of this investigation required the development of suitable procedures for the separation and isolation of constituents.

Centrifugation and dialysis techniques were first carried out to remove insoluble material, low molecular weight species and particulate matter from the fluid. Gel filtration chromatography separated the fluid proteins into two components (1 and 2). The apparent molecular weights of each component were then estimated. Anion exchange chromatography on 1 and 2 showed that the fluid is composed of nine proteinaceous constituents. The details are presented in this chapter.

Experimental Methods

Materials

Sephadex G-200, G-25, DEAE-A50, human serotransferrin (81,000), bovine serum albumin (68,000), bovine carbonic

anhydrase B (29,000), and bovine myoglobin (17.200) were purchased from Sigma Chemical Company and used without further purification. Human γ-globulins (160,000) and Dextran Blue were gifts of the Biochemistry Department at the University of New Hampshire. All other materials were obtained from several commercial sources.

Separation of Protein Components

Step 1: Centrifugation, dialysis and concentration of native fluid. Centrifuged-dialyzed fluid was prepared as described in Chapter 3. In a typical preparation, centrifuged-dialyzed fluid was preconcentrated from 20 ml to 5 ml using an ultrafiltration cell model 12 (Amicon Corp.) fitted with a PM-10 membrane (MW cutoff 10,000) and under nitrogen pressure (∿15 psi).

Step 2: Gel filtration chromatography. A Sephadex G-200 (Pharmacia) column, 1.5 x 55 cm, was equilibrated with several bed volumes of 0.05M Tris-HCl buffer, 0.02% NaN_3, pH 7.5, under a hydrostatic pressure of 20 cm to remove soluble carbohydrate material. The sample (approximately 40 mg in 5 ml) obtained from the previous step was applied to the column and eluted with the equilibrating buffer at a flow rate of 6 ml per hour. Fractions of 2 ml were collected and analyzed for protein content at 280 nm on a Bausch and Lomb Spectronic 710 spectrophotometer. Two different fractions were detected and each was pooled for ion exchange chromatography.

Step 3: Anion Exchange Chromatography. DEAE-50 anion exchanger was suspended in 0.05M Tris-HCl buffer, pH 7.5,

0.02% NaN_3 for 48 hours. A column, 2.0 x 20 cm, was poured with a slurry of the resin and allowed to settle by gravity. 0.5 cm of G-25 Sephadex was added to the top of the column to protect the bed surface. Components 1 and 2 obtained from the gel filtration step were each applied to the column and eluted with the Tris-HCl buffer and a linear salt gradient to 1.0M NaCl. The flow rates were maintained at 10 ml/hour under a hydrostatic pressure of 10 cm. Fractions of 3 ml volume were collected and analyzed for protein content as described in Step 2. Fractions associated with each peak (1A-B, 2A-G) were pooled, dialyzed exhaustively against distilled-deionized water, and stored at 4°C.

Molecular Weight Determination of Components 1 and 2

The apparent molecular weights of components 1 and 2 were determined according to the method of Andrews[74] using a Sephadex G-200 column equilibrated as before. Elution positions were determined by absorbance at 280, 410, or 660 nm for the standard proteins and the unknowns (see Materials section). The apparent molecular weights were determined by comparison of the observed distribution coefficient, Kd, with a calibration curve of log molecular weight vs. Kd prepared with the standard proteins of known molecular weights (vide supra).

Results

The chromatograph of the extrapallial fluid separated on Sephadex G-200 is given in Figure 4.1. In a routine

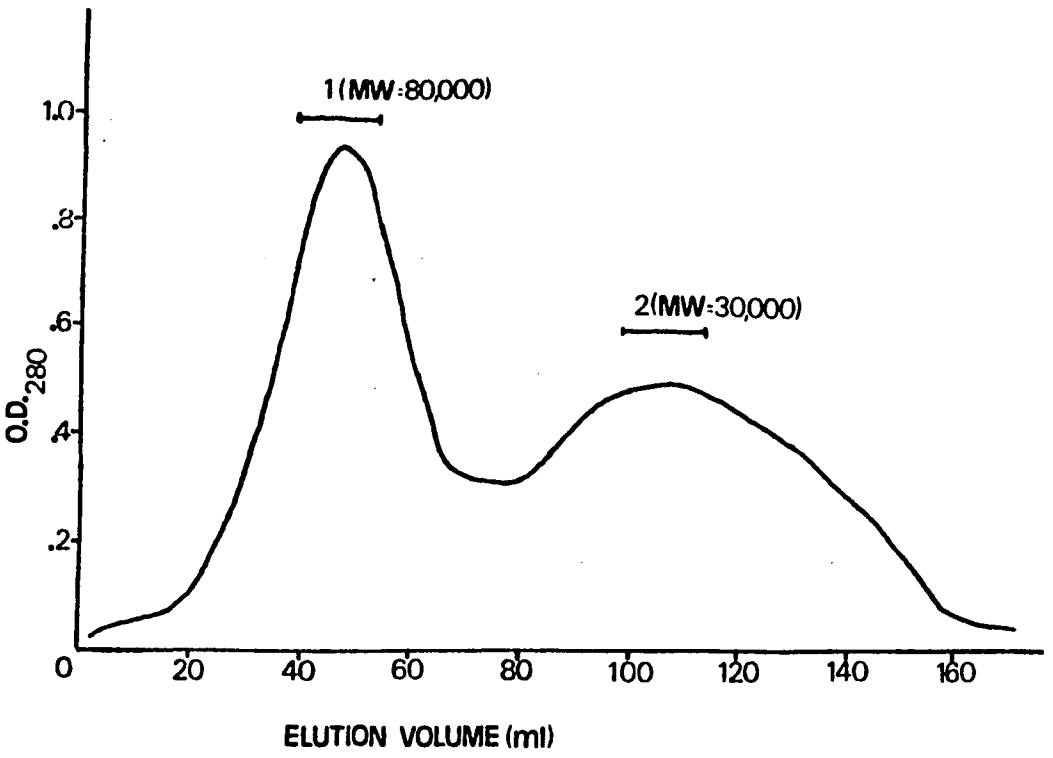

Figure 4.1. Elution profile of centrifuged-dialyzed fluid chromatographed on Sephadex G-200. The bars above each peak denote those fractions which were pooled for further experiments.

experiment 40 mg of centrifuged-dialyzed fluid applied to the G-200 column yielded 20 mg of component 1 and 8 mg of component 2. Approximately 6 mg of soluble carbohydrate material was detected in the void volume by the anthrone reaction.[52]

The apparent molecular weights of each component were determined by gel filtration chromatography and employing the standard curve in Figure 4.2. Component 1 eluted as a single peak on a Sephadex G-200 column with a distribution coefficient Kd, slightly higher than that of human serotransferrin (HST) which corresponds to an apparent molecular weight of ∿80,000 daltons for component 1 (Figure 4.2). Similar treatment of component 2 yielded a Kd value slightly lower than that of carbonic anhydrase (CA) and an apparent molecular weight of 30,000 daltons.

Application of component 2 to Sephadex DEAE-A50 yielded seven peaks (Figure 4.3) which were not examined further. Similar treatment of component 1 produced two peaks 1A and 1B (Figure 4.4) which were subjected to further analysis.

Discussion

It has been demonstrated that the extrapallial fluid of M. edulis, like other physiological fluids, contains carbohydrate matter and several protein components. A three-step procedure was developed to separate the various macromolecules. Proteins in the fluid were first separated from low molecular weight solutes by dialysis. Sample concentration prior to chromatography was done by ultrafiltration techniques.

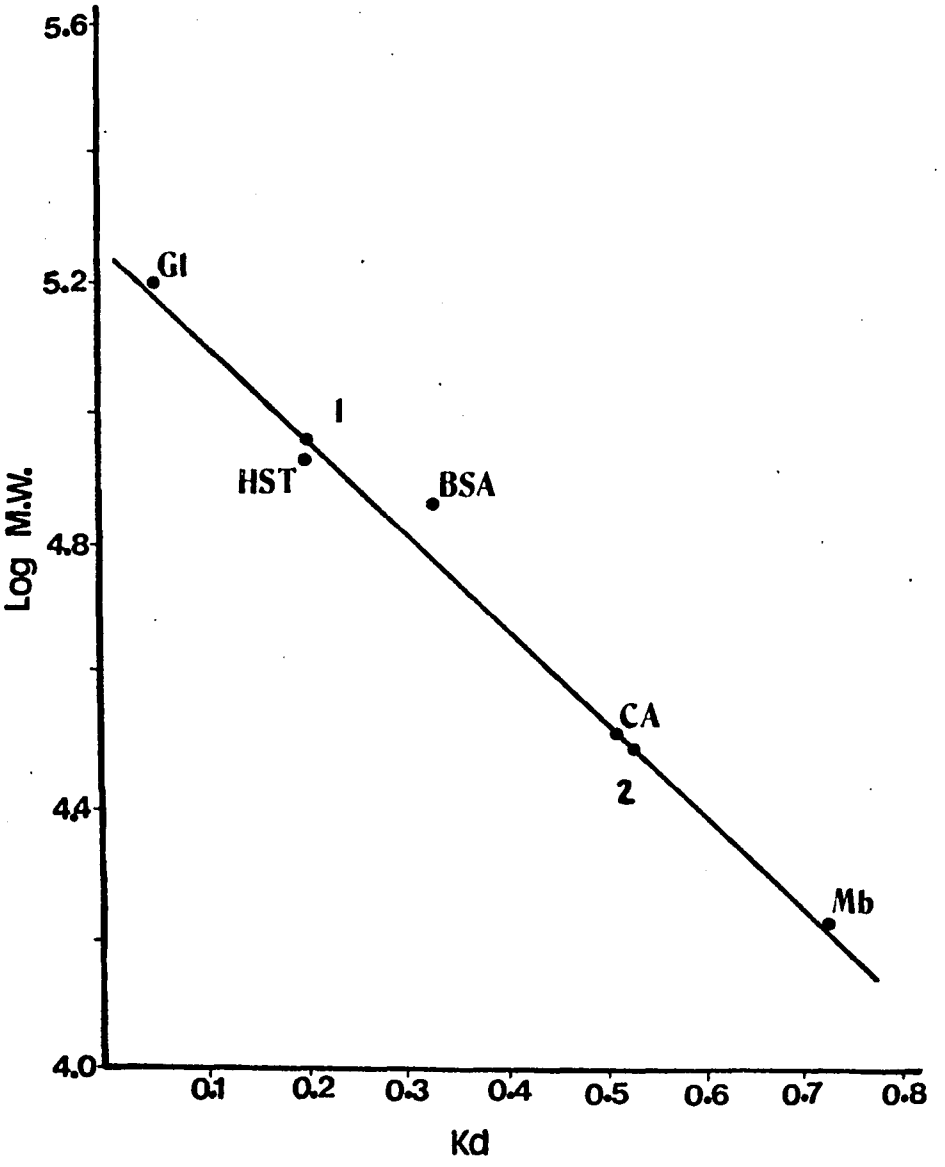

Figure 4.2. Estimation of the molecular weights of components 1 and 2 by gel filtration chromatography.

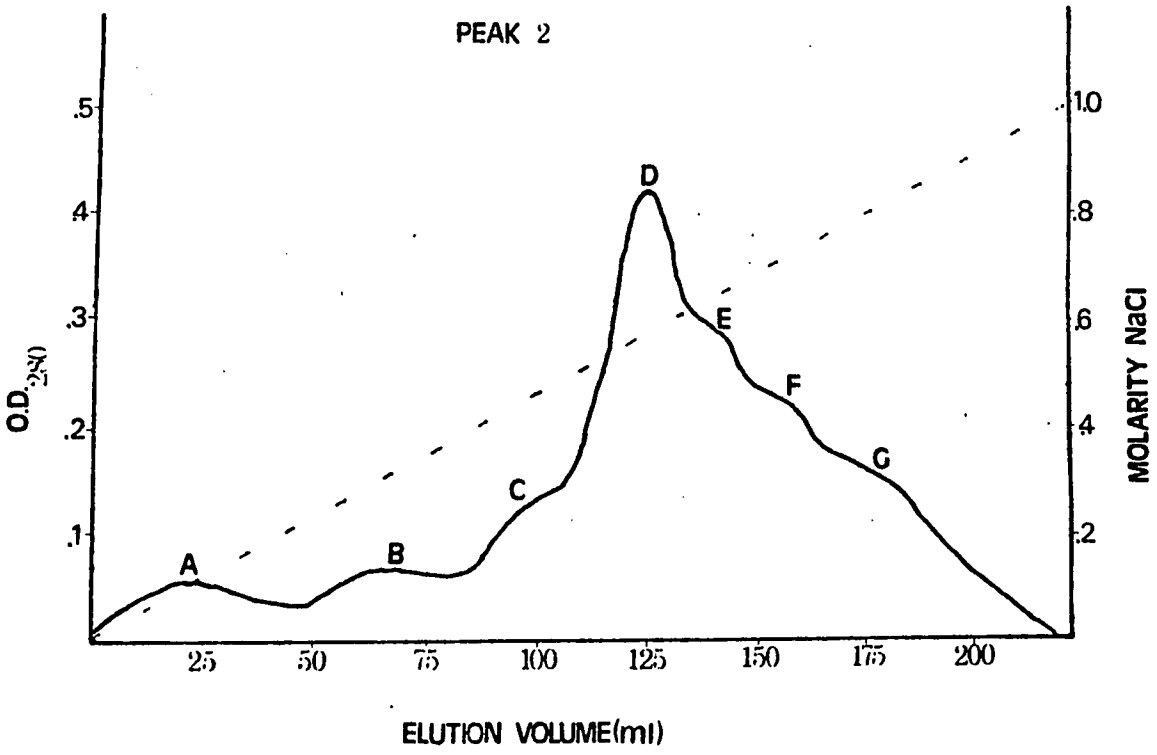

Figure 4.3. Chromatographic separation of component 2 on Sephadex DEAE-A50. Elutant: 0.05M Tris-HCl buffer, pH 7.5, with a linear salt gradient to 1.0M NaCl.

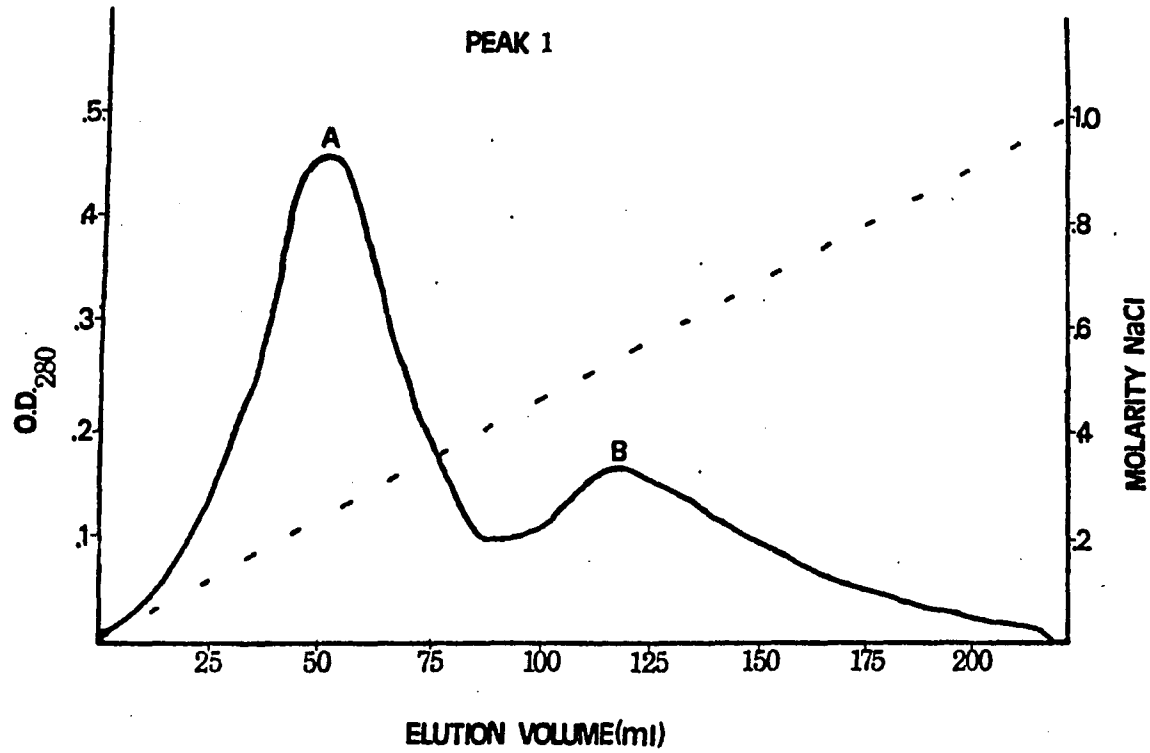

Figure 4.4. Chromatographic separation of component 1 on Sephadex DEAE-A50. Elutant: 0.05M Tris-HCl buffer, pH 7.5, with a linear salt gradient to 1.0M NaCl.

Gel filtration chromatography of centrifuged-dialyzed fluid sorted the proteins into two components: 1 and 2. The apparent molecular weights of each component were then determined. Component 2 (Figure 4.3) contains seven species (2A-G) that have molecular weights around 30,000. Carbonic anhydrase, with a molecular weight near 30,000 and found in some molluscs,[18,19] might be present in this fraction.

Component 1, with a molecular weight around 80,000 contains two species, 1A and 1B. 1A accounted for 68% of the total protein composition in the fluid while 1B was only detected periodically in very small amounts (3% of total protein content). These results support the concept that some proteins in the fluid are present as stable components while others (i.e., enzymes) vary according to the current rate or stage in shell formation of the animal.[32] Interestingly, Jope[75] found shell proteins of M. edulis to consist of one main polypeptide and other proteins in smaller amounts, in accord with my findings in the extrapallial fluid.

In addition to proteins, carbohydrates are also candidates for the regulation of calcium carbonate deposition. The results obtained in Chapters 3 and 4 show that 40% of dialyzed extrapallial fluid is polysaccharide material. This material can be separated into two fractions. Almost 10% of the calcium in extrapallial fluid is bound to an insoluble carbohydrate fraction. This binding is probably accomplished by sulfate groups present in this component. Eighteen percent of centrifuged-dialyzed fluid is soluble

high molecular weight polysaccharide material. Upon reviewing the literature, I found only one other experimental study undertaken in this area. Analysis of the non-dialyzable material in the extrapallial fluid of M. mercenaria, showed that polysaccharide accounted for 91% of the impermeate.[16] The large differences in polysaccharide content of M. mercenaria and M. edulis extrapallial fluids cannot be explained at this time. Further work to examine the possible relationship between polysaccharides and mineralization is in order.

In summary, the extrapallial fluid of Mytilus edulis contains several proteins and significant amounts of carbohydrate. These species are probably necessary for synthesis of an organic matrix capable of binding and depositing calcium carbonate crystals in a characteristic crystalline configuration. Subsequent studies were carried out to characterize components 1A and 1B with respect to structure, elemental analysis, spectroscopic properties, and functional groups.

Chapter 5

Partial Characterization, Metal Binding Properties and Proposed Function of a Purified Glycoprotein (1A)

Molluscan biomineralization is characterized by a high degree of organization due primarily to involvement of organic macromolecules. These components have a wide variety of possible roles such as crystal orientation and initiation, metal transport, and catalysis of specific reactions. In order to understand their function, the composition and structure of these macromolecules must be determined.

Virtually all previous investigations have focused on the macromolecular components in the shell. Organic matrices within the crystallites of molluscan shells have been identified,[42,76-78] analyzed for amino acid composition,[56,79,80] and reported to consist of more than one macromolecule.[57] Molecular conformation studies of proteins constituting the molluscan shell have been reported by Hotta.[81] The infrared spectra of several decalcified shell layer films have been studied in the 4000 to 7000 cm^{-1} region. The protein structure is coiled and has a β conformation.

The only report on the extraction and partial purification of a shell protein comes from Crenshaw,[42] who isolated a glycoprotein from Mercenaria mercenaria. The glycoprotein was evenly distributed throughout the shell and proved to be

homogeneous as determined by gel filtration chromatography and electrophoresis. The apparent molecular weight was 160,000 daltons. Titration of this component in the presence of excess sodium, potassium, and magnesium showed that calcium was selectively bound. Calcium binding was eliminated at urea concentrations above 3M. Crenshaw[42] suggested that the glycoprotein plays a role in initiation of calcification. The present chapter describes the first isolation and partial characterization of a glycoprotein component, 1A, from the extrapallial fluid of a mollusc.

Experimental Methods

Materials

$LaCl_3 \cdot 7H_2O$ and EGTA [ethylenebis (oxyethylenenitrilo)]-tetraacetic acid were purchased from Alfa Inorganics.[45] $CaCl_2$ (2m Ci) and Bray's solution were bought from New England Nuclear. Calcium, magnesium, and manganese chlorides were all of analytical grade. All other inorganic, organic, and biochemicals were, when possible, of reagent grade or better.

Electrophoresis

The disc gel electrophoretic system (Hoefer Scientific, Model DE-102), described by Hedrick and Smith,[54] was utilized to estimate the purity of 1A at pH 8.9 and varying gel concentration. Samples containing approximately 1 mg/ml were applied in 100 µl volumes to the gels (10 cm in length). Electrophoresis was carried out at room temperature toward

the anode at a constant current of 1mA/sample. The gels were stained with Napthol Blue Black and destained with a Quick Gel Destainer (Hoefer Scientific).

Carbohydrate and Amino Acid Analysis

The carbohydrate content of 1A was determined by the anthrone reaction.[52] Spectral measurements were carried out with a Bausch and Lomb Spectronic 710 spectrophotometer using 5 cm quartz cells and a wavelength of 620 nm. Samples for amino acid analyses were hydrolyzed in 6N HCl under reduced pressure in sealed tubes at 105° for 24 hours. The hydrolysates were dried under reduced pressure and then redissolved in 0.2M sodium citrate buffer, (pH 2.2), and analyzed on a Beckman 120C analyzer by the method of Guire et al.[53]

Determination of ε_{280} (Molar Absorbance)

Purified samples were weighed carefully by a technician and placed in appropriate volumes of buffer to give 1 mg/ml concentrations. The absorbance at 280 nm was measured on three samples. The values obtained were used for further work in estimating protein concentration.

Metal Analyses

A Varian Techtron Model AA-3 spectrometer modified with AA-5 electronics was used for atomic absorption analyses of calcium and magnesium. The wavelengths and slit widths employed were 422.6 nm (100 μ) and 285.2 nm (100 μ) respectively. All samples and standards were acidified and made

1% in $LaCl_3$ to suppress matrix effects. A Baird Associates Eagle Mount grating spectrograph was used for optical emission measurements. The protein sample was ashed first to remove organic matter.

Removal of Metals

Metal removal from 1A was accomplished by the scheme shown in Figure 5.1. The fraction was first dialyzed for 48 hours against 10mM EDTA in Tris-HCl buffer, pH 7.7 at 20°C. Exhaustive dialysis against distilled-deionized water, pH 7.0, for 48 hours removed most of the EDTA present. Samples were then dialyzed against 10mM $NaClO_4$, pH 7.2, for 48 hours to remove the rest of the chelate. Final dialyses were against distilled-deionized water for 48 hours, pH 7.0, to remove Na^+ and ClO_4^- ions. After this procedure, normally 0.15 ± 0.06 gram-atoms of magnesium remained. These protein samples were formulated as $Ca_3$1A (Figure 5.1, top).

To remove both Mg^{2+} and Ca^{2+}, the following procedure was employed (Figure 5.1, bottom). Samples of 1A were dialyzed against 100mM EDTA, pH 4.6, for 48 hours at 20°C, then 4mM sodium citrate buffer, pH 4.5, for 48 hours to remove EDTA. The pH of this dialysate was carefully brought to 7.0 with 0.1M NaOH and dialysis was resumed for 24 hours. Finally, the samples were dialyzed for an additional 24 hours against distilled-deionized water to remove sodium and citrate ions. These samples were formulated as "Apo" 1A. To check for EDTA binding to protein, $VOSO_4$ (10^{-4}M) was added to various 1A samples at pH 7.5 and the EPR spectrum

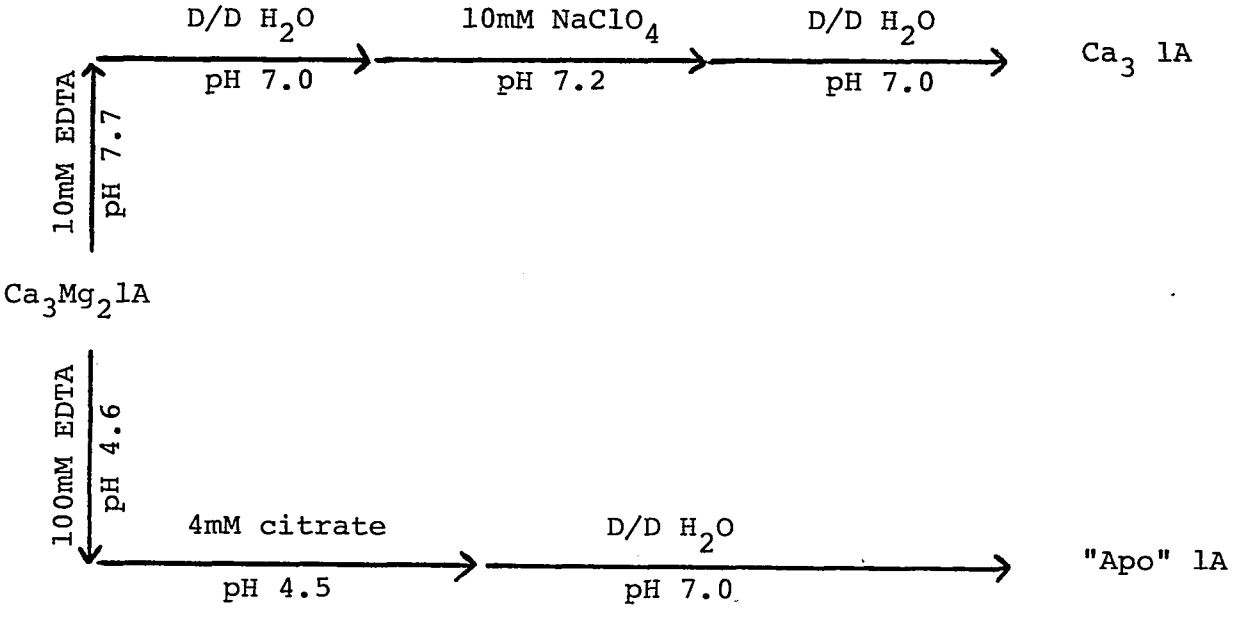

Figure 5.1. Dialysis scheme to remove Ca^{2+} and Mg^{2+} from the glycoprotein.

was recorded. No EPR signals due to either a VO^{2+}-1A or VO^{2+}-EDTA complex were observed, indicating no binding of the chelate to the macromolecule. All samples were dialyzed against 500 fold excess of the appropriate buffer prior to metal binding experiments.

Electron Paramagnetic Resonance Spectroscopy (EPR) Mn^{2+} and Mg^{2+} Binding

All solutions were made in 0.1M Tris-HCl buffer, pH 7.4. In the presence of "Apo" 1A, the free manganese was measured by the intensity of its EPR spectrum at room temperature using a Varian E-4 spectrometer operating at X-band frequency (∿9.5G Hz), and 100K Hz magnetic field modulation.

Procedures for a typical binding experiment were as follows. Exactly 300 µl of 14 x 10^{-6}M "Apo"1A were added to a capillary flat cell. A 2000G scan (2400 - 4400G) was recorded to detect the presence of any paramagnetic transition metal ions in the sample. Mn^{2+} was then added to the flat cell. The contents were carefully withdrawn by a 500 µl syringe twice and reinserted into the cell to insure thorough mixing of the metal and protein. The flat cell was positioned very carefully into the instrument cavity and the spectrum was recorded. To insure that the instrument was tuned properly, the sample was removed, then reinserted and retuned, and the spectrum was rerecorded until a consistent signal height (± 3%) was obtained. This procedure was followed upon successive additions of metal throughout the titration such that the final solutions covered the range of 0.3 to 5.5

equivalents Mn^{2+} per equivalent 1A. After the manganese titration was complete, the concentration of free manganese was redetermined on the sample containing 5.5 equivalents Mn^{2+} per 1A equivalent. Aliquots of Mg^{2+} were then added to the sample and the relative signal intensity of the free manganese ion was recorded. Final protein dilution effects were small (∿6%).

Flow Dialysis - Ca^{2+} Binding

The calcium binding properties of the protein were investigated in a flow dialysis system similar to that described by Colowick and Womack.[82] Solutions for all experiments in this section were made in 0.1M Tris-HCl buffer, pH 7.9. All experiments were conducted at room temperature (20°C). The dialysis cell consisted of an upper chamber containing the protein sample (typically 1-2 x 10^{-5}M) and $^{45}Ca^{2+}$ (1-2 x 10^{-6}M), separated by a membrane from a lower chamber through which buffer was pumped at a constant rate and from which the effluent was sampled for radioactivity (Figure 5.2). The cell (1 ml size) was adapted from a Technilab cell (Bel-Art Products) for flow dialysis. The upper chamber (19mm in diameter x 5mm) was deepened to 9mm to make the capacity to 1.8 ml (with stir bar) and a hole (3.2mm in diameter) was drilled through the center to permit additions of small amounts of metal ion to the protein solution during the course of a binding measurement. To the lower chamber (19mm in diameter x 10mm) a hole (3.2mm in diameter) was drilled 180° from one already there. The

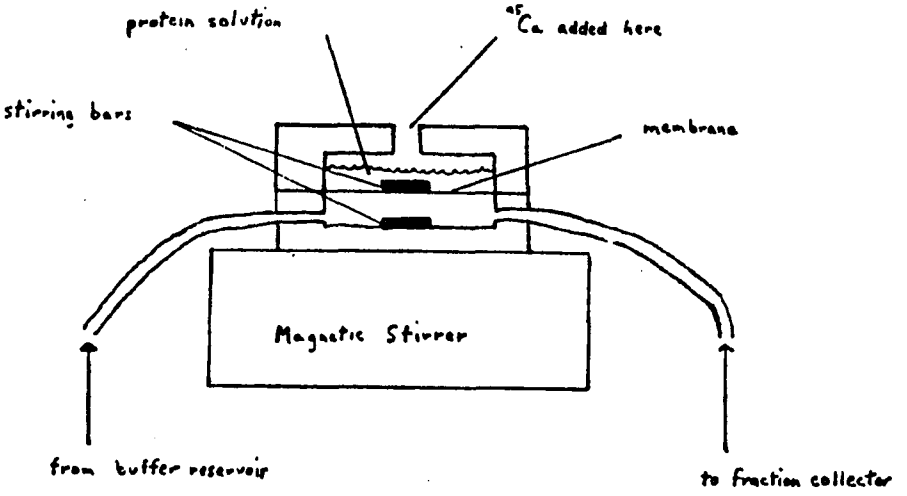

Figure 5.2. Diagram of the apparatus for measuring Ca^{2+} binding to 1A by flow dialysis.

PLEASE NOTE:

In all cases this material has been filmed in the best possible way from the available copy. Problems encountered with this document have been identified here with a check mark ✓.

1. Glossy photographs _____
2. Colored illustrations _____
3. Photographs with dark background _____
4. Illustrations are poor copy _____
5. Print shows through as there is text on both sides of page _____
6. Indistinct, broken or small print on several pages ✓ throughout _____
7. Tightly bound copy with print lost in spine _____
8. Computer printout pages with indistinct print _____
9. Page(s) _____ lacking when material received, and not available from school or author _____
10. Page(s) _____ seem to be missing in numbering only as text follows _____
11. Poor carbon copy _____
12. Not original copy, several pages with blurred type _____
13. Appendix pages are poor copy _____
14. Original copy with light type _____
15. Curling and wrinkled pages _____
16. Other _____

University Microfilms International

300 N. ZEEB RD., ANN ARBOR, MI 48106 (313) 761-4700

lower chamber had a capacity of 2.0 ml (with stir bar). The membrane, a square piece of Spectrapor 132650 membrane tubing (MW cutoff 6-8,000), was clamped between the two chambers by stainless steel screws.

The flow rate in all measurements (with and without protein) was 8 ml/min and the effluent was collected in 2 ml aliquots with a Gilson model FC-80E Microfractionator (Gilson Electronics). One ml samples from even numbered fractions were added to 10 ml of scintillation fluid and were counted in a Unilux model 6850 liquid scintillation counter. Protein concentrations were checked before and after each experiment. Dilution effects and protein loss through leaks of the membrane were small (±5%).

Ultrafiltration Techniques - Mg^{2+} Binding

An Amicon Model 12 stirred cell with a 25mm, PM-10 membrane (Amicon Corp.) was used to study the magnesium binding properties of the protein. All solutions were made in 0.1M Tris-HCl buffer, pH 7.9. The apparatus is shown in Figure 5.3. The entire assembly was made firm by clamping. A magnetic stirrer was placed below to effect mixing. This maintained a uniform bulk composition in the compartment and also prevented adhesion of protein to the membrane surface. Accordingly, preliminary experiments were performed with 1A in the sample cell to study any exchange. No detectable binding or absorption to the membrane was observed.

It was necessary to evaluate the permeation of diffusible ions through the membrane in order to (1) measure

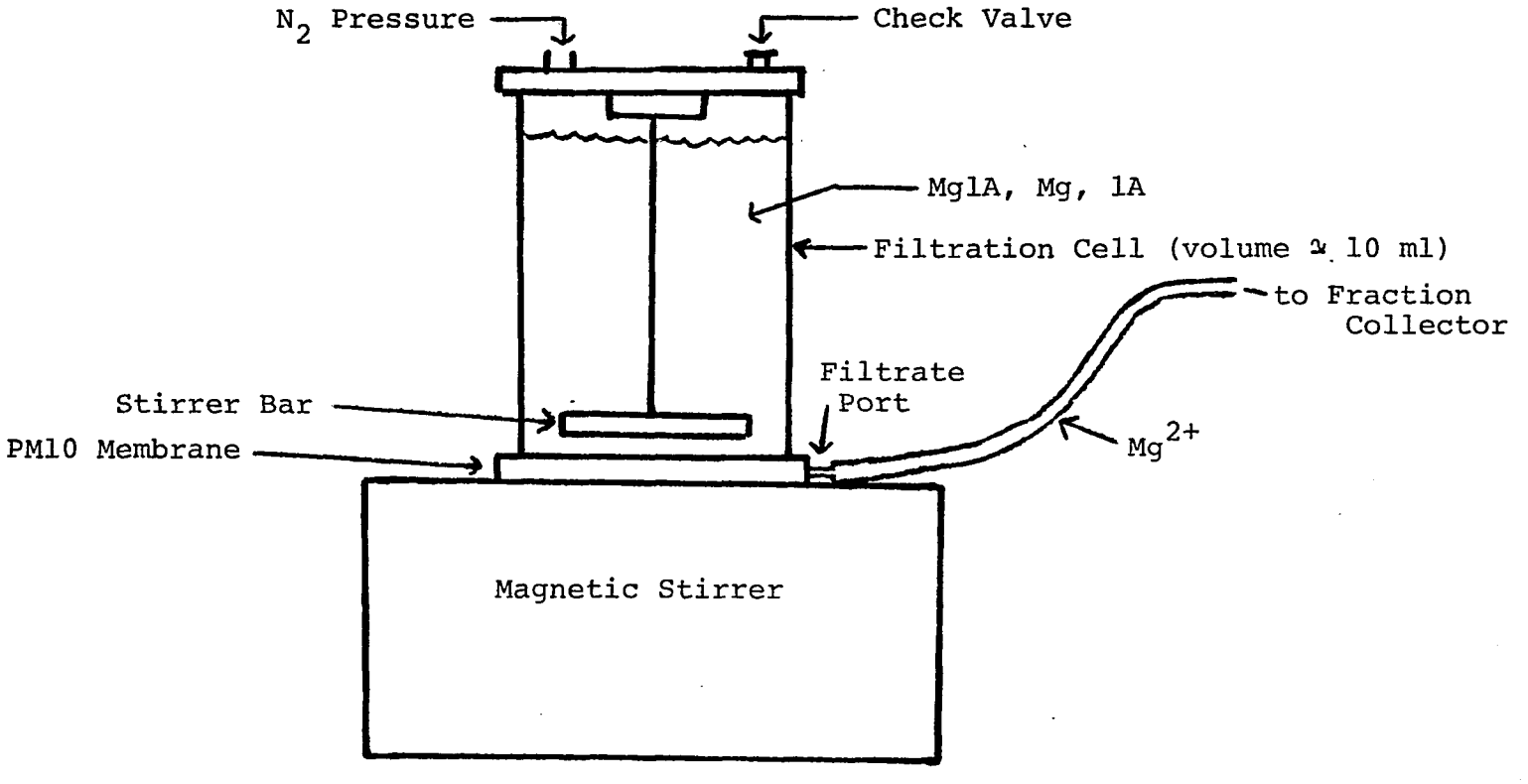

Figure 5.3. Diagram of the apparatus for measuring Mg^{2+} binding to lA by ultrafiltration.

the void volume of the effluent collection assembly and (2) to determine possible binding of metal ions to the membrane. The void volume of the system was determined in the following manner. The entire apparatus (including tubing from the filtrate port to the fraction collector) was weighed (179.90 g). Exactly 10 ml of distilled-deionized water was added to the cell and ultrafiltration was carried out until the void volume was filled with effluent. The volume of the remaining contents in the cell was 6.3 ml, while the apparatus with the filled void volume weighed 183.70 g. The void volume of the system was therefore 3.75 ml.

The permeability of the membrane to Mg^{2+} solutes was determined by passing fixed volumes of magnesium ions through the membrane and comparing the effluent concentration to the original. Concentrations of 10 and 100 x 10^{-6}M Mg^{2+} were found to vary ±7% as determined by atomic absorption spectroscopy. Diffusion between the void volume and cell contents was checked with a dye solution (0.01% Napthol Blue) and found to be small.

Binding profiles of magnesium to Ca_3 1A and "Apo" 1A were determined accordingly. The void volume of the assembly was completely filled with buffer. Exactly 10 ml of 1A solution ($\sim 10^{-5}$M) were added to the cell and stirred for 10 minutes. The solution was filtered down to 1 ml with 18 psi N_2 pressure; two fractions (4.5 ml each) were collected in the fractionator. Next, 9 ml of buffer with Mg^{2+} were added to the ultrafiltration cell and stirred for 10 minutes.

Again, the solution was filtered until 1 ml of protein concentrate remained in the cell. This procedure was repeated several times with varying concentrations of Mg^{2+} in the 9 ml of the added buffer. Effluent samples were analyzed for magnesium content by atomic absorption spectroscopy. Total magnesium (free plus bound) concentration in the cell was measured upon completion of the binding experiment.

Results

Purity and Chemical Characterization of 1A

The purity of component 1A was estimated by disc gel electrophoresis employing a Tris-HCl buffering system and using gels of 7, 10, and 17% acrylamide concentration (Figure 5.4). As seen, the component migrates as a single species in each of the gels. A plot of log (mobility x 100) versus percentage gel shows a linear relationship. These results indicate that the protein is homogeneous with respect to charged isomers.[54] Recent findings with SDS (sodium dodecyl sulfate) disc gel electrophoresis indicate that the protein consists of two identical subunits of 40,000 daltons each.[45]

The amino acid analysis of 1A is reported in Table 5.1. The carbohydrate content is 30%, which suggests a glycoprotein. Preliminary isoelectric focusing experiments reveal an isoelectric point of 4.6,[45] a result consistent with the large amounts of glutamic and aspartic acid residues present. Protein concentration was estimated by the absorbance at 280 nm. The molar absorbance, ε, based on 1 mg/ml samples, is 5.4 x $10^4 M^{-1} cm^{-1}$, using the molecular weight of 1A as 80,000 daltons (Chapter 4).

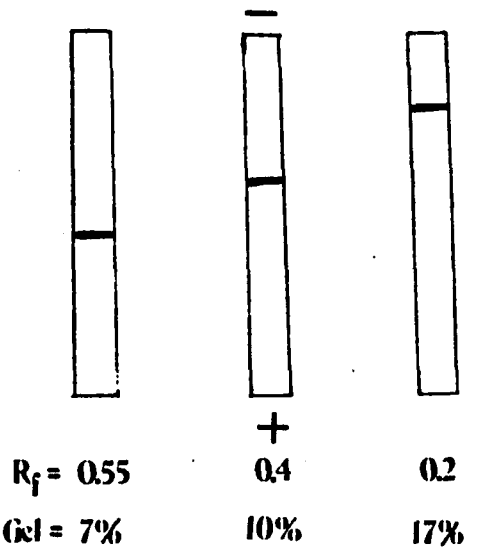

Figure 5.4. Disc gel electrophoresis analysis of component 1A in 7, 10, and 17% gel concentrations.

Table 5.1

Amino Acid Composition of 1A[3]

	Residues/1000 amino acid residues
Lysine	41
Histidine	12
Arginine	24
Aspartic acid[1]	217
Threonine	73
Serine	68
Glutamic acid[2]	114
Proline	12
Glycine	140
Alanine	69
Cysteine	11
Valine	31
Methionine	13
Isoleucine	41
Leucine	64
Tyrosine	30
Phenylalanine	40

[1]Value is given as sum of asparagine and aspartic acid.

[2]Value is given as sum of glutamine and glutamic acid.

[3]Precision to within 6%.

Metal Content and Stoichiometry

Qualitative optical emission spectroscopy on lyophilized 1A samples indicate that calcium, magnesium and sodium are present. Calcium and magnesium stoichiometries were determined on several 1A samples by atomic absorption spectroscopy. The molar ratios of calcium and magnesium to protein were found to be 3.1 ± 0.3 and 1.8 ± 0.2 respectively, based on an apparent molecular weight of 80,000 daltons. Therefore 1A is formulated as $Ca_3Mg_2$1A.

Dialysis of the native protein, $Ca_3Mg_2$1A against the chelating agent EDTA at pH 7.7 removed both Mg^{2+} ions but not the three Ca^{2+} ions, yielding the component $Ca_3$1A. Dialysis against the chelate at pH 4.6 induces removal of both metal ions ("Apo" 1A). It appears that the calcium sites are accessible to EDTA only through reductions in pH or possible conformational changes brought about at its isoelectric point (pI 4.6).

Binding of Mn^{2+} and Mg^{2+} Using EPR

This spectroscopic method was done by measuring the intensities of the EPR peaks of the free manganese ion. EPR has been used previously for determining association constants of manganese complexes with proteins.[57,83] The measurement is based on the fact that the broad, room-temperature EPR signal of the protein bound manganese has a neglible contribution to the free manganese signal.[84]

In this study, a constant "Apo" 1A concentration (1.4×10^{-5}M) was titrated in the concentration range 10^{-6}

to 10^{-4}M. The pH, checked before and after the experiment, was 7.9 ± 0.2. The amounts of free manganese were determined from a calibration curve while bound manganese was determined by the relationship:

$$[Mn^{2+}]_{bound} = [Mn^{2+}]_{added} - [Mn^{2+}]_{free}$$

To determine the binding constant, number, and classes of sites, the data was cast in the form of a Scatchard plot.[64] This type of plot is described by the law of mass action:[85]

$$\tilde{v} = \sum_{i=1}^{n} \frac{n_i K_i [Mn^{2+}]f}{1 + K_i [Mn^{2+}]f}$$

where $\tilde{v}$ = moles of manganese bound per mole of "Apo" lA; n_i = the number of sites per class, i; K_i = the association constant for type i sites and $[Mn^{2+}]f$ = free manganese concentration. If there is one class of sites, a plot of $\tilde{v}/[Mn^{2+}]f$ versus $\tilde{v}$ should yield a straight line such that when $\tilde{v} = 0$, $\tilde{v}/[Mn^{2+}]f = nK$ and when $\tilde{v}/[Mn^{2+}]f = 0$, $\tilde{v} = n$ and the slope of the line = -K.

When the titration data is put into such a form, the data obtained in Table 5.2 are obtained. Figure 5.5 shows the Scatchard plot of this data and indicates, within experimental error, that there is only one class of sites. There are approximately two sites with an association constant of $1.1 \times 10^{5} M^{-1}$.

Table 5.2

Data from the Titration for Scatchard Plot

$[Mn^{2+}]_{free}$ (x 10^{6}M)	$[Mn^{2+}]_{bound}$ (x 10^{6}M)	$\tilde{v}$	$\frac{\tilde{v}}{[Mn^{2+}]_{free}}$ (x 10^{-5}M)
2.08	4.59	0.33	1.58
4.43	8.91	0.64	1.44
7.68	12.32	0.87	1.15
16.20	17.14	1.23	0.76
26.38	20.29	1.46	0.55
32.47	20.87	1.50	0.46
39.08	20.92	1.51	0.38
45.70	20.97	1.51	0.33
50.99	22.35	1.61	0.31

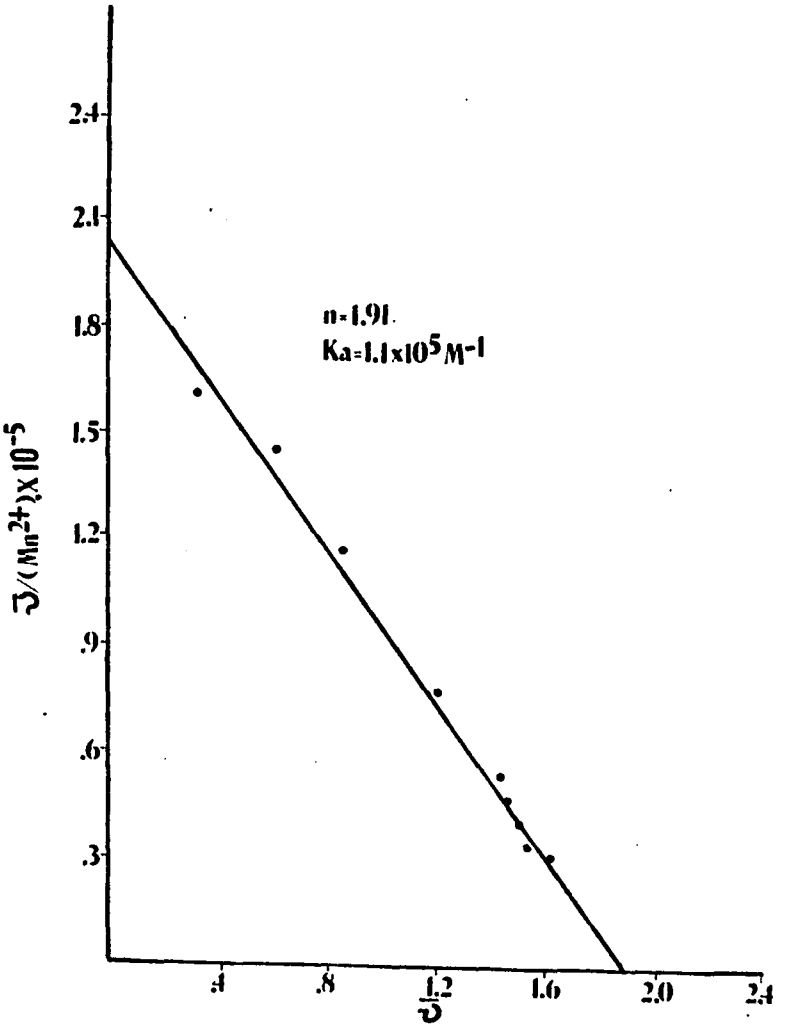

Figure 5.5. Scatchard plot of the titration of "Apo" 1A with Mn^{2+}.

Competitive Binding between Mn^{2+} and Mg^{2+}

Figure 5.6 shows the displacement of Mn^{2+} from its sites by Mg^{2+}. Here, the relative EPR signal intensity of free manganese is plotted as a function of Mg^{2+} added to the final Mn^{2+}-1A solution from the previous experiment. Mg^{2+} displaces Mn^{2+} completely as evidenced by the sharp increase in the Mn^{2+} free EPR signal intensity which levels off after ∿2 equivalents of Mg^{2+} are added. These results indicate high affinity of the sites for Mg^{2+}.

From the equation:

$$K_{Mg} = \frac{[Mg^{2+}\ 1A]}{[Mg^{2+}]_{free}[1A]}$$

where: $[Mg\ 1A]\alpha$ = the increase in $[Mn^{2+}]_{free}$ as measured by EPR

$$[Mg^{2+}]_{free} = [Mg^{2+}]_{added} - [Mg^{2+}1A]$$

and $$[1A] = n[1A]_{total} - [Mg^{2+}1A],$$

the lower limit for K_{Mg} for each site can be determined. In this experiment $n[1A]_{total} = 28 \times 10^{-6}M$ which equals the increase in the concentration of free Mn^{2+} after two equivalents of Mg^{2+} are added. The uncertainty in $[Mn^{2+}]_{free}$ is on the order of ∿5%; therefore the $[Mg^{2+}]_{free}$ can only be measured down to ∿5% of $[Mg^{2+}]_{added}$. Accordingly, this places a lower limit on K_{Mg} of $2.5 \times 10^{6}M^{-1}$.

Ca^{2+} Binding by 1A - Flow Dialysis

Flow dialysis is based on the principle that the rate of diffusion across a membrane is proportional to the

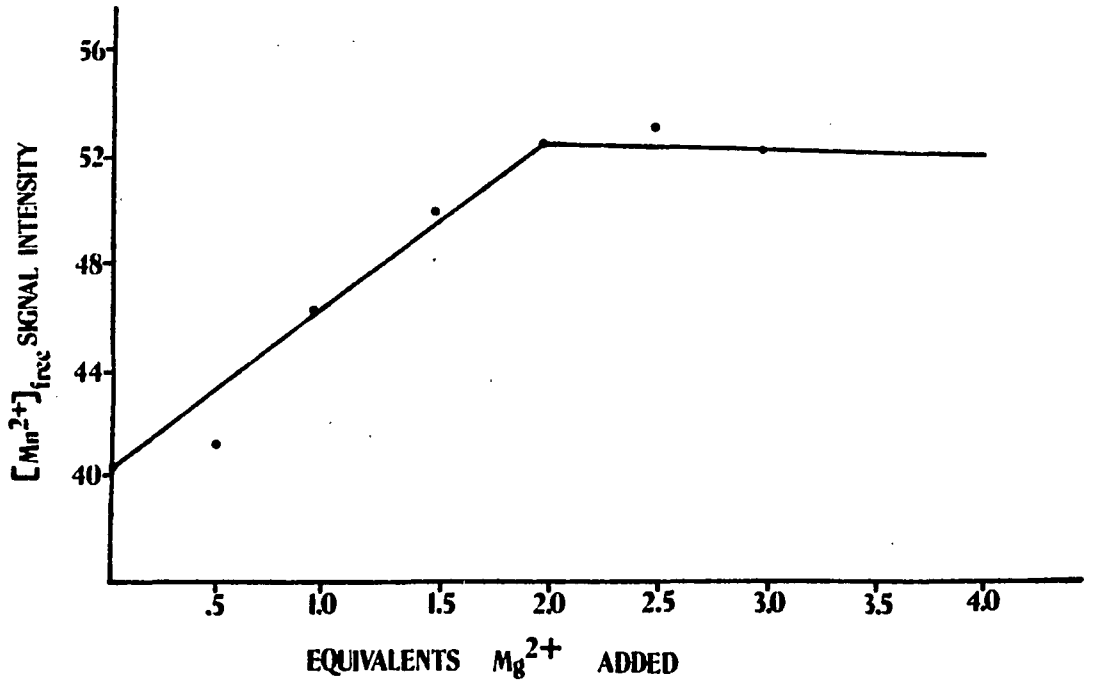

Figure 5.6. Plot of Mn^{2+} free signal intensity versus equivalents Mg^{2+} added.

concentration of free diffusible $^{45}Ca^{2+}$ ions; the rate will be constant when equilibrium is achieved with the protein in the upper chamber and a steady state flow in the lower chamber is maintained. Equilibrium is reached in a few seconds, and constant diffusion rate occurs within 1.5 minutes when the effluent volume pumped through the lower chamber is about four times the volume of the lower chamber.[82]

At the beginning of a metal binding experiment, $^{45}Ca^{2+}$ was introduced into a solution in the upper chamber at a concentration ($\sim 10^{-6}$M) below that of the macromolecule ($\sim 10^{-5}$M). As soon as a constant diffusion rate was reached, $^{40}Ca^{2+}$ was added to the upper chamber. A new equilibrium was reached. An increased fraction of the total metal was free and hence diffusible. Because of the exchange, the $^{45}Ca^{2+}$ diffusing across the membrane is a measure of the total free Ca^{2+}. Additions of $^{40}Ca^{2+}$ were made repeatedly, and a series of values was obtained for the fractions of free metal ion at each concentration of $^{40}Ca^{2+}$. The final $^{40}Ca^{2+}$ concentration ($\sim 10^{-2}$M) was in large excess relative to the protein concentration, hence the fraction of bound metal became negligible.

Figure 5.7 shows a typical $^{45}Ca^{2+}$ diffusion rate profile of calcium binding to "Apo" 1A in the presence of 1mM Mg^{2+}. At time zero 1 x 10^{-6}M $^{45}Ca^{2+}$ was added to the medium in the presence or absence of protein. The medium and dialysis buffer contained 0.1M Tris-HCl buffer (pH 7.9) and 1mM Mg^{2+}. The upper curve is a control curve in the absence

Figure 5.7. Measurement of calcium binding to "Apo"1A in presence of 1 mM Mg^{2+} at varying calcium concentrations.

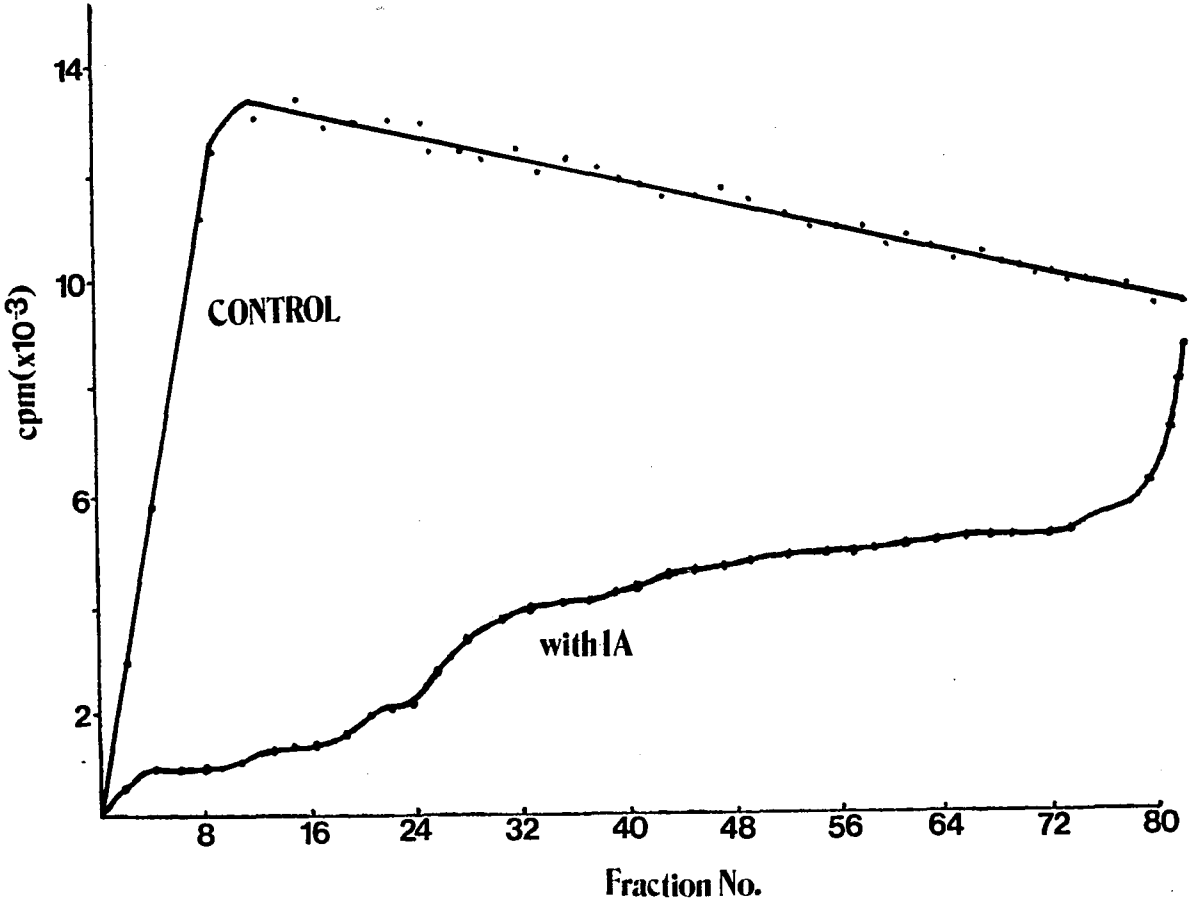
14
10
6
2
cpm(x10-3)
CONTROL
with IA
8
16
24
32
40
48
56
64
72
80
Fraction No.

of protein. The lower curve represents the diffusion rate profile of $^{45}Ca^{2+}$ in the presence of "Apo" 1A (2.6×10^{-5}M) at various $^{40}Ca^{2+}$ concentrations as indicated in Table 5.3. Eight 2 ml fractions were collected before the next aliquot of $^{40}Ca^{2+}$ was added. The data for these experiments were first plotted in this manner to allow calculation of the extent of Ca^{2+} binding for each step. Values of free and bound Ca^{2+} were then derived. For example, from Figure 5.7 and Table 5.4, at a total Ca^{2+} concentration of 2×10^{-5}M, the fraction of Ca^{2+} free is $\frac{2,519 \text{ counts/min}}{12,502 \text{ counts/min}}$ or 0.2, so that the values of free and bound Ca^{2+} are 0.4×10^{-5}M and 1.6×10^{-5}M respectively. From these values and the protein concentration, a Scatchard plot can be constructed. If there is more than one type of site, the plot should yield a curve which is concave upward. When the parameters of each site are known and the value of $\tilde{\nu}$ corrected for these contributions, the final plots are straight lines.

The Scatchard plot shown in Figure 5.8 reveals two classes of sites for Ca^{2+} binding to "Apo" 1A in the presence of excess Mg^{2+}; a high affinity site accommodating $1Ca^{2+}$ ($n = 0.86$) and $K_{Ca} = 6 \times 10^{5}M^{-1}$ and weak sites with $K_{Ca} = 3.3 \times 10^{4}M^{-1}$ and a stoichiometry of ~ 2 ($n = 2.36$). No observable binding of Ca^{2+} to $Ca_3Mg_2$1A could be detected by flow dialysis or calcium ion specific electrode methods. These results do not preclude the possibility of other low affinity Ca^{2+} binding sites with $K < 10^{3}M^{-1}$ however.

The binding of Ca^{2+} to component $Ca_3$1A was examined.

Table 5.3

Concentrations of Unlabeled Calcium Added at Various Intervals in Figure 5.7

Fraction No.	$[^{40}Ca^{2+}]$ (x 10^{5}M)
8	1.0
16	2.0
24	3.0
32	5.0
40	7.0
48	9.0
56	12.0
64	15.0
72	10^{-2}M

Table 5.4

Data for Scatchard Plot of Ca^{2+} Binding to "Apo"1A in Presence of 1mM Mg^{2+}

$[Ca^{2+}]_{free}$ (x 10^{6}M)	$[Ca^{2+}]_{bound}$ (x 10^{6}M)	$\tilde{v}$	$\frac{\tilde{v}}{[Ca^{2+}]_{free}}$ (x 10^{-4}M)
1.0	9.0	0.35	35.0
4.0	16.0	0.62	15.0
9.3	20.7	0.80	8.6
19.0	31.0	1.20	6.3
29.9	40.1	1.55	5.2
43.1	46.9	1.81	4.2
63.4	56.6	2.19	3.4
83.6	66.4	2.56	3.1

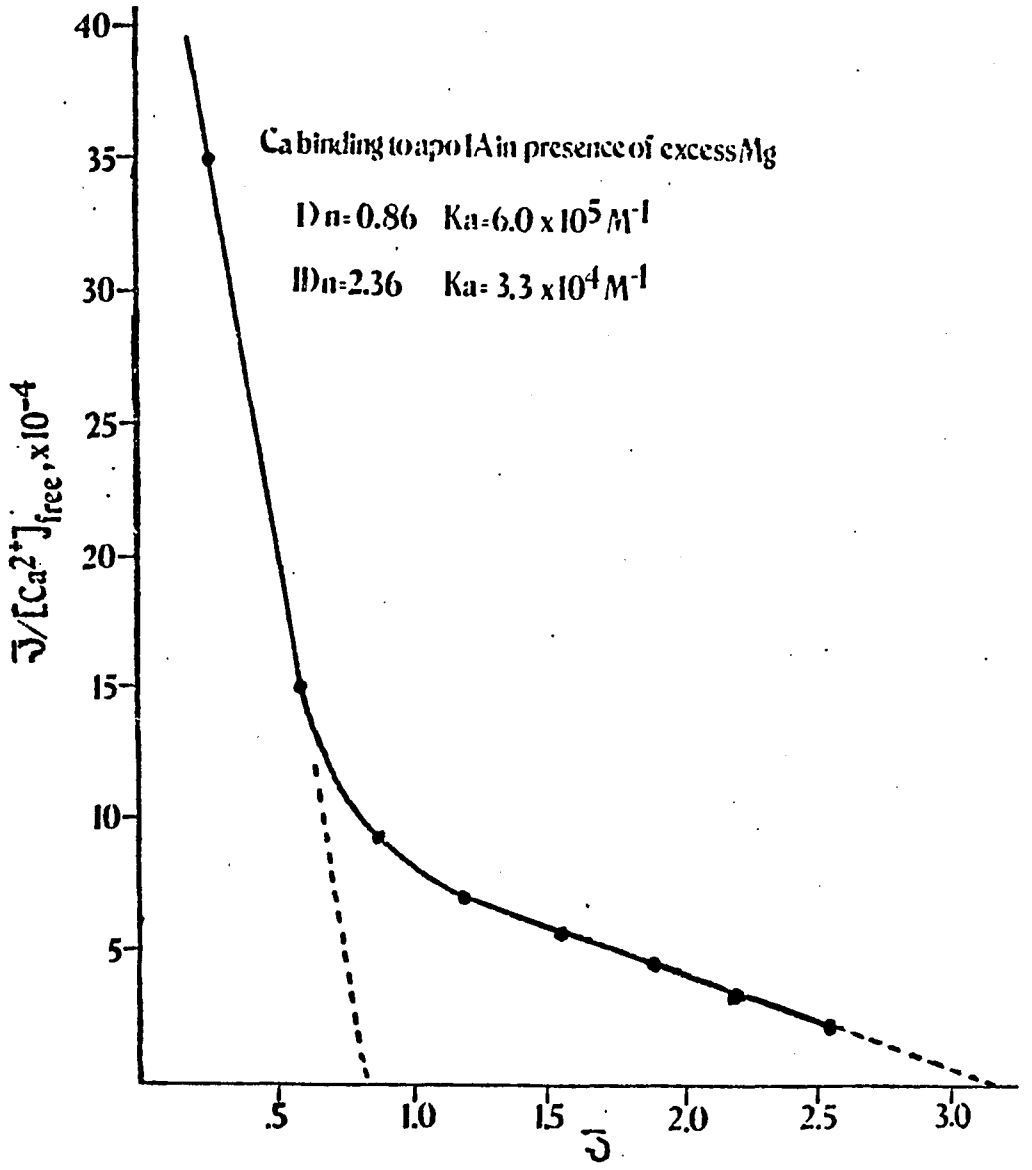

Figure 5.8. Scatchard plot of the data derived from the steady state values in Figure 5.7.

Data for this experiment is presented in Table 5.5 and cast into a Scatchard plot (Figure 5.9). One class of sites accommodating ∿2 Ca^{2+} ions (n = 2.34) and an association constant of 2.5 x $10^4 M^{-1}$ is evident.

<u>Mg^{2+} Binding to 1A - Ultrafiltration and Atomic Absorption Spectroscopy</u>

For the simple reaction of a metal such as Mg^{2+} binding to a protein,

$$Mg^{2+} + P \rightleftharpoons Mg^{2+}P$$

the equilibrium constant for 10 ml of solution in an ultrafiltration cell is

$$K_0 = \frac{[Mg^{2+}P]_0}{[Mg^{2+}]_0\ [P]_0}$$

where $[Mg^{2+}]_0$ = the concentration of free Mg^{2+}, $[P]_0$ = the concentration of unbound protein, and $[Mg^{2+}P]$ = the concentration of bound Mg^{2+}. When the solution is concentrated down to 1 ml, the new equilibrium expression is

$$K_1 = \frac{[Mg^{2+}P]_1}{[Mg^{2+}]_1\ [P]_1}$$

Since $[Mg^{2+}P]_1 = 10[Mg^{2+}P]_0$, $[P]_1 = 10[P]_0$ and $[Mg]_0 = [Mg]_1$; then $K_0 = K_1$ as it should be. Since we know $[Mg^{2+}]_{total}$, and can measure $[Mg^{2+}]_{free}$, we can calculate $[Mg^{2+}P]$ from the

Table 5.5

Data for Scatchard Plot of Ca^{2+} Binding to Ca_3 1A

$[Ca^{2+}]_{free}$ ($\times 10^{6}$M)	$[Ca^{2+}]_{bound}$ ($\times 10^{6}$M)	$\tilde{v}$	$\frac{\tilde{v}}{[Ca^{2+}]_{free}}$ ($\times 10^{-4}$M)
5.1	4.9	0.27	5.3
10.9	9.1	0.51	4.7
16.7	13.3	0.74	4.4
31.2	18.8	1.04	3.3
44.6	25.4	1.41	3.2
62.5	27.5	1.53	2.4
90.4	29.6	1.64	1.8
118.9	31.1	1.73	1.4

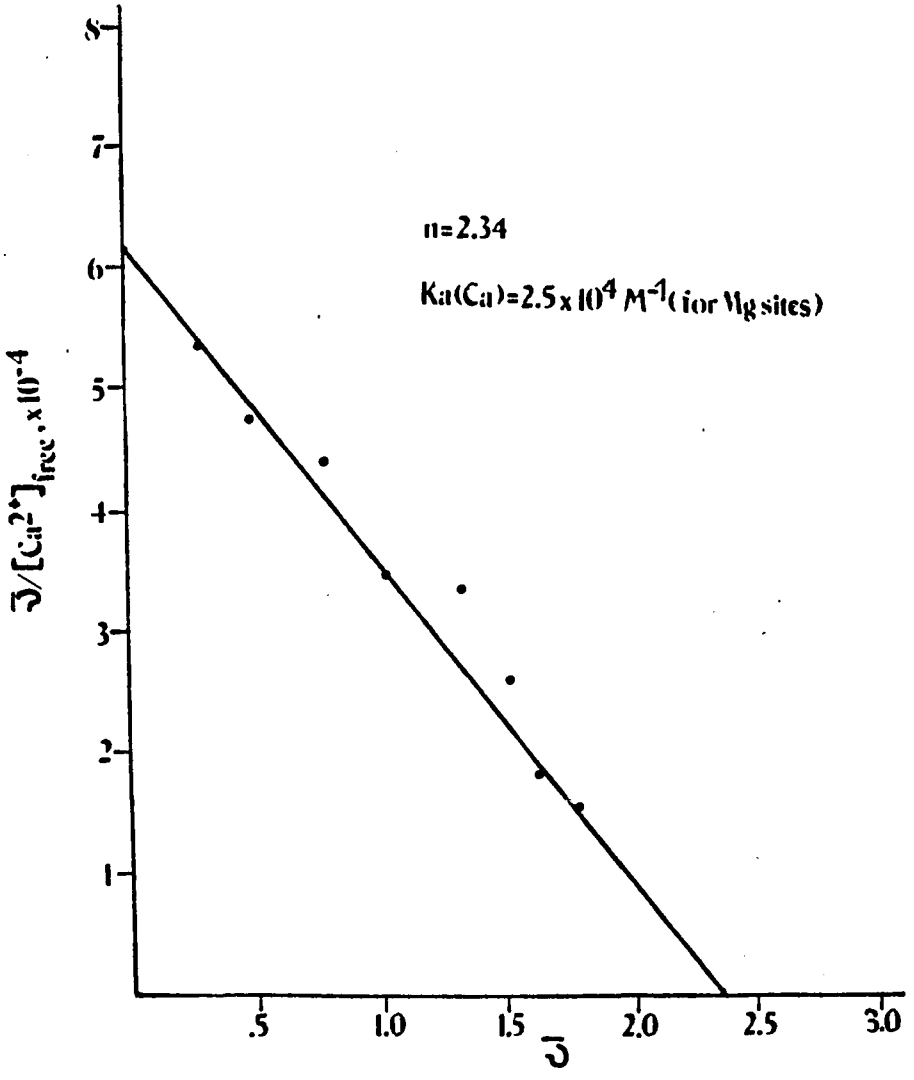

Figure 5.9. Scatchard plot of $Ca_3$1A binding to calcium using flow dialysis.

expression $[Mg^{2+}]_{total} = [Mg^{2+}P] + [Mg^{2+}]_{free}$. When more Mg^{2+} and buffer are added to the system and the volume brought to 10 ml, $[Mg^{2+}]_{total} = [Mg^{2+}]_{added} + [Mg^{2+}P] + \frac{[Mg^{2+}]_{free}}{10}$. From here the calculation of Mg^{2+} binding at various metal concentrations can proceed. Data for the binding of Mg^{2+} to "Apo" 1A and Ca_3 1A using this method are shown in Tables 5.6 and 5.7 respectively. Total Mg^{2+} (free plus bound) was measured after completion of each binding experiment.

The results for Mg^{2+} binding to "Apo" 1A and Ca_3 1A are shown in Figures 5.10 and 5.11 respectively. In Figure 5.10, the plot of $[Mg^{2+}]_{bound}$ (●) versus equivalents of Mg^{2+} added is linear and breaks off sharply at approximately 2 equivalents of Mg^{2+} added. This establishes that there are 2 magnesium binding sites on the macromolecule. A plot of $[Mg^{2+}]_{free}$ (▲) versus equivalents of Mg^{2+} added implies that site 1 has a higher affinity for Mg^{2+} than site 2. This can be explained by the resulting increase in $[Mg^{2+}]_{free}$ in the region where 1-2 equivalents of Mg^{2+} are added. Similarly, the same trend for component Ca_3 1A can be shown using metal binding data in Table 5.7 and Figure 5.11.

The lower limit of KMg for site 1 can be approximated from step #2 from each metal binding experiment. Calculation for this value can be done using the conditions below:

$$Mg^{2+} + 1A \rightleftharpoons Mg^{2+}1A$$

Table 5.6

Data for Equivalence Plot for Titration of "Apo"1A with Mg^{2+}. ["Apo"1A] = 1.75×10^{-5}M

Step #	$[Mg^{2+}]_{bound}$ ($\times 10^{6}$M)	$^{1}[Mg^{2+}]_{free}$ ($\times 10^{6}$M)	Equivalents Mg^{2+} Added
1	5.0	<0.3	0.29
2	10.0	<0.3	0.58
3	19.5	0.5	1.14
4	27.8	1.9	1.69
5	33.1	5.2	2.19
6	33.2	22.1	3.16
7	31.0	24.7	3.18
8	28.9	29.4	3.22
9	29.0	110.	5.85

[1]Detection limit for Mg^{2+} by atomic absorption spectroscopy = 3×10^{-7}M.

Table 5.7

Data for Equivalence Plot of the Titration of Component Ca_3lA with Mg^{2+}

$[Ca_3lA] = 2.1 \times 10^{-5}M$

Step #	$[Mg^{2+}]_{bound}$ ($\times 10^{6}M$)	$^{1}[Mg^{2+}]_{free}$ ($\times 10^{6}M$)	Equivalents Mg^{2+} Added
1	5.0	<0.3	0.26
2	10.0	<0.3	0.52
3	20.0	<0.3	1.05
4	30.0	<0.3	1.58
5	38.0	2.0	2.10
6	41.0	17.0	3.30
7	43.3	19.4	3.43
8	44.2	20.9	3.49
9	42.8	107.5	6.14

[1]Detection limit for Mg^{2+} by atomic absorption spectroscopy = $3 \times 10^{-7}M$.

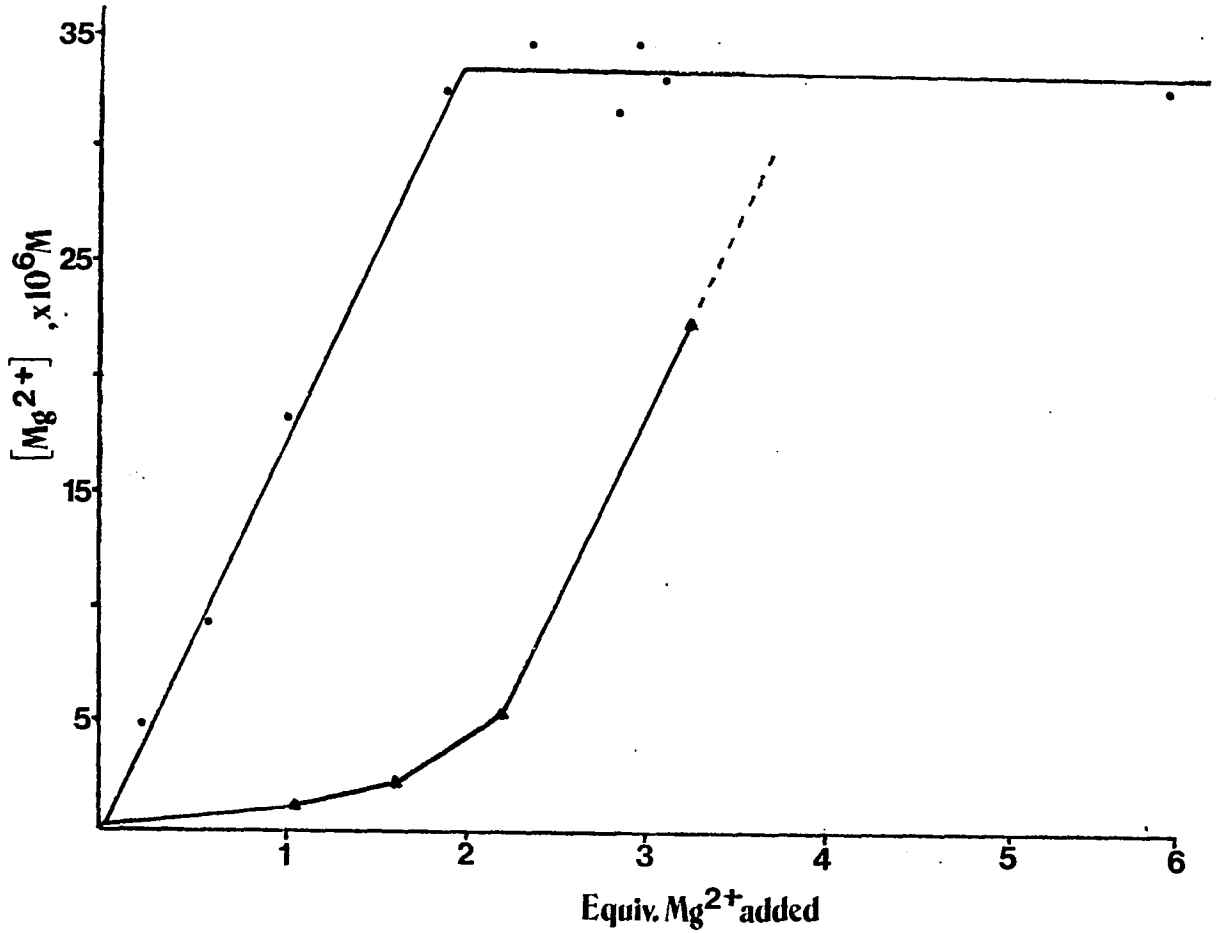

Figure 5.10. Plot of $[Mg^{2+}]_{bound}$ versus equivalents of Mg^{2+} added for magnesium binding to "Apo"1A. (●) = bound Mg^{2+}; (▲) = free Mg^{2+}.

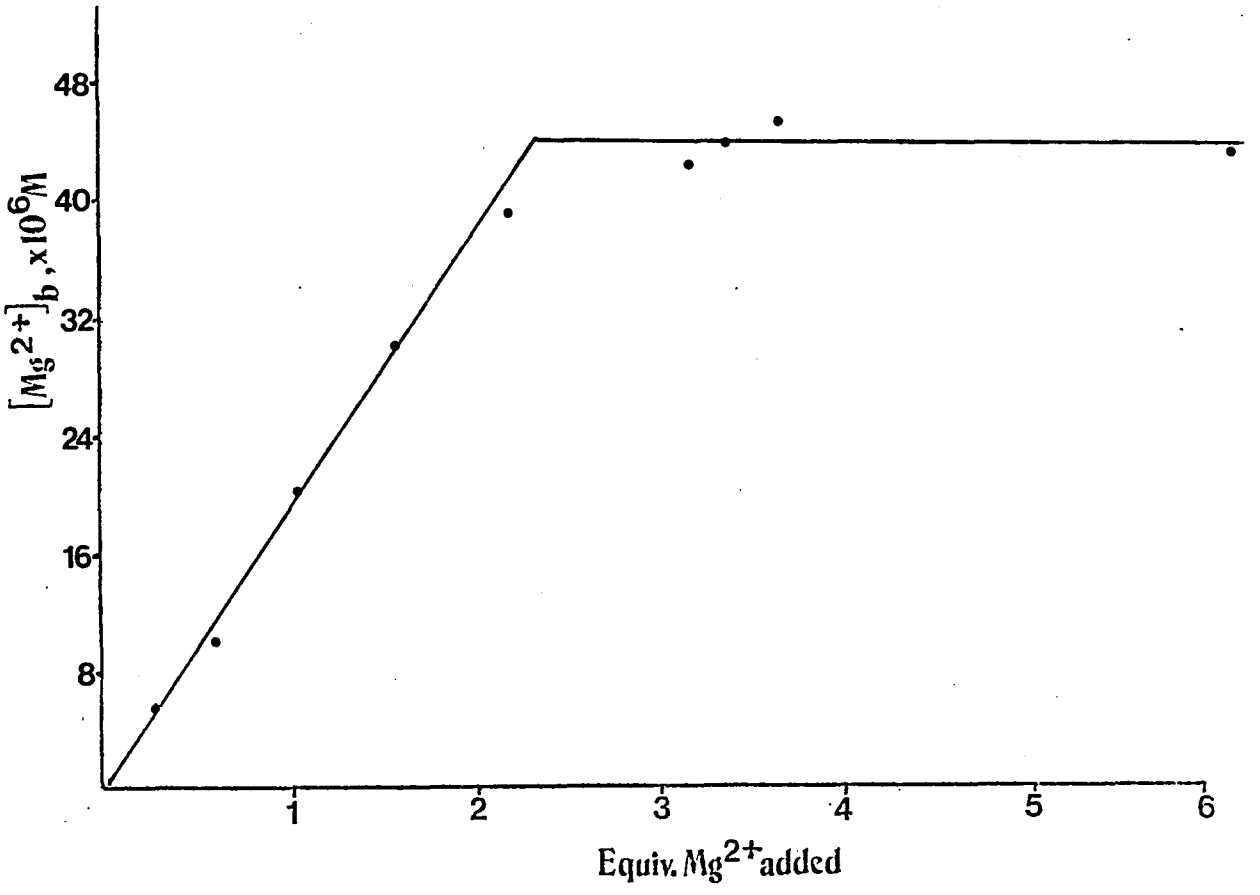

Figure 5.11. Plot of $[Mg^{2+}]_{bound}$ versus equivalents Mg^{2+} added for magnesium binding to $Ca_3$1A.

$$K_1Mg = \frac{[Mg^{2+}1A]}{[Mg^{2+}]_{free}\,[1A]_1}$$

where $[1A]_1 = [1A]_{total}$ (for site 1) - $[Mg^{2+}1A]$, $[Mg^{2+}]_{free}$ is the detection limit for Mg^{2+} by atomic absorption spectroscopy ($3 \times 10^{-7}M$), and $[Mg^{2+}1A]$ is calculated. K_1Mg for site 1 $\geq 3.9 \times 10^{6}M^{-1}$.

To determine K_2Mg for site 2, we use these conditions:

$$Mg^{2+}1A + Mg^{2+} \rightleftharpoons Mg_2{}^{2+}1A$$

$$K_2Mg = \frac{[Mg^{2+}1A]}{[Mg^{2+}]_{free}\,[1A]_2}$$

where $[1A]_2 = [1A]_{total}$ (for site 2) = $[1A]_{total}$ - ($Mg^{2+}1A$ + $Mg_2{}^{2+}1A$), $[Mg^{2+}]_{free}$ is measured, and $[Mg_2{}^{2+}1A]$ is calculated. from step #5 in each metal binding experiment, we calculate $K_2Mg = 1.8 \times 10^{6}M^{-1}$ for site 2. The values for K_1Mg and K_2Mg are in good agreement with values obtained with EPR measurements.

These results suggest that Mg^{2+} does not bind to the Ca^{2+} sites but does bind to the Mg^{2+} sites tightly.

Discussion

The three-step isolation procedure described in Chapter 4 yielded a calcium-magnesium binding glycoprotein (1A) from the extrapallial fluid. The electrophoretic properties

of the component indicated the absence of any major protein contaminants.

Several molecular properties of 1A have been characterized. 1A has a high content of carbohydrate (30% by weight). Although uncharacterized, the carbohydrate portion may contain acidic side groups (e.g., sulfate) that can bind metal ions. The low isoelectric point (4.6) of 1A appears compatible with its amino acid composition (Table 5.1) and is due to the presence of acidic side chains on the proteinaceous or carbohydrate portions of the molecule. The high proportion of dicarboxylic amino acids (33% in 1A) is also found in other high affinity calcium binding proteins.[86-89] In addition, such proteins have normally been found to have pI's in the range of 4 - 5.

Mathjia and Degens[91] and Wilbur and Simkiss[57] have proposed that binding of calcium by carboxyl groups of glutamic and aspartic acid residues could concentrate calcium ions. However, Crenshaw[92] states that these residues are present as their amides which would bind little or no calcium. The small amount of basic amino acid residues (e.g., lysine and arginine) present and the low pI of 1A seem to refute this finding but no conclusions should be drawn until the carbohydrate portion is characterized.

1A has a molecular weight of 80,000 (Chapter 4) and appears to consist of two subunits of identical size.[45] The interaction of these subunits appears to be disulfide-dependent. Further, other factors such as Ca^{2+} or Mg^{2+} ions might also be involved in the subunit assembly of the protein.

Qualitative optical emission spectroscopy on 1A shows the presence of calcium and magnesium. Atomic absorption spectroscopy on several purified samples indicates there are three Ca^{2+} ions and two Mg^{2+} ions associated with each molecule. The native component for metal binding studies was formulated $Ca_3Mg_2$1A.

Ensuing dialysis experiments to remove the divalent metals suggests that the binding sites are located in different regions of the protein. Dialysis of $Ca_3Mg_2$1A against EDTA at physiological pH readily removes the two Mg^{2+} ions but not Ca^{2+} ($Ca_3$1A). The Mg^{2+} sites are probably located on the surface of the molecule. The three Ca^{2+} ions are only removed upon dialysis against a chelating agent at pH 4.6, the isoelectric point of the protein. It appears that the Ca^{2+} sites are located in the interior of the molecule and become accessible only through a reduction in pH to where the net charge of the molecule is zero and possible alteration of the protein occurs. This is substantiated by recent findings. When "Apo" 1A was reconstituted with Ca^{2+} and dialyzed against EDTA or EGTA at pH 7.0, the metal was readily removed, suggesting that the Ca^{2+} sites on the protein have been altered after a reduction in pH to 4.6.

My findings reveal that the metal binding properties of 1A are unique. The results are summarized in Table 5.8. 1A contains one Ca^{2+} binding site that has an affinity of $6.0 \times 10^5 M^{-1}$ and two with an affinity of $3.3 \times 10^4 M^{-1}$. These sites appear highly specific for calcium, as evidenced by

the absence of Mg^{2+} or Mn^{2+} binding. These results suggest that the protein possesses three binding sites with a high degree of stereospecificity and that Ca^{2+} binding is not a result of simple electrostatic or ionic interactions.[1] Since solubilized calcium is continually available in the fluid ($\sim 10^{-2}$M), the calcium affinity of 1A should guarantee that the protein is bound with its full complement of Ca^{2+} ions. If binding to the protein portion of the molecule is assumed, the magnitude of the association constant can be compared with stability constants for Ca^{2+} binding to model compounds.[93] The results suggest that three or more carboxyl groups of 1A are coordinated with each Ca^{2+} ion.

Recently carboxylic groups of eggshell matrix have been modified according to the procedure of Hoare and Koshland.[94] When the groups were blocked with water-soluble carbodiimides, the Ca^{2+} binding affinity of the matrix decreased rapidly.[95] The implied dependence of Ca^{2+} binding to 1A on the presence of ionized carboxyl groups is important and needs to be resolved. Further studies along these lines are needed.

1A also contains two Mg^{2+} binding sites which also bind Mn^{2+} and Ca^{2+}. The order of affinities for these three cations is as follows: $Mg^{2+} > Mn^{2+} > Ca^{2+}$. This selectivity series can be rationalized by their corresponding radii (Table 5.8) and suggests that radial size is an important factor in determining binding affinity for these particular sites. Mg^{2+} appears to have the optimum radial size for

Table 5.8

Summary of Metal Binding Studies for the Glycoprotein 1A

Metal	Method of Study	Component Used	Mg^{2+} "high affinity" Sites	Ca^{2+} Specific Sites
Mn^{2+} (r=0.80Å)	EPR spectroscopy	"Apo" 1A	One class of sites n=1.91, $K_{Mn}=1.1x10^{5}M^{-1}$	No binding
Mg^{2+} (r=0.65Å)	Indirect EPR spectroscopy	Mn_2^{2+} 1A	$K_{Mg}\geq 2.5x10^{6}M^{-1}$	No binding
	Ultrafiltration and AA spectroscopy	"Apo" 1A and Ca_3 1A	K_{1Mg}(site1) $\geq 3.9x10^{6}M^{-1}$ K_{2Mg}(site2)=$1.8x10^{6}M^{-1}$	No binding
Ca^{2+} (r=1.06Å)	Flow dialysis	Ca_3Mg_2 1A	No binding	No binding
	Flow dialysis	"Apo" 1A with 1mM Mg^{2+}	No binding	Two classes of sites n=0.86, $K_{Ca}=6.0x10^{5}M^{-1}$ n=2.36, $K_{Ca}=3.3x10^{4}M^{-1}$
	Flow dialysis	Ca_3 1A	One class of sites n=2.34, $K_{Ca}=2.5x10^{4}M^{-1}$	-----

these sites which appear to be tight and preferential for Mg^{2+}.

To summarize the metal binding data here, the glycoprotein 1A contains five cation binding sites: three Ca^{2+}-specific sites that do not bind Mn^{2+} or Mg^{2+} and two Mg^{2+} sites that also bind Mn^{2+} and Ca^{2+}.

The role of Mg^{2+} is not clear. Speculation about the function of Mg^{2+} seems unwarranted without more evidence. The role of the bound Ca^{2+} ions might very well be in maintaining protein structural integrity. Clearly these sites are altered significantly upon reduction in pH to 4.6, the pI of the protein. This suggests that the metal has an important role in protein conformation. Additionally, calcium has been shown to impart thermal stability to several proteins.[88-90]

At present there are several proteins which have been reported to possess specific and/or physiologically significant calcium and magnesium binding activity.[1] Many of these proteins are associated with metal-transporting systems, including intestines,[96] kidneys,[97] the parathyroid gland,[98] the pancreas,[99] and avian shell glands.[100] Calcium-magnesium binding proteins are also present in several intracellular metal-regulating systems, e.g., mitochondria and the sarcoplasmic reticulum.[1]

The exact function of this glycoprotein in relation to the calcification process is not clear. Normally three events take place in metal transport systems: (1) selective

binding of a metal to a carrier molecule, (2) transport of the metal-carrier species to various locations, and (3) release of the metal by a change in the binding affinity of the carrier molecule. Since 1A meets criterion (1) by having a selective affinity for Ca^{2+}, further studies to meet criteria (2) and (3) might prove beneficial in defining additional properties of the protein. However, since the calcium bound by this protein is such a small fraction of the total calcium in the fluid, 1A is probably not important in metal transport.

1A might act as a localizer of calcium at the inner shell surface, providing Ca^{2+} for the next step in the biomineralization process. Further, 1A appears to exist in several polymeric forms, depending on the concentration of Ca^{2+}.[45] This implies that the quaternary structure is changed by the presence of Ca^{2+}. The protein could in effect serve as a template for crystal initiation and growth.

Chapter 6

Partial Characterization of an

Isolated Phenoloxidase (1B)

The enzyme phenoloxidase is responsible for tanning reactions throughout the phylogenetic scale. Many, but not all, phenoloxidases are capable of catalyzing two distinct reactions: (1) the ortho hydroxylation of phenols and (2) the dehydrogenation of catechols to form quinones.

(1) 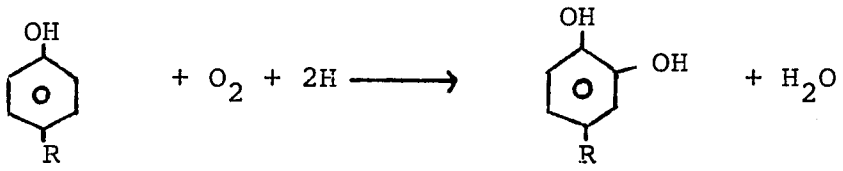

(2) 2 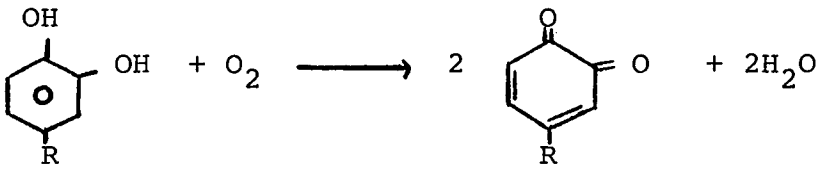

Quinones from reaction 2 are thought to initiate the browning process by crosslinking proteins in an undetermined manner.[51]

Phenoloxidase has been detected in the mantles and periostraca of the molluscs Pteria martensii, Cristaria plicata and Modiolus demissus.[51] The enzyme presumably aids in the crosslinking of presclerotin protein subunits of the periostracum.

A phenoloxidase (1B) from the extrapallial fluid of Mytilus was isolated and partially characterized. The electrophoretic properties, activity, amino acid content and metal association are reported.

Experimental Methods

Materials

3,4-L-dihydroxyphenylalanine (L-dopa), L-tyrosine, and α chymotrypsin, gifts of the Biochemistry Department, University of New Hampshire. All other chemicals were reagent grade or better.

Isolation of 1B

Details of the isolation of 1B are described in Chapter 4. In brief, centrifuged-dialyzed fluid was prepared and chromatographed as previously for enzyme studies with the exception that 0.1M Tris-HCl buffer, pH 7.9, was used for all experiments.

Electrophoresis and Amino Acid Analysis

The disc gel electrophoretic system described by Hedrick and Smith,[54] employing a Tris-HCl buffering system at pH 8.9 was utilized to estimate the number of protein bands in 1B at two different gel concentrations. Samples containing approximately 0.5-1 mg/ml were applied in 200 µl volumes to the gels. Electrophoresis was run at room temperature using Bromphenol Blue as the tracker dye. The gels were stained with Napthol Blue Black and destained with a Quick Gel Destainer (Hoefer Scientific).

Samples for amino acid analyses were prepared in the same manner as for 1A (Chapter 5).

Determination of ε_{280}

Lyophilized samples of 1B were weighed out by a technician and placed in appropriate amounts of buffer to give 1 mg/ml concentrations. The absorbance at 280 nm was measured on the samples using a Bausch and Lomb Spectronic 710 spectrophotometer. Values obtained were used for further studies in estimating 1B concentrations.

Metal Analyses

A Baird Associates Eagle Mount grating spectrograph was used for optical emission analyses. A Varian Techtron Model AA-3 spectrometer was used for atomic absorption analyses of copper. The wavelength and slit width employed were 324.7 nm and 50 μ, respectively.

Enzyme Assay

For 3,4-L-dihydroxyphenylalanine (L-dopa) as a substrate, one unit of enzyme activity is defined as 1 μmole of L-dopa oxidized per minute in 0.1M Tris-HCl buffer (pH 7.2, 25°C). The oxidation product of the reaction, dopachrome (2-carboxy-2,3 dihydroindole-5,6 quinone), absorbs maximally at 475 nm with an extinction coefficient of 3600 $cm^{-1}M^{-1}$.[101] Activity measurements were carried out with a Bausch and Lomb Spectronic 710 spectrophotometer using 1 cm quartz cells in which the sample cell contained 0.1M Tris-HCl buffer (pH 7.9), 1 mM L-dopa, 25 μg/ml chymotrypsin and

enzyme. The reference cell contents were identically prepared with the exception that the enzyme solution was heated in a water bath at 90°C for 30 minutes.

Results

Characterization of 1B

The purity of 1B was estimated using polyacrylamide disc gel electrophoresis (Figure 6.1). In 7% gel, the component migrated as a single sharp band. In contrast, three closely spaced bands were observed in the 17% gel. Many previous studies have shown that preparations of this enzyme may be separated by electrophoretic techniques into several enzymatically active species. It is therefore possible that 1B contains three isozymes.

The amino acid analysis is presented in Table 6.1. The enzyme contains a large amount of aspartic acid. Consistent with the analyses reported for other phenoloxidases,[105-107] 1B was also found to be free of carbohydrate.

Protein concentration was estimated by absorbance at 280 nm. The molar absorbance, ε, based on 1 mg per ml samples, is $1.4 \times 10^{5} M^{-1} cm^{-1}$, using the molecular weight of 1B as 80,000 (Chapter 4).

Optical emission spectroscopy on lyophilized samples indicate that copper, iron, and sodium are associated with 1B. Copper and iron stoichiometries were determined by atomic abosrption spectroscopy. The molar ratio of copper to protein was 1.5 while the ratio of iron to 1B was 0.9, based on a molecular weight of 80,000 daltons. EPR

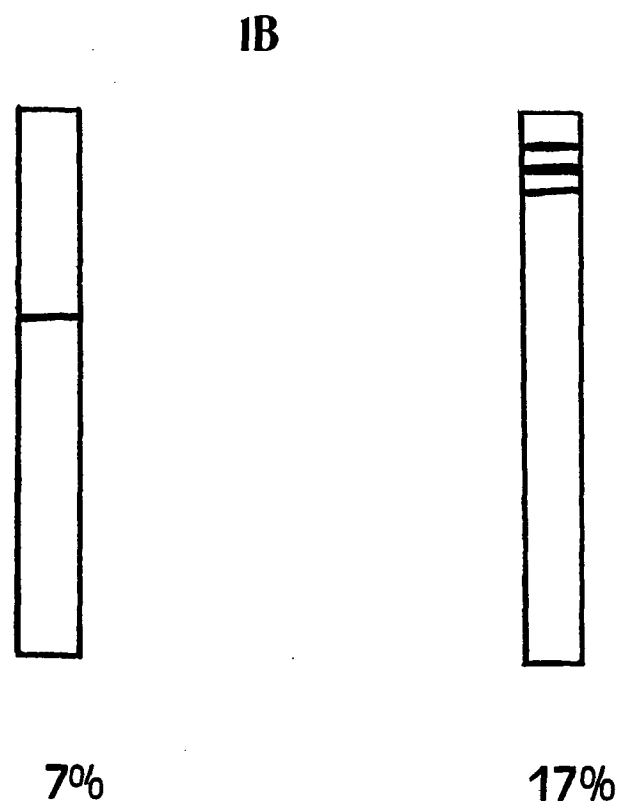

Figure 6.1. Disc gel electrophoresis analysis of component 1B in 7% and 17% gel concentrations.

Table 6.1

Amino Acid Composition of 1B[1]

	Residues/1000 amino acid residues
Lysine	74
Histidine	47
Arginine	22
Aspartic Acid	257
Threonine	56
Serine	59
Glutamic Acid	66
Proline	13
Glycine	62
Alanine	58
Cystine	14
Valine	39
Methionine	18
Isoleucine	65
Leucine	77
Tyrosine	47
Phenylalanine	26

[1]Estimated error = 6%.

measurements with native solutions of the enzyme suggest that all or most of the copper is present as Cu(I) as in all other phenoloxidases. When the enzyme is lyophilized however, and reconstituted into distilled-deionized H_2O, pH 7.0, a distinctive EPR signal due to Cu(II) is apparent, suggesting alteration of the protein. Figure 6.2 shows the 77°K EPR spectrum of reconstituted 1B (2.5×10^{-4}M) in the g = 2 region. The observed hyperfine structure is suggestive of two nitrogen ligands around the copper nucleus. This observation is in agreement with Fling et al.[102] who postulate that two histidine residues are bound to the copper atom at the active site in Neurospora crassa phenoloxidase. In addition, a high spin Fe(III) signal in the g = 4.3 region can be observed in lyophilized enzyme samples.

Initial assay experiments to detect phenoloxidase activity in the centrifuged-dialyzed fluid showed the presence of the enzyme (Figure 6.3). At t = 0, 300 µl of 10 mM L-dopa was added to 2700 µl of chymotrypsin treated solutions in the sample and reference cells. The contents in the reference cell had been boiled prior to the assay. Maximal activity was achieved after 45 minutes.

Gel filtration chromatography on the centrifuged-dialyzed fluid showed that phenoloxidase was totally associated with component 1 (Chapter 4). Further fractionation of peak 1 to Sephadex DEAE-A50 indicated that 1B exhibits the majority of enzyme activity in the fluid.

Figure 6.2. 77°K EPR spectrum in the g = 2 region of reconstituted fluid phenoloxidase. Modulation aptitude = 6.3G; Microwave power = 5mW; Scan rate = 200G/min; Time constant = 1 sec.; Frequency =~9.175 GHz.

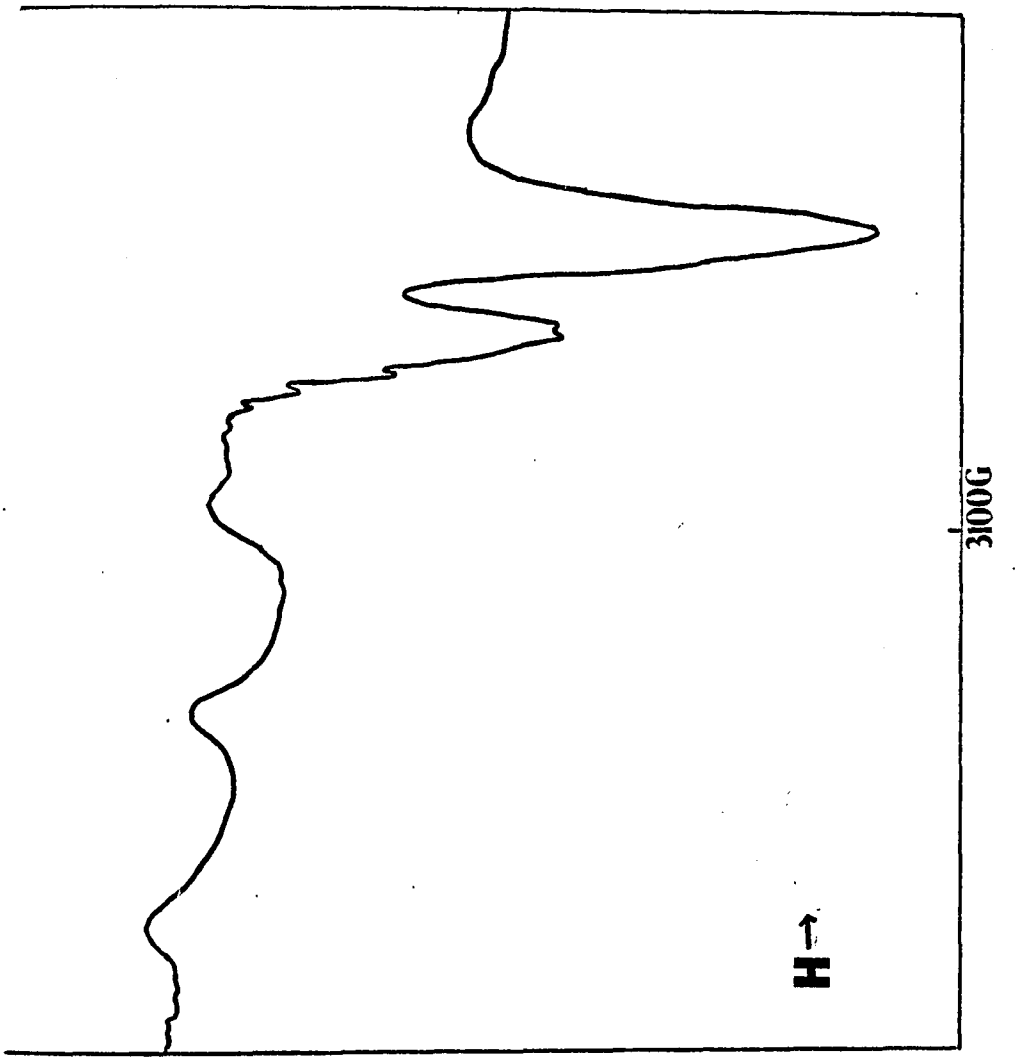
3100G
H

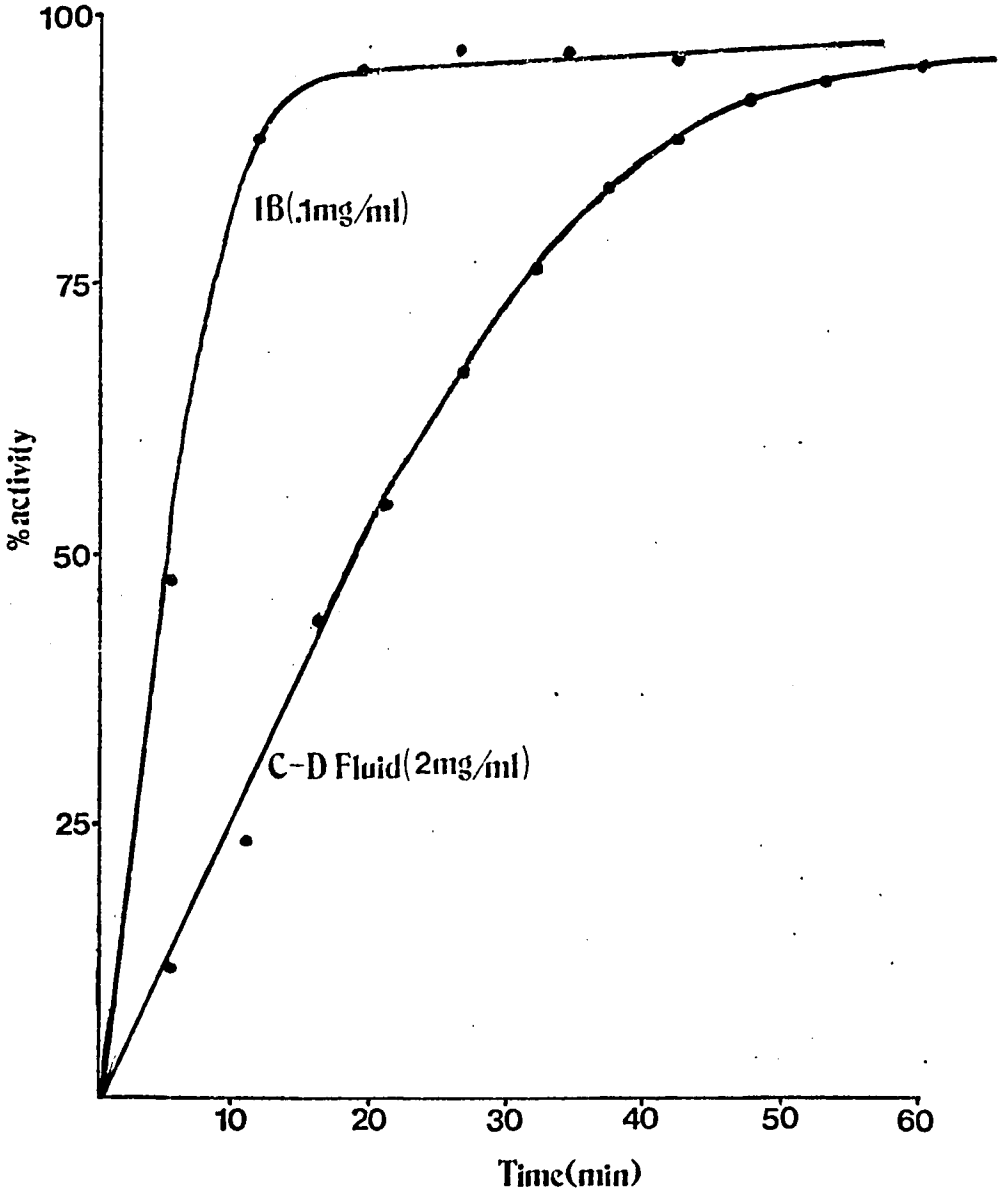

Figure 6.3. Phenoloxidase activity profile of centrifuged-dialyzed fluid and component 1B.

Specific Activity of 1B

One unusual feature of the fluid phenoloxidase is the dependence on chymotrypsin for activation. Little activity could be observed in any fluid samples without prior additions of the proteolytic enzyme.

Figure 6.3 shows the activity profile of 1B (1.25×10^{-6}M). Maximal activity was achieved after ten minutes. The specific catecholase activity of 1B was determined by the method of Fling et al.[102] and found to be 0.33 units/mg. Table 6.2 shows the specific activities of 1B and other phenoloxidases from the work of others. The activity of the fluid enzyme appears to be quite low when compared to phenoloxidases from other sources. Two different explanations can account for this: (1) the separation method described in Chapter 4 is unable to separate inactivated molecules of phenoloxidase from those which retain their activity or (2) the requirements of the animal are such that only a low activity enzyme is needed. Interestingly, the specific activity of a partially purified phenoloxidase from the mantle of M. demissus is also low (see Table 6.2).

Cresolase activity was attempted by an assay procedure using L-tyrosine as a substrate.[103] Surprisingly, no cresolase activity was observed with any fluid samples.

pH Effects on Activity

Partially purified 1B was used for estimation of the optimal pH for this enzyme. In the range pH 6-10.5, maximal activity was observed in the interval pH 7.5-8.0 (Figure 6.4).

Table 6.2

Specific Activities of Various Phenoloxidases

Using L-dopa as a Substrate

Source	Specific Activity[1] (units/mg protein present)
Mantle, *M. demissus*[51]	0.24
Extrapallial fluid, *M. edulis*	0.33
Periostracum, *M. demissus*[51]	212.0
N. crassa[104]	398.0
A. bisporus[107]	900.0

[1]One unit of enzyme activity is defined as 1 μmole of 3,4-L-dihydroxyphenylalanine (L-dopa) oxidized per minute.

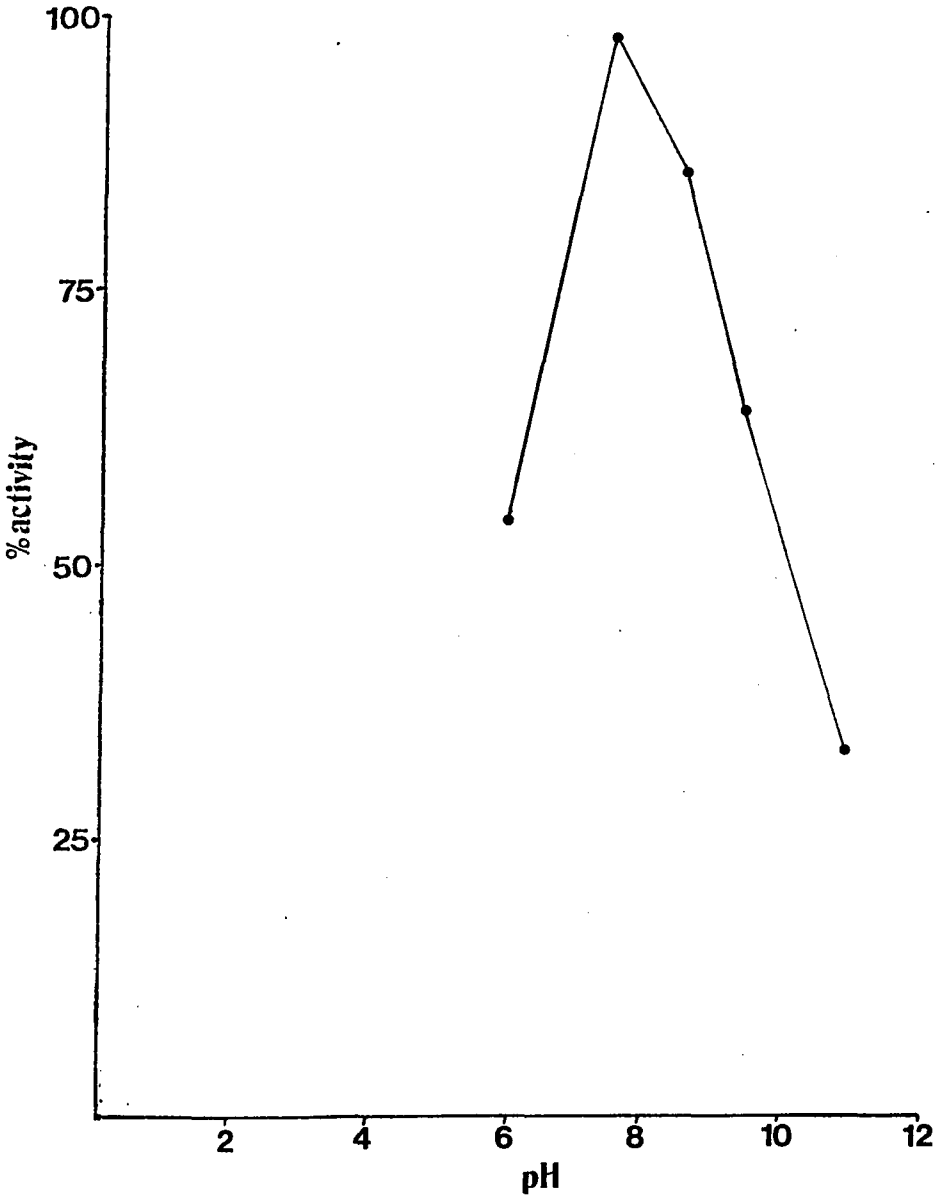

Figure 6.4. Effect of pH on the activity of fluid phenoloxidase.

Discussion

A phenoloxidase was isolated from the extrapallial fluid of Mytilus and is unusual in two respects. The fluid enzyme differs from classically described phenoloxidases in its (1) apparent low specific activity and (2) its dependence on chymotrypsin for activation. The absence of activity with L-tyrosine as a substrate is surprising but does not preclude the possibility of phenoloxidase activity toward other phenolic substrates.

The fluid enzyme is presumably stored in mantle cells lying along the epithelial edge.[51] The cellular storage of phenoloxidase and activation after secretion are important biological adaptations because the reaction catalyzed by the enzyme is harmful to living cells. Phenoloxidases in mantles and periostraca of some molluscs also undergo activation by chymotrypsin.[51] Although nothing is known about the activating mechanism in the fluid, it is very possible that one of the seven species observed in component 2 (Chapter 4) is a proteolytic enzyme.

1B appears to exist as at least three different forms. Multiple forms of phenoloxidase have been reported in mushrooms,[104] potatoes,[105,106] and mammalian tumors.[107,108] In a detailed study of the multiplicity of mushroom phenoloxidase,[109] it was found that the isozymes are interconvertible, depending on conditions of pH, ionic strength, and protein concentration. Several reasons have been suggested for the multiplicity of phenoloxidases: (a) various degrees

of polymerization of like subunits, (b) various combinations of unlike subunits, (c) conformational changes of a single protein, or (d) combinations of the three.

Van Holde[110] has assembled data for a number of proteins, classifying them as "single chain" or "multi-chain" and correlating this with the percentage of five hydrophobic residues (leucine, isoleucine, proline, valine, and phenylalanine). A hydrophobic residue content over 30% constitutes single chain proteins while less than 30% indicates multi-chain proteins. In 1B, the content of these five hydrophobic residues is 22.0%, indicative of a multi-chain protein and consistent with electrophoretic results.

Metal analyses indicate the presence of copper and iron with the enzyme. The iron is probably a contamination that is generally observed with many marine samples. Like all phenoloxidases, 1B contains copper in significant amounts. The copper content is 0.12%, as compared to 0.19% for other phenoloxidases.[104-108] This suggests that samples of the fluid enzyme might contain inactivated molecules and could help explain the apparent low specific activity observed. Total copper was determined on lyophilized samples of 1B. These particular samples gave a characteristic Cu^{2+} EPR signal (Figure 6.2). It is well known that inactivation of the enzyme is associated with the presence of EPR detectable copper. When the EPR spectrum is taken on unlyophilized samples of 1B, no signal due to a Cu^{2+}-polymer species is observed. The fluid enzyme might be immobilized upon lyophilization.

Molluscan mantles have been shown to be abundant in aromatic compounds, including L-dopa, halogenated tyrosine and halogenated tryptophan.[111-113] Since no catecholic substrate has yet been identified in the fluid, more studies along these lines are in order.

Chapter 7

Future Studies

So much accomplished, so much left to be done. In the final chapter, I have divided prospective studies into three areas: (1) protein components, (2) carbohydrate components, and (3) dialyzable material. Each area is multifaceted and could provide interesting research opportunities for analytical, physical or bioinorganic chemists. The objective of this chapter is to present a basic plan of attack and generate interest for other chemists to enter this field of research.

Protein Components

Component 2--Isolation and Characterization

Peak 2, composed of seven different species, was not examined in this work. These species are undoubtedly important in the mineralization process. Examination of these components, particularly peak 2D (see Figure 4.3), appears crucial in furthering our knowledge.

Detection of Carbonic Anhydrase and Alkaline Phosphatase

These two enzymes have been detected in the mantles and periostraca of molluscs and are likely present in the extrapallial fluid.

Alkaline phosphatase activity can be measured routinely in the fluid by following any release of p-nitrophenol from p-nitrophenyl phosphate through the change in absorbance at 410 nm.[114]

Carbonic anhydrase activity can be detected similarly by measuring the amount of p-nitrophenol produced from the hydrolysis of p-nitrophenyl acetate.[115] If detected, these enzymes could be isolated by procedures similar to those developed here.

Binding of Tb^{3+} to 1A

The trivalent lanthanide ions have approximately the same charge ratio radius (~1.00Å) and form electrostatic complexes analogous to those of calcium. In contrast to the calcium ion, however, the rare earth metal ions exhibit a wide range of magnetic and spectroscopic properties. Consequently, there has been great interest in the use of these ions to probe calcium binding sites in biopolymers.[116-118]

Certain lanthanides (i.e., Tb^{3+}), when complexed with organic ligands, exhibit characteristic fluorescence spectra. These spectra arise from intramolecular energy transfer from the electronic states of the ligands to the 4f levels of the lanthanide ions.[119] Strong emission is observed when the ligand has a triplet state lying above the 4f level of the ion. Thus proteins, being abundant in aromatic residues, are amenable to such studies.[119] The intensity of the fluorescence spectrum of Tb^{3+} is greatly enhanced upon the

binding to several proteins.[120-122] I have observed similar effects with 1A as described below:

Fluorescence measurements were recorded on a Mark I spectrofluorimeter (Ferand Optical). All solutions were made in 10 mM MOPS buffer (Morphilinopropane sulfonic acid), pH 6.53. The inherent fluorescence intensity of Tb^{3+} solutions at various concentrations (0-0.2 M) were then recorded. The excitation and emission wavelengths used were 295 nm and 545 nm respectively. To 1500 µL of a 6.2 x 10^{-5} M 1A solution was added 1500 µL of 0.1 M Tb^{3+} and allowed to equilibrate overnight. The fluorescence intensity of the sample was recorded at 545 nm on the spectrofluorimeter. The intensity was enhanced upon the binding of the metal ion to the protein. Aliquots of 10 mM Ca^{2+} were then added to the sample. After each addition the contents were withdrawn with a 500 µL syringe and reinserted into the fluorescence cell to ensure thorough mixing. The emission intensity at 545 nm was recorded after five minutes.

The results of this titration are shown in Figure 7.1. Ca^{2+} completely displaces Tb^{3+} until 1.56 equivalents are added. It is not clear whether Tb^{3+} is bound to the 2 inherent Mg^{2+} sites or Ca^{2+} sites. Future studies with components $Ca_3$1A and "Apo" 1A will help determine which sites are involved. The magnitude of the fluorescence enhancement could also be used to characterize these metal binding sites further by determining:

A. The Ka's for Tb^{3}-1A complexes

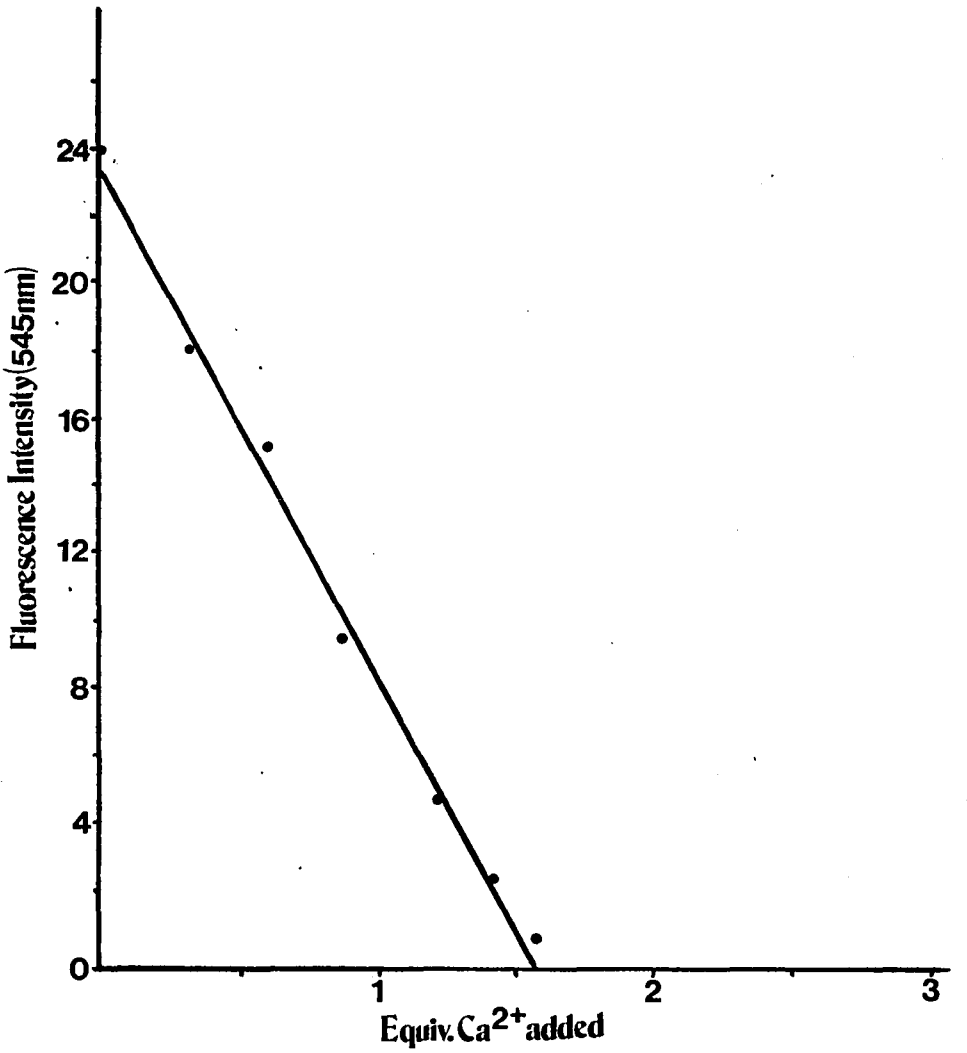

Figure 7.1. Plot of intrinsic fluorescence intensity of Tb^{3+}-1A complex versus equivalents of Ca^{2+} added.

B. The pK's of the coordinating ligands

C. Number of H_2O molecules bound to the metal ion

D. The distance between the metal binding sites.

Structure of lA in Solution--
Circular Dichroism

In recent years, much use has been made of circular dichroism (CD) to investigate the structure of proteins in solution.[123] There are now standard proteins which exhibit CD spectra characteristic of their structural content (α helix, β structure, or random). Comparison of these spectra would qualitatively determine the conformation of lA and its components ("Apo" lA, Ca_3Mg_2lA, Ca_3lA) and enable us to determine whether the metal ions are involved in maintenance of protein integrity.

Carbohydrate Components

Soluble and insoluble carbohydrate material has been found in the fluid and binds almost 10% of the calcium present. The structure and function of this material remains to be investigated.

Dialyzable Material

Organic Material

This dissertation suggests that molluscan calcification appears to be controlled by the chelation of calcium by small molecules. The theory could be confirmed by determining the identity and concentration of the chelates. The presence of amino acids in the ultrafiltrate has been shown (Chapter 3).

Chromatography of the fluid by the method of Barker and Summerson[124] would determine the presence and amount of various metabolic acids. The presence of simple sugars could be tested with the anthrone reaction.

Aromatic compounds that are candidates as substrates for the phenoloxidase could also be tested for accordingly.

Metals

There are seventeen metals present in the fluid. It seems likely that the metal content in shells would reflect the composition of this fluid. No work has been done to establish if such a correlation exists. Determination of the concentrations of the metals would help in evaluating whether the calcification process has an important role in incorporating metals into the shell.

Nd^{3+} Binding to Small Chelates--
pK's of Ligands

The 4f orbitals of the lanthanides are not significantly involved in bonding. However, the f-f transitions that do arise are very sensitive to complex formation. The f-f transitions of trivalent neodymium (Nd^{3+}) in the 500-600 nm region have been found to be particularly useful in detecting spectral changes.[125] These changes are quite small and a difference spectrum must be recorded to observe them. The Nd^{3+} difference spectrum observed with extrapallial fluid ultrafiltrate (MW 10,000) is shown in Figure 7.2. The sample cell contained 1500 µL of 0.1 M $NdCl_3$ and 1500 µL of ultrafiltrate. The reference cell contained 1500 µL of 0.1 M

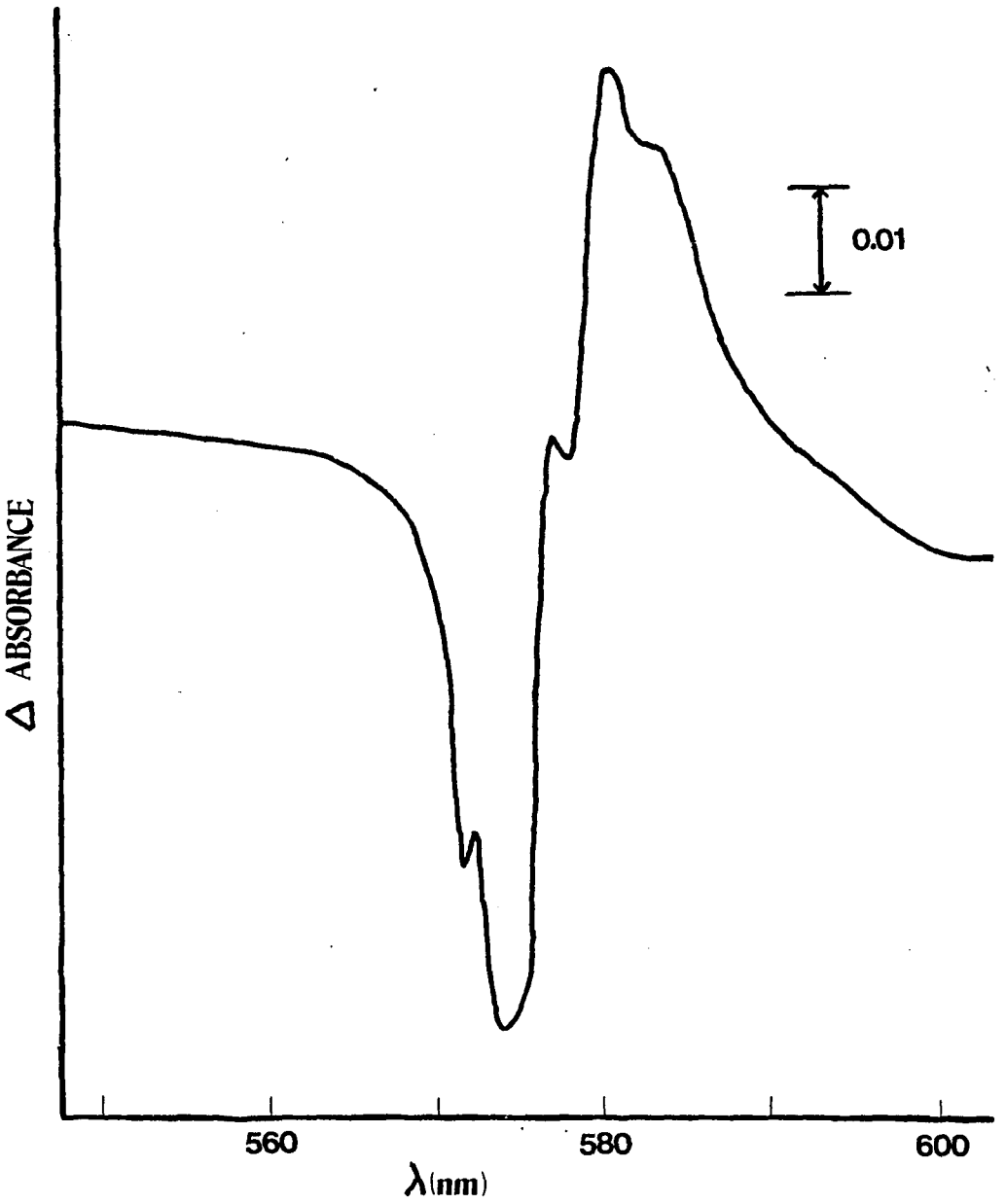

Figure 7.2. Difference absorption spectrum of a 0.05M Nd^{3+} solution in ultrafiltrate (MW ≤ 10,000) portion of the fluid.

$NdCl_3$ and 1500 μL of distilled-deionized H_2O. The pH of both samples was 6.1 and the spectrum was obtained on a Cary 14 spectrophotometer using a 0-0.1 absorbance slidewire. It is clear that intensity changes have occurred. The intensities of difference spectra obtained with ligands in other studies vary markedly with pH.[126] It is obvious from this spectrum that complexing agents are present in the fluid. The pH dependence of the spectral intensity could be used for determining the pK's of the coordinating fluid ligands.

Bibliography

1. R. H. Kretsinger, Ann. Rev. Biochem., 239(1976).
2. K. Towe, Biomineralization, 4, 1(1972).
3. W. F. Newman, Fed. Proc., 28, 1846(1969).
4. J. D. Taylor and J. W. Kennedy, Calc. Tiss. Res., 3, 274(1969).
5. P. Tasch, "Paleobiology of the Invertebrates," John Wiley and Sons, New York, N.Y., p. 312 (1970).
6. D. F. Travis, J. Ultra. Res., 23, 183(1968).
7. A. L. Heinz and D. P. Abbott, Science, 188, 363(1975).
8. G. Bevelander and H. Wakhara, Cal. Tiss. Res., 3, 84(1969).
9. N. Watabe, J. Ultra. Res., 12, 351(1965).
10. C. H. Brown, Quart. J. Micros. Sci., 93, 487(1952).
11. R. E. Hillman, Science, 134, 1754(1961).
12. K. Simkiss, Endeavor, 33, 119(1974).
13. H. J. Schatzman, J. Physiol. Lond., 235, 551(1973).
14. P. F. Baker, Prog. Biophys. Molec. Biol., 24, 177(1972).
15. R. D. Keynes, Q. Rev. Biophys., 2, 177(1969).
16. M. A. Crenshaw, Biol. Bull., 143, 506(1972).
17. T. Marin, Physiol. Rev., 47, 595(1967).
18. S. A. Nielson and E. Frieden, Comp. Biochem. Physiol., 418, 461(1972).
19. J. B. Polya and A. J. Wirtz, Enzymologia, 29, 27(1965).
20. K. M. Wilbur, Shell Growth and Regeneration. In "Physiology of Molluscs," Vol. I. K. M. Wilbur and C. N. Yonge, eds., Academic Press, New York, 243-282.
21. J. W. Campbell and K. V. Speeg, Nature, Lond., 224, 725(1969).

22. R. F. Pitts, Amer. J. Physiol., 203, 11 (1962)

23. T. Morimoto and R. E. Johnson, Nature, 216, 813(1967).

24. K. Simkiss, Biochem. J., 111, 647(1969).

25. P. S. B. Digby, Symp. Zool. Soc. Lond., 22, 903(1968).

26. K. Wada and T. Fryinuki, 1976. Biomineralization in bivalve molluscs with emphasis on the chemical composition of the extrapallial fluid. In "The Mechanism of Mineralization in the Invertebrates and Plants." K. Wilbur and N. Watabe, eds. University of South Carolina Press, Columbia, South Carolina. Pp. 175-190.

27. R. de Waele, Mem. Acad. Roy. Belg. Classe Sci., 10, 1 (1930).

28. M. Florkin and G. Bosson, C. R. Soc. Biol., 118, 1222 (1935).

29. S. Koboyashi, Biol. Bull., 126, 414(1964).

30. A. Abolins-Krogis, Ark. Zool., 13, 159(1960).

31. R. Durning, Ark. Zool., 18, 85(1965).

32. J. Pietrzak, J. M. Bates and R. M. Scott, Biol. Bull., 144, 391(1973).

33. M. A. Crenshaw, Amer. Zool., 9, 383(1969).

34. M. A. Crenshaw and S. D. Young, unpublished results, 1972.

35. K. Wada, Bull. Jap. Soc. Sci. Fish, 33, 613(1967).

36. K. Wada, Bull. Jap. Soc. Sci. Fish, 33, 1007(1967).

37. A. C. Neville,Biol. Rev., 42, 421(1967).

38. P. Greenaway, J. Exp. Biol., 54, 199(1971).

39. D. F. Travis, J. Untrastructure Res., 23, 183(1968).

40. S. Blanchard and N. D. Chasteen, J. Phys. Chem., 80, 1362(1976).

41. J. Skrabak, B. S. Thesis, University of New Hampshire, 1977.

42. M. A. Crenshaw, Biomineralization, 6, 6(1972).

43. G. Krampity, J. Engels, and C. Cagaux, Biochemical studies on water-soluble proteins of gastrapod shells. In "The Mechanism of Mineralization in the Invertebrates and Plants." K. Wilbur and N. Watabe, eds. University of South Carolina Press, Columbia, South Carolina. Pp. 155-173.

44. S. Weiner and L. Hood, Science, 190, 987(1975).

45. M. Borowski, personal communications.

46. M. J. Carter, Biol. Rev., 47, 465(1972).

47. A. S. Salenddin, Malacologia, 9, 501(1969).

48. J. R. Bradfield, Biol. Rev., 25, 113(1950).

49. D. B. Kroon, Acta Anat., 15, 317(1952).

50. K. Simkiss, Biol. Rev., 39, 487(1964).

51. J. Waite and K. M. Wilbur, J. Exp. Zool., 195, 359(1976).

52. J. H. Roe, J. Biol. Chem., 212, 335(1955).

53. P. Guire, P. Riquetti and B. G. Hudson, J. Chromatog., 90, 350(1974).

54. J. L. Hendrick and A. J. Smith, Arch. Biochem., 126, 155(1969).

55. J. Fitzgerald and N. D. Chasteen, Anal. Biochem., 60, 170(1974).

56. V. R. Meenakshi and K. M. Wilbur, Comp. Biochem. Physiol., 611(1969).

57. K. M. Wilbur and K. Simkiss, 1968. Calcified sheels. In "Comprehensive Biochemistry." M Florkin and E. H. Stotz, eds. Elsevier, New York. Pp. 224-295.

58. A. G. Gornall, C. G. Bardawill, and M. M. David, J. Biol. Chem., 177, 757(1949).

59. S. Hunt, 1970. "Polysaccharide-Protein Complexes in Invertebrates." Academic Press, New York. Pp. 146-155.

60. A. S. Mildvan and M. Cohn, Biochem., 2, 911(1963).

61. B. Burgess, N. D. Chasteen, and H. E. Gaudette, Anal. Geochem., 1, 171(1976).

62. N. D. Chasteen and J. Francavilla, J. Phys. Chem., 80, 867(1976).

63. J. Francavilla and N. D. Chasteen, Inorg. Chem., 14, 2680(1975).

64. G. Scatchard, Ann. N. Y. Acad. Sci., 51, 660(1949).

65. W. T. Oosterhuis, Struct. and Bond., 20, 59(1974).

66. J. F. Boas and B. Window, J. Chem. Phys., 51, 965(1969).

67. K. Wada, Bull. Natl. Pearl Res. Lab., 9, 1087(1964).

68. A. Abolins-Krogis, L. Z. Zellforsch, 142, 225(1973).

69. N. M. Holyk, M.S. Thesis, University of New Hampshire, (1978).

70. S. Blanchard and N. D. Chasteen, Anal. Chem. Acta, 82, 113(1976).

71. L. K. White, N. D. Chasteen, A. S. Szabo, and P. Carkner, J. Phys. Chem., 81, 1420(1977).

72. R. M. Garrels and M. E. Thompson, Am. J. Sci., 260, 57 (1962).

73. S. E. Ingle, C. H. Culberson, J. E. Hawley and R. M. Pythowicz, Mar. Chem., 1, 295(1973).

74. P. Andrews, Biochem. J., 91, 222(1964).

75. M. Jope, Comp. Biochem. Physiol., 45B, 17(1973).

76. N. Watabe, J. Ultrastructure Res., 12, 351(1965).

77. H. Mutnu, Biomineralization, 2, 48(1970).

78. V. R. Meenakshi, P. E. Hare, and K. M. Wilbur, Comp. Biochem. Physiol., 40B, 1037(1971).

79. R. W. G. Wyckhoff, "The Biochemistry of Animal Fossils," Scientichnitise, Bristol, U. K., 1972.

80. C. Grégoire, Biol. Rev., 42, 653-688(1967).

81. S. Halta, Earth Sci. Tokyo, 23, 133-140(1969).

82. S. P. Colowick and F. C. Womack, J. Biol. Chem., 244, 774-777(1969).

83. B. G. Malmstrom, Biochem. Biophys. Acta, 30, 1(1958).

84. M. Cohn and J. Townsend, Nature, Lond., 173, 1090(1954).

85. J. Francavilla, M.S. Thesis, University of New Hampshire, (1974).

86. T. Tsugii, Mie Ken Daig Suisan Gak Kizo, 5, 378-383(1962).

87. G. Sattacassa, Biochem. Biophys. Res. Comm., 407, 808 (1972).

88. C. E. Nicholds, Proc. Natl. Acad. Sci. U.S., 69, 581 (1972).

89. S. Ebashi, S. Ohnishi, S. Abe, and K. Marayama, J. Biochem (Tokyo), 69, 441(1971).

90. C. S. Fullmer and R. H. Wasserman, Biochem. Biophys. Acta, 317, 172(1968).

91. J. Mathejea and E. T. Degens, Neues. Jb. Geol. Paleont. Mh., 4, 215(1968).

92. M. A. Crenshaw, personal communication, (1976).

93. H. P. Baker and H. A. Saroff, Biochem., 4, 1670(1965).

94. D. G. Hoare and D. E. Koshland, J. Biol. Chem., 242, 2447(1967).

95. G. Abontangelo, Calc. Tiss. Res., 26, 247(1978).

96. E. E. Stauffer and R. S. Treptow, Biochem. Biophys. Acta, 295, 457(1973).

97. A. N. Taylor and R. H. Wasserman, Arch. Biochem. Biophys., 119, 536(1967).

98. S. B. Oldham, C. D. Arnaud and J. J. Jowsey, Biochem., 13, 4790(1974).

99. D. T. Zolock and R. L. Morrisey, Fed. Proc., 35, 1609 (1976).

100. C. S. Fullmer, Proc. Soc. Exp. Biol. Med., 152, (1976).

101. H. S. Mason, J. Biol. Chem., 172, 83(1948).

102. M. Fling, N. H. Horowitz and S. F. Heineman, J. Biol. Chem., 238, 2045(1963).

103. H. W. Duckworth and J. E. Coleman, J. Biol. Chem., 245, 1613(1970).

104. D. Kertesy, G. Rotilio, M. Brunori, R. Zito, and E. Antonini, Biochem. Biophys. Res. Comm., 49, 1208(1972).

105. A. S. Sussman, Arch. Biochem. Biophys., 95, 407(1961).

106. D. Kertesy and R. Zito, Biochem. Biophys. Acta, 96, 447 (1965).

107. S. S. Patul and M. Zucker, J. Biol. Chem., 240, 3938 (1965).

108. S. H. Framerantz, J. Biol. Chem., 238, 2351(1963).

109. R. L. Jolley, D. A. Robb, and H. S. Mason, J. Biol. Chem., 244, 1593(1969).

110. K. E. Van Holde in T. H. Hayashi and A. G. Szent-Gyargi (Editors), "Symposium on molecular architecture in cell physiology," Prentice-Hall, Inc., 1966. P. 81.

111. E. T. Degens and J. Mathejea, Comp. Biochem. Physiol., 20, 553(1967).

112. S. T. Hunt and S. W. Brener, Biochem. Soc. Trans., 1, 215(1973).

113. A. Bubel, Mar. Biol., 23, 2(1973).

114. D. J. Plocke, Biochem., 1, 373(1962).

115. Y. Pocker and J. T. Stone, Biochem., 6, 668(1967).

116. E. R. Birnbaum, J. Amer. Chem. Soc., 92, 5287(1970).

117. J. Reuben, Biochem., 10, 2834(1971).

118. J. Reuben, J. Phys. Chem., 75, 3164(1971).

119. A. D. Sherry and G. L. Cottam, Arch. Biochem. Biophys., 156, 665(1973).

120. J. Reuben, Naturwissenchaften, 62, 172(1975).

121. M. Epstein, A. Levitzki and J. Reuben, Biochem., 13, 1777(1974).

122. C. K. Luk, Biochem., 10, 2838(1971).

123. W. P. Saxena and D. B. Wettaufer, Proc. Nat. Acad. Sci. USA, 68, 969(1971).

124. S. B. Barker and W. H. Summerson, J. Biol. Chem., 138, 534(1941).

125. A. Gafni and I. Z. Steinberg, Biochem., 13, 800(1974).

126. E. R. Birnbaum and D. W. Durnall, Bioinorg. Chem., 3, 15(1973).

127. R. M. Pytowicz, Am. Zool., 9, 673(1969).

128. M. Whitfield, Geochim. et. Cosmochim. Acta, 39, 1545(1975).

129. C. Mehrbach, C. H. Culberson, J. E. Hawley and R. M. Pytkowicz, Limnol. Oceanogr., 18, 897(1973).